INVESTIGATING NEURAL RESPONSES IN MODELS OF NEUROCYSTICERCOSIS.

by

Hayley Sarah Tomes
TMSHAY001

Department of Human Biology

SUBMITTED TO THE UNIVERSITY OF CAPE TOWN

In fulfilment of the requirements for the degree

Doctor of Philosophy in *Neuroscience*

Supervisor:

Dr Joseph Valentino Raimondo

Department of Human Biology
University of Cape Town

Co-supervisor:

E/Prof Lauriston Kellaway

Department of Human Biology
University of Cape Town

December 2019

The National Research Foundation, Oppenheimer Memorial Trust and the University of Cape Town are acknowledged for financial support.

Declaration

I, **Hayley Sarah Tomes**, hereby declare that the work on which this dissertation/thesis is based on my original work (except where acknowledgements indicate otherwise) and that neither the whole work nor any part of it has been, is being, or is to be submitted for another degree in this or any other university.

I empower the university to reproduce for the purpose of research either the whole or any portion of the contents in any manner whatsoever.

Signature: Signed by candidate

Date: **03 April 2020**

Abstract

Epilepsy is more frequent in sub-Saharan Africa than the rest of the world due to high levels of brain infections by larvae of the pig cestode *Taenia solium*, a condition termed neurocysticercosis. Despite the large nature of the problem, little is known about how neurocysticercosis modulates neuronal responses to result in the development of seizures. In this thesis I have used the cestode *Taenia crassiceps* to develop multiple *in vitro* and *in vivo* models of neurocysticercosis in rodents. Utilising patch-clamp electrophysiology in organotypic hippocampal brain slices and chronic, wireless electrocorticographic recordings in freely moving animals I have explored how cestode larvae affect neuronal excitability in the brain across a range of time scales. First I demonstrate that homogenate of *Taenia crassiceps* larvae has a strong, acute excitatory effect on neurons, which is sufficient to trigger seizure-like events. The excitatory component of the homogenate was found to strongly activate glutamate receptors and not acetylcholine receptors nor acid-sensing ion channels. An enzymatic assay showed that the larval homogenate contains high levels of glutamate, explaining its acute excitatory effects on neurons. In the second part of my thesis I demonstrate that longer-term incubation of *Taenia crassiceps* homogenate with organotypic brain slices over the course of a day does not affect the intrinsic properties of pyramidal neurons nor the excitability of the neuronal network. In the final part of my thesis I established an *in vivo* model of neurocysticercosis. I found that intradermal inoculation together with multiple intracerebral injections of *Taenia crassiceps* homogenate did not result in the development of seizures over 3 months of chronic electrocorticography recordings. In addition, the seizure-threshold to picrotoxin, an excitotoxin, was not altered by *Taenia crassiceps* homogenate injection. Immunohistological analysis of the tissue below the injection site revealed no difference in astrocytes nor the number of microglia. However, microglial processes were observed to be retracted in the *Taenia crassiceps* group reflecting a moderate neuroinflammatory response. Together the data in my thesis provides novel insight into the acute and chronic effects of *Taenia crassiceps* homogenate on the excitability of neuronal networks with relevance to our understanding of neurocysticercosis.

Acknowledgements

Most of all I would like to thank my supervisor Joe, for not only mentoring me in science but in life as well. I could not have picked a better human to tackle this doctorate with than you - an all-round “groovy” person who has created such an amazing lab with an emphasis on the well-being of its people as well as the excellence of its science.

Shannagh! Thank you for constantly checking in with me in the gentlest way possible and for proof raeding most of this document – your suggestions were incredibly astute and helpful. It calmed me greatly to know that my writing was making any sense!

Richard, thank you for being such a patient and caring partner through this marathon and for giving the very best pep talks. I’m so excited for post-thesis adventures with you. Love you!

Thank you so much to my family for their tireless support, even from afar. Thank you mom and Kel for all the phone calls and messages of encouragement! Dad and MC - thank you for stuffing me full of good food at every opportunity.

I’m so fortunate to have such wonderful friends and housemates who have checked in with me even when I was in full lock-down mode. You are the most wonderful humans that I am privileged to share life with. Tabitha, thank you for knowing me so darn well and being my reference point in all things.

My epic lab filled with the loveliest bunch of nerds! Thank you for creating such a special environment in which to do science. A special thank you to the other half of (the OG) Team Tapeworm – Anja de Lange. You have been a science buddy of note and I appreciate the hell out of our friendship!

Finally I would like to extend an unexpected thank you to the two litters of foster kittens who were the best anti-anxiety elixir during the last stressful weeks of this thing.

Table of Contents

List of Figures

List of Tables

List of Abbreviations

Symbol	Description
aCSF	Artificial cerebro-spinal fluid
ANOVA	Analysis of variance
ASICs	Acid-sensing ion channels
ATP	Adenosine triphosphate
BBB	Blood-brain barrier
Ca^{2+}	Calcium
Cl^-	Chloride
CNS	Central nervous system
CT	Computed tomography
ECoG	Electrocorticography
GABA	γ-aminobutyric acid
GluRs	Glutamate receptors
GFAP	Glial fibrillary acidic protein
Iba1	Ionized calcium binding adaptor molecule 1
IL-1β	Interleukin-1β
IL-6	Interleukin-6
ip	Intraperitoneal
IQR	Interquartile range
K^+	Potassium
LH	Left hemisphere
LPS	Lipopolysaccharide
M. corti	*Mesocestoides corti*
Na^+	Sodium
nAchRs	Nicotinic acetylcholine receptors
NF-κB	Nuclear Factor Kappa-light-chain-enhancer of activated B cells
NK1R	Neurokinin-1 receptor
NMDA	N-methyl-D-aspartate
OCT	Optimal Cutting Temperature
OSI	Open Source Instruments
PBS	Phosphate buffered saline
sc	Subcutaneous
SEM	Standard error of the mean
SLE	seizure-like event
T. crass.	*Taenia crassiceps*
T. solium	*Taenia solium*
TNF-α	Tumour necrosis factor-α
WHO	World Health Organisation

Chapter 1

INTRODUCTION

1.1 DISORDERS OF THE NERVOUS SYSTEM AND THEIR PREVALENCE IN THE DEVELOPING WORLD

Neurological disorders contribute 6.3% to the global burden of disease in terms of disability-adjusted life years and constitute 11.7% of total deaths, according to the most recent, but dated, World Health Organisation (WHO) report focusing on neurological disorders and the public health challenges they are associated with (WHO, 2006, pages 34-35).

These include; epilepsy, cerebrovascular disease, Alzheimer's and other dementias, neuro-infections, Parkinson's disease, nutritional deficiencies and neuropathies, multiple sclerosis, neurological injuries, migraine, poliomyelitis, tetanus, meningitis and Japanese encephalitis (WHO, 2006). Many are life threatening if left untreated while others result in an extremely diminished quality of life.

Parasitic infections of the nervous system are an important cause of neurological disease, but are significantly understudied as they predominantly occur in the developing world, where limited resources are available (Singhi 2011; Hotez *et al.* 2008; Wagner and Newton 2009).

Parasitic infections affecting the nervous system are more common in children and are particularly problematic as they can cause permanent deficits in learning and memory with debilitating long-term socioeconomic impacts (Mafojane *et al.* 2003; Ndimubanzi *et al.* 2010).

Neurocysticercosis (NCC) is the most prevalent parasitic infection of the central nervous system (CNS) (Diop *et al.* 2003; Preux and Druet-cabanac 2005) and is listed as one of the WHO's prioritised 20 most Neglected Tropical Diseases ("Neglected Tropical Diseases", accessed July 2019).

1.2 NEUROCYSTICERCOSIS: ITS IMPACT AND PREVALENCE

NCC is the leading cause of acquired epilepsy in the developing world (Mejia Maza *et al.* 2019). It is thought to account for 50 000 deaths annually and up to 70% of those infected will

eventually develop seizures (Preux and Druet-cabanac 2005; Román *et al.* 2000). It is caused by larvae of the tapeworm *Taenia solium* lodging in the brain (Trevisan *et al.* 2016).

1.2.1 Prevalence

NCC is most prevalent in the developing world, spanning the continents of South America, Africa and Asia (see Figure 1.1). In addition, it is increasingly becoming apparent in developed countries as people emigrate in search of better prospects.

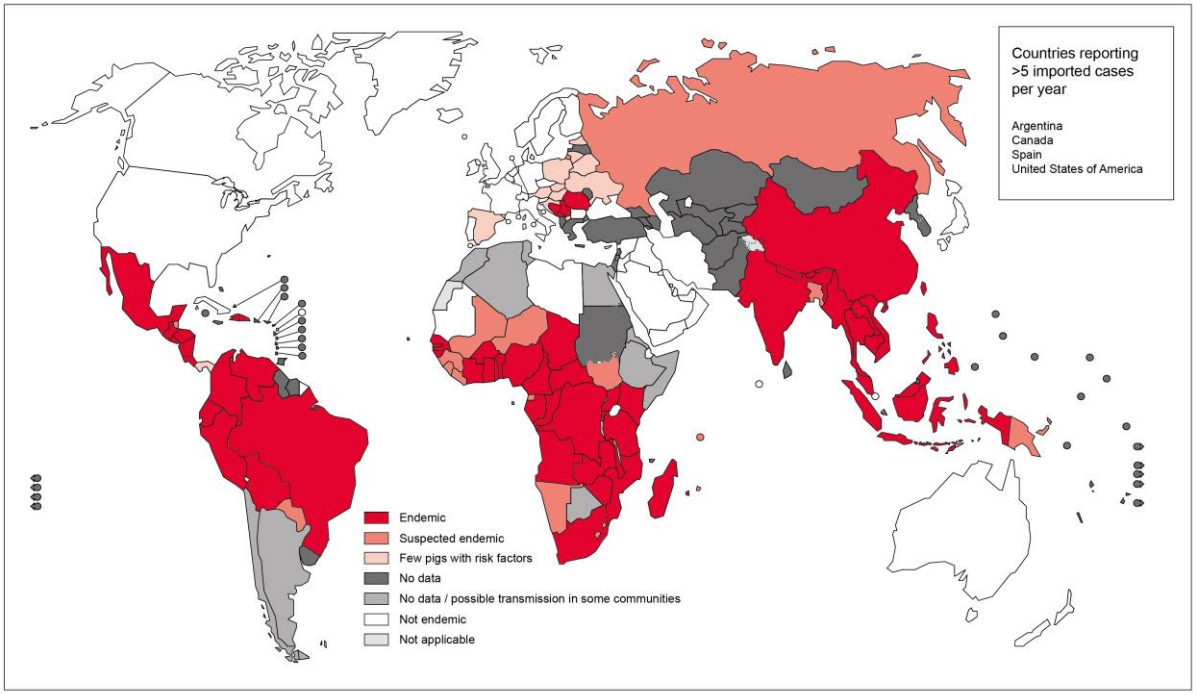

Figure 1.1 Prevalence of Neurocysticercosis.
Areas in the world endemic to *Taenia solium* and in which Neurocysticercosis is prevalent, taken from a WHO fact sheet ("Endemicity of *Taenia solium* " 2015, accessed August 2019).

NCC is a difficult disease to diagnose definitively as it requires a computed tomography (CT) scan, which is expensive and not typically accessible in rural areas where the disease is endemic (Mafojane *et al.* 2003; Ndimubanzi *et al.* 2010). Furthermore NCC can remain asymptomatic for years and as such is likely to be heavily under diagnosed in both rural areas and the urban areas to which people have relocated (Stringer *et al.* 2003; Y. Sun *et al.* 2014). South Africa has a paucity of studies which have attempted to estimate the prevalence of NCC, and yet it is one of the more studied populations on the African continent (Mafojane *et al.* 2003).

A 1965 report by Heinz and MacNab estimates that on average 10% people living in rural areas have cysticercosis (infection of the body with *T. solium* larvae). Cysticercosis may not be specific to the brain but since the larvae preferentially penetrate brain and muscle tissue it

is likely that NCC will develop (Carpio, Escobar, and Hauser 1998). In a study of 200 male black African mine workers, 9.5% had *Taenia* eggs in their stool, which, if combined with improperly managed sanitation, creates a large risk for NCC infection (Bird, Heinz, and Klintwork 1962; Garcia and Del Brutto 2005).

The prevalence of NCC may be as high as 20% in certain regions of South Africa, most notably the Eastern Cape, where free-range pig farming is common (Heinz and MacNab 1965; Campbell and Farrell 1987). This area is so endemic that one study conducted at the Groote Schuur Hospital in Cape Town (over 1200 kilometres away) found that 88% of patients presenting with NCC over a 15 year period (N = 239) were originally from the Eastern Cape region (A. J. G. Thomson 1993).

Cysticercosis is an eradicable disease but, unfortunately, no longer features on the International Task Force for Disease Eradication's list of focal diseases ("International Task Force for Disease Eradication,", accessed July 2019) despite previously being designated as such (International Task Force for Disease Eradication 2008).

1.2.2 The *Taenia* parasite life cycle

Neurocysticercosis infection occurs when a person accidentally ingests *Taenia solium* eggs from human faecal matter, often via unwashed vegetable produce in areas where pigs are in close proximity to humans and sanitation is poor, or if there is a tapeworm carrier in the household (Figure 1.2, left) (Diop *et al.* 2003; Garcia and Del Brutto 2005). Since tapeworm are hermaphroditic and each proglottid comprises both gonads, they are able to self-fertilise their eggs once they mature. When the tapeworms eggs are fertilised the proglottid is known to be gravid (Figure 1.2, right) and is shed into the faeces where the individually encapsulated eggs may then be eaten by the intermediate host (Willms and Zurabian 2010). The parasite eggs are converted to larvae or oncospheres when they come into contact with the host's gastric acid and intestinal juices and attach to the host's intestinal mucosal membrane with projections of their membrane (Johnston *et al.* 2016; Verastegui *et al.* 2015). They secrete proteases in order to facilitate burrowing through the membrane in order to enter the circulatory system where they are able to travel to other bodily tissues, preferentially the brain, skeletal muscle, eye and subcutaneous tissue (Nash *et al.* 2015; Mahanty and Garcia 2010; Carpio, Escobar, and Hauser 1998; Id *et al.* 2018).

The oncospheres, upon entry into the brain, form cysticerci. The development of the cysticerci is divided into four stages; the vesicular or viable stage, the colloidal stage, the granular-nodular stage and the calcified stage (see Figure 1.3) (Carpio, Escobar, and Hauser 1998).

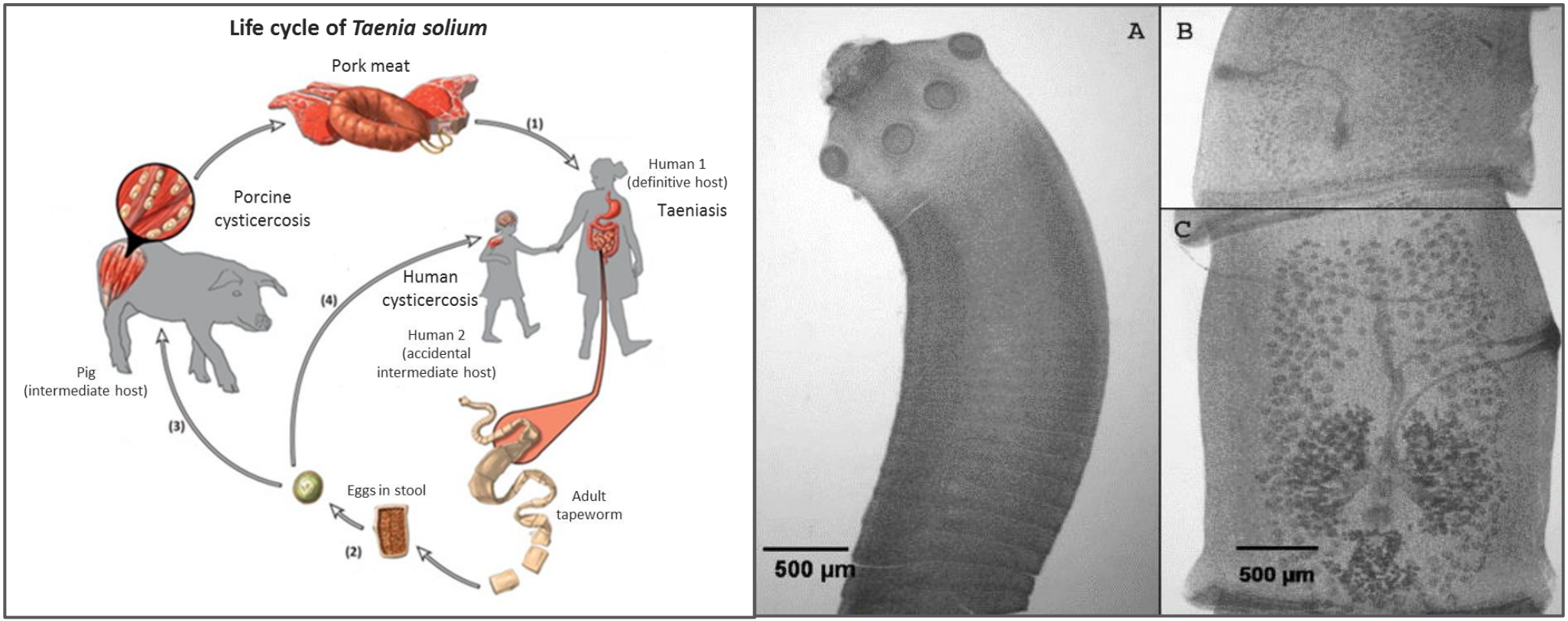

Figure 1.2 The Taenia Parasite.
Left: Life cycle of ***Taenia solium***. (1) A person eats undercooked, infected meat and an adult tapeworm develops in the intestine and (2) sheds gravid proglottids with eggs in their host's faeces. (3) The eggs in the stool are ingested by the designated intermediate host, the pig, or (4) they are ingested by an accidental intermediate host, the human, resulting in human (neuro)cysticercosis. (Diagram modified from Rasamoelina-Andriamanivo, Porphyre, and Jambou 2013). Right: Tapeworm recovered from a 30 day hamster infection, whole mounts stained with carmine red. (A) the head (scolex) and initial formation of proglottids, (B) immature proglottid, (C) mature 'gravid' proglottid showing eggs (Diagram from Willms and Zurabian 2010).

The exact mechanism by which NCC leads to epilepsy is largely unknown. It has been hypothesized that seizures develop as a result of the host's immune response to dying cysts, as live parasites are associated with negligible inflammation (Stringer *et al.* 2003; Y. Sun *et al.* 2014). However, it has not been determined whether the mediator of the seizures is a substance released by the dying parasite or one produced by the surrounding inflammatory cells (Stringer *et al.* 2003). The stage of the cysticerci may also play a role.

1.2.2.1 Cyst stages and seizure development

The host will generally remain asymptomatic, for weeks to months, while the vesicular cysticerci mature (Foyaca-sibat *et al.* 2009). This is suggested to be because the parasite is able to use host molecules to mask their surface structures and secrete immunomodulatory molecules (Restrepo *et al.* 2001; Dzik 2006). Following the sequencing of the *Taenia solium* genome in 2013 other evolved adaptions were discovered, including a specialised metabolism, nutrient scavenging abilities and specific detoxification pathways (Tsai *et al.* 2013).

Once the cysticerci begin to die, the resulting focal reaction can result in acute symptomatic seizures for some (around 7.5%) and in others triggers the beginning of the inflammatory process, which can result in seizures, or remain asymptomatic for years, or even the entire lifetime of the host (Foyaca-sibat *et al.* 2009; Stringer *et al.* 2003). The progression from a mature cyst to a colloidal or inflamed cyst is often referred to as the 'silent period' (Figure 1.3) (Garcia, Gonzalez, and Gilman 2003).

Fully inflamed cysticerci, over the course of approximately a month, go on to produce a chronic granuloma (amalgamation of immune cells and parasite material), resulting in the so-called granular-nodular stage (Figure 1.3) (Garcia, Gonzalez, and Gilman 2003). It can take over a year for the granuloma to eventually calcify (Figure 1.3) (Garcia, Gonzalez, and Gilman 2003). The calcification corpuscle, made up of host protein taken up by the parasite (Flores-Bautista *et al.* 2018), can lead to the formation of an epileptogenic zone in approximately half of people (Diop *et al.* 2003). The manifestation of phenotypical symptoms is variable and may only occur 4 - 5 years after infection in some cases (Stringer *et al.* 2003; Y. Sun *et al.* 2014), seizures may also either be generalized or partial depending on the brain area affected (Diop *et al.* 2003; Agnes Fleury *et al.* 2004).

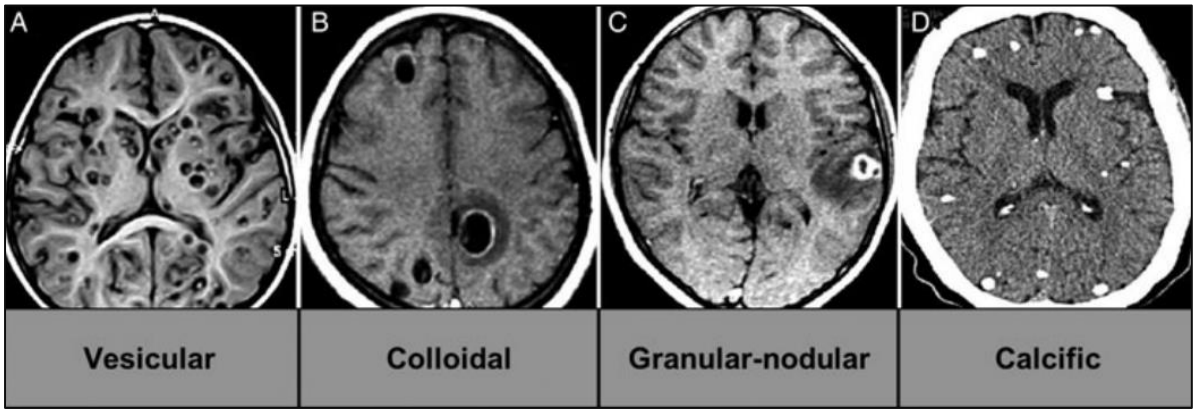

Figure 1.3 The evolution of parenchymal cysticerci in the accidental human host.
(A) MRI of vesicular cysticerci. **(B)** MRI of colloidal (inflamed) cysticerci. **(C)** MRI of a degenerating cysticercus forming a granuloma. **(D)** CT scan of calcified cysticerci. (Images from Carpio and Romo 2014 and Lange, Mahanty, and Raimondo 2018).

Importantly, the exact correlation between cyst stage and symptom presentation, mainly seizures, is still not clear. It is generally believed, however, that seizures are more likely when a degenerating cyst is present (colloidal or granular-nodular stages) (Verma *et al.* 2010) or when the cyst has calcified (Nash, Pretell, and Garcia 2002). In contrast, there is evidence that seizures can also occur whilst the cysts are viable. For example, Naidoo *et al.* (1987) found that 12.9 % of epileptic patients with NCC had only viable cysts (N = 70), whereas Campbell and Farrell (1987) found this percentage to be 18.5 % (N = 106). In addition, evidence of calcified cysts has also been found in asymptomatic individuals (Prasad *et al.* 2009) and Foyaca-sibat *et al.* (2009) have shown a similar distribution of parasite load and degenerating stages of the cyst (past the vesicular stage) in both symptomatic and asymptomatic people with NCC. It should be noted that these studies are relatively old and improved CT scanning imaging resolution together with the advent of MRI will allow for more accurate staging of cysts in order to better correlate cyst development with seizure onset.

As described above, although the propensity for seizure development may change depending on the time since infection and the cyst-stage, it is clear that seizures can occur at any point. The variability in terms of when, or whether, seizures emerge suggests that there are likely multiple mechanistic processes involved in the development of seizures in NCC. This thesis therefore studies the effects of tapeworm homogenate over a range of different time scales to explore different possible processes which may be relevant to the epileptogenic process in NCC.

1.2.3 Symptoms

1.2.3.1 Seizures

The main symptom of NCC is seizures, either focal or generalized, often resulting in epilepsy, which is characterised by recurrent seizures in a person. In fact, the correlation between NCC and epilepsy is so well established that NCC is widely recognised as the leading cause of acquired epilepsy in adults (Preux and Druet-cabanac 2005; Román *et al.* 2000). It is estimated that between 30 and 50 % of all adult-onset or acquired epilepsy in developing countries is due to NCC (Garcia and Del Brutto 2005; Garcia, Gonzalez, and Gilman 2003; Ndimubanzi *et al.* 2010).

One of the more recent reviews collating incidence of NCC among epilepsy patients in eastern and southern african regions found numbers mostly in agreement with the above (Mafojane *et al.* 2003). Those that had lower incidence were often relying solely on serological testing which is known to underestimate numbers (Mafojane *et al.* 2003). In many areas the prevalence is still unknown or is on the rise after not being considered endemic for decades prior (Mafojane *et al.* 2003).

In South Africa the number of epilepsy patients who also have a tapeworm infection in endemic areas is similar to the international picture, with Naidoo *et al.* (1987) finding 30 % of patients, Campbell and Farrell (1987) finding up to 50.9 % of patients, Foyaca-sibat *et al.* (2009) finding between 37 and 47 % of patients and van As and Joubert (1991) finding 28 % of patients to be infected. Furthermore, studies of epileptic children who also had NCC found a prevalence of 43 % in one study (Thomson *et al.* 1984) and 45.2 % in another of under 20 year olds (Foyaca-sibat *et al.* 2009). The local data is therefore consistent with international studies which find that on average, in endemic areas, approximately 29 % of people with epilepsy have NCC (Ndimubanzi *et al.* 2010).

1.2.3.2 Other

Other symptoms include; increased intracranial pressure, which can result in migraines, headaches and dizziness; focal neurological deficit; meningo-encephalitis and hydrocephalus (Nash, Pretell, and Garcia 2002; Prasad *et al.* 2008; Thomson *et al.* 1984).

The symptoms of NCC are often specific to the number of cysts and brain location affected, particularly in cases where the larvae enter the ventricles of the brain, which can result in the larvae obstructing the flow of cerebrospinal fluid (García *et al.* 2003; Prasad *et al.* 2008). Focal deficits occur depending on what brain tissue degenerates as a result of the space occupied by and inflammatory effects of the calcified cyst.

1.3 SEIZURES AND EPILEPSY

Epilepsy constitutes a serious medical condition whereby bouts of excessive, synchronous hyperexcitability (seizures) result in significant morbidity and mortality. It can be genetic in origin, result from an anoxic incident, from a CNS infection or trauma or a combination of multiple insults.

The WHO estimates that epilepsy accounts for 0.5 % of the global burden of disease and that close to 80 % of all cases occur in the developing world (WHO 2006; Diop *et al.* 2003). In fact, epilepsy is the most common neurological disorder in sub-Saharan Africa (Winkler *et al.* 2009). The syndrome affects many more people in the developing world, ≥ 190 per 100 000 people compared to only 24 per 100 000 people in Europe, due to the high incidence of head trauma and NCC (WHO 2006, page 58). The prevalence of epilepsy in South Africa is even higher and was found to affect between 220 and 370 per 100 000 people in two rural populations (N = 400 000) (Diop *et al.* 2003; Bird, Heinz, and Klintwork 1962).

Epilepsy is highly stigmatised in sub-Saharan Africa. The afflicted person can be believed to have been cursed with bad spirits which, furthermore, are believed to be contagious, which can result in social isolation from the village (Winkler *et al.* 2009). Not only does this have an immense emotional impact but it can also be medically dangerous for someone who is epileptic to live entirely alone.

Status epilepticus is another possible complication of epilepsy caused by NCC. Status epilepticus is a continous seizure, or a state of sequential seizures without recovery of consciousness. It is considered a medical emergency and can result in debilitating neurological sequelea if not treated urgently.

The brain mechanisms that go awry to result in seizures and ultimately epilepsy are complex, and are best understood as network disruptions resulting from alterations to specific brain cell types and transmembrane ion gradients, amongst a host of other factors.

1.4 NEURAL SIGNALLING AND THE EXCITATION: INHIBITION BALANCE

The brain is arguably one of the most complex signalling systems known. Successful neural transmission relies upon a stable balance of excitatory and inhibitory signalling. Neurons, the basic computational units of the CNS, are densely connected, each receiving thousands of synaptic inputs, and are able to sense changes in the environment, translate these changes to other cells and evoke a bodily response (Bear, Connors, and Paradiso 2007). Although

neurons do the bulk of informational processing, glial cells are also essential to the functioning of neural transmission and their role will be examined in section 1.5.

1.4.1 Different neuronal types

This balance between excitatory and inhibitory activity in the brain depends upon the collaborative actions of many different cell types and many different neuron types. Activation of a neuron typically results in the release of neurotransmitter from the axon terminal into the synaptic cleft and the activation of ligand-gated receptors on the postsynaptic neuron, causing current flow and voltage signals that may or may not result in an output known as an action potential (Bear, Connors, and Paradiso 2007). Different types of neurons release many different neurotransmitters (typically only one kind of neurotransmitter per neuron) which have different effects on their postsynaptic targets (Bear, Connors, and Paradiso 2007).

Pyramidal neurons are large cells abundant in the cerebral cortex and hippocampus. They serve as the primary excitatory neurons in the brain and release the neurotransmitter glutamate. Ubiquitous across the brain are inhibitory interneurons, which function to quieten the network by releasing the inhibitory neurotransmitter γ-aminobutyric acid (GABA). Broadly speaking these two cell types control the firing rates and excitability of neuronal networks (Bear, Connors, and Paradiso 2007).

1.4.2 Transmembrane ion gradients

How each synaptic input results in a voltage change in the postsynaptic neuron is down to the action of ion channels and transmembrane ion gradients (Raimondo *et al.* 2015). The opening of channels allows ions, which are charged, to move down their electrochemical gradient and by doing so change the membrane voltage of the cell. If more positive ions, such as sodium (Na^+) or calcium (Ca^{2+}), flow into the cell this raises the membrane voltage or 'depolarises' the cell. Conversely when chloride (Cl^-) ions flow into the cell or K^+ ions flow out of the cell this lowers the membrane potential or 'hyperpolarises' the cell. Ion gradients are maintained between channel openings by the actions of enzymatic pumps and transporters. The most fundamental of which is the Na^+ / K^+ ATPase enzyme, which utilises the energy from ATP to establish opposing transmembrane gradients for Na^+ and K^+ (Raimondo *et al.* 2015). This is characterised by a high intracellular K^+ concentration (typically ~100 mM) and a low extracellular concentration (typically ~3 mM) (Raimondo *et al.* 2015). The opposite is true for Na^+ where the intracellular concentration is low (typically ~10 mM) and the extracellular concentration is high (~145 mM) (Raimondo *et al.* 2015). A host of secondary transporters then use these gradients established by the Na^+ / K^+ ATPase enzyme to establish transmembrane gradients for other ions such as Cl^- (Raimondo *et al.* 2015).

Ion channels harness these ion gradients to generate ion flux and voltage signals in neurons. Ion channels are often gated, meaning that their opening is dependent on an environmental signal. For example, some ion channels are ligand-gated whilst others may be voltage-gated (Bear, Connors, and Paradiso 2007). Ligand-gated ion channels are specific to the type of neurotransmitter that binds to them, whereas voltage-gated ion channels are only able to open at certain voltages (Bear, Connors, and Paradiso 2007).

Voltage-gating is in fact critical for the generation of an action potential in the postsynaptic cell. An excitatory post-synaptic potential causes some depolarisation of the membrane which can lead to the opening of voltage-gated Na^+ channels (Bear, Connors, and Paradiso 2007). If enough voltage-gated Na^+ channels are activated, the resulting depolarisation leads to further opening of voltage-gated Na^+ channels initiating a positive feedback phase whereby rapid depolarisation, constituting an action potential, is generated. With continued depolarisation, voltage-gated Na^+ channels start to close again. At the same time voltage-gated K^+ channels also open allowing K^+ to flow out of the cell (repolarising and then hyperpolarising the cell) (Bear, Connors, and Paradiso 2007). This second phase is critical for the cell's ability to respond to subsequent signalling.

Some ion channels may exhibit both voltage-gated and ligand characteristics. For example, the N-methyl-D-aspartate (NMDA) receptor, which is effectively a hybrid ligand and voltage-gated glutamate receptor. At hyperpolarised potentials a magnesium molecule blocks the channel pore. At depolarised potentials the magnesium molecule is displaced which means that concurrent glutamate binding will open the channel (Bear, Connors, and Paradiso 2007). Thus in order for the channel to be open, it needs both glutamate binding and a relatively positive membrane potential.

K^+ leak-channels are constitutively open ion channels and play a critical role in setting the negative membrane potential of neurons by allowing K^+ to flow down its electrochemical gradient from inside to outside the cell (Lesage 2003). Raising the extracellular K^+ concentration is a common method for inducing seizure-like activity *in vitro* as it slows the K^+ flux through the leak channels by creating a less steep ion gradient, thereby depolarizing the neuronal resting membrane potential (Wang *et al.* 2016). Furthermore, genetic alterations to K^+ channels are known to result in inherited epilepsies (Villa and Combi 2016). At least 80 genes in the human genome encode for K^+ channels, which represents the largest of the ion channel groups (Villa and Combi 2016).

1.4.3 Different receptor types and neurotransmitters

Different receptors respond to different neurotransmitters released from the presynaptic neuron resulting in either a depolarisation or hyperpolarisation of the postsynaptic cell. The

correct functioning of these receptors helps maintain the balance of excitation and inhibition in the network.

1.4.3.1 Glutamate receptors

Glutamate is the main excitatory neurotransmitter in the CNS and has three main ionotropic or fast acting receptors; AMPA, NMDA and Kainate receptors (Bear, Connors, and Paradiso 2007). All three are cation channels that result in a depolarisation, but each is selective for which cations it allows through its channel. AMPA and Kainate receptors are permeable to Na^+, K^+ and sometimes Ca^{2+}, whereas NMDA channels are permeable to Na^+, K^+ and Ca^{2+} (Bear, Connors, and Paradiso 2007). An imbalance resulting in an increased activity of these channels could result in runaway excitation or even seizure development. Especially because NMDA receptors are voltage-gated and thus open for longer than AMPA receptors allowing for much more Ca^{2+} influx which in turn can stimulate further neurotransmitter release. In fact glutamate is so potent in its effect that astrocytes assist neurons in buffering it out of the synaptic cleft once it has been released.

1.4.3.2 Acetylcholine receptors

While the neurotransmitter, acetylcholine plays a more complex role in the central nervous system, it is also released at the neuromuscular junction where it is responsible for muscle contraction. It has a broadly depolarising effect on both pyramidal neurons and inhibitory interneurons resulting in a combination of excitatory and inhibitory effects on the network (McQuiston 2014). There are two types of acetylcholine receptors: nicotinic and muscarinic.

Nicotinic receptors are ionotropic (permeable to Na^+, K^+ and Ca^{2+}) mixed cation channels and are responsible for fast synaptic transmission (Bear, Connors, and Paradiso 2007). Conversely, muscarinic channels are metabotropic and responsible for much slower transmission, mediated by second messenger cascades (Bear, Connors, and Paradiso 2007). The nicotinic receptors are therefore the more likely of the two to result in any kind of excitation imbalance, either through direct excitation of pyramidal neurons or reduction in nicotinic activation of interneurons. Additionally if the GABAergic interneurons become transiently excitatory in nature during seizures, through a process known as chloride loading (Raimondo *et al*. 2012), then acetylcholine release and activation of these interneurons could also conceivably contribute to a pro-seizure environment.

1.4.3.3 Acid Sensing Ion Channels

Acid Sensing Ion Channels (ASICs) are a type of cation channel, permeable mainly to Na^+ but also somewhat to Ca^{2+} that have a depolarising effect when activated. They are activated at low pHs (maximally at a pH of 5) due to proton binding. In addition, they have also been known to be bound by other molecules that can activate or inhibit them outside of their usual pH range

(Baron, Waldmann, and Lazdunski 2002; Weng *et al.* 2004; Osmakov *et al.* 2017). There are at least two types of ASICs currently known to be expressed in the hippocampus (Baron, Waldmann, and Lazdunski 2002; Weng *et al.* 2004).

Relevant to this thesis, tissue acidosis is a common feature following seizures as well as ischemia and may activate ASICs (Johnson *et al.* 2001), indicating a potential role in the modulation of network excitability. Therefore any sort of activation of ASICs leads to some excitation and should a seizure occur the resulting tissue acidosis may lead to prolonged ASICs activation which may in turn further propagate the seizure state.

1.4.3.4 Substance P receptors

Substance P is a peptide widely abundant in the peripheral nervous system, where it is responsible for the neurogenic inflammatory response (Douglas and Leeman 2011). Its function in the CNS, however, is associated with sensory transmission, pain, inflammation, stress related responses, depression and anxiety (Douglas and Leeman 2011). Its multiple roles means that it is likely relevant in the modulation of excitability in the context of neuroinflammation (Robinson *et al.* 2012), as will be discussed in section 1.5.

Substance P binds to the Neurokinin-1 receptor (NK1R), which is a G-protein coupled metabotropic receptor that acts as a neuro-immune modulator and can lead to the activation of enzymes and secondary messenger cascades. Furthermore, activation of the NK1R results in Nuclear Factor Kappa-light-chain-enhancer of activated B cells (NF-κB) activation and cytokine production (Douglas and Leeman 2011). NK1Rs are constitutively expressed in inhibitory interneurons in the hippocampus, among other brain regions (Sloviter *et al.* 2001; Chun *et al.* 2019; Martin and Sloviter 2001). Substance P is expressed in the terminals of hippocampal principle neurons, but possibly only during seizure states (Liu *et al.* 2002).

Since Substance P receptors are found on interneurons, it is predicted to have an inhibitory effect, however, the exact mechanisms of Substance P's action remains unclear. For example, Substance P can result in effects further afield by enhancing the function of NMDA channels and increasing intracellular Ca^{2+} in the granule cells of the dentate gyrus, the cells which control activation of the whole hippocampal network (Lieberman and Mody 1998). The large number of Substance P positive fibres relative to the small number of cells expressing Substance P receptors in the hippocampus suggests that Substance P may be exerting some of its effect by non-synaptic diffusion (Czeh *et al.* 2005). This may be how it affects the NMDA receptors of the granule cells, causing them to remain open for longer, and resulting in an overall excitatory effect, in contrast to its prior mentioned inhibitory action (Czeh *et al.* 2005). All things considered it is plausible that the dysregulation of Substance P could result in a pro-seizure environment.

1.5 NEUROINFLAMMATION AND NETWORK EXCITABILITY

Neuroinflammation is a state characterised by the activation of glial cells, including microglia and astrocytes, as well as the release of cytokines. It may originate in the brain or be acquired systemically through a disruption of the blood-brain barrier (BBB).

1.5.1 Glial cells

Microglia are the main immune surveillance cells of the CNS and respond to disruptions in balance, whether resulting from a seizure or foreign particulate entering the CNS (Y. Sun *et al.* 2014). They also function to enhance synapse activity and thus have a critical role in maintaining network synchronization (Akiyoshi *et al.* 2018). Furthermore, activated microglia produce various cytokines that can be strongly seizure promoting (Rana and Musto 2018; Shabab *et al.* 2017). Activation of microglia, following neuroinflammation, results in a phenotypic change, specifically the enlarging of the soma and the retracting of branched processes (Hui *et al.* 2019), as shown in Figure 1.4.

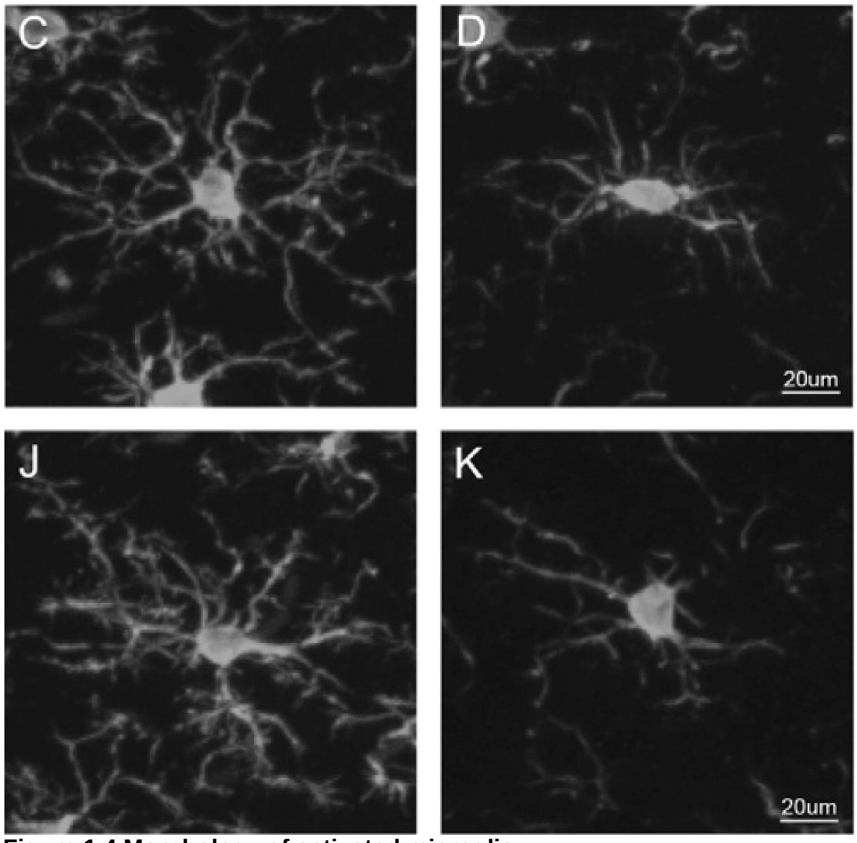

Figure 1.4 Morphology of activated microglia.
Microglia labelled with an anti-Iba1 antibody in sham-operated (left, C & J) and lesioned (right, D & K) rat brains demonstrating some of the phenotypic characteristics of activated microglia; retracted processes and reduced arbourisation. Images taken from Hui *et al.* (2019, figure 6).

Astrocytes are ubiquitous throughout the CNS and serve many functions under normal conditions including; metabolic support for neurons, glutamate and pH buffering, maintenance of the extracellular environment and BBB formation (Sofroniew 2005). Astrocytes become

reactive in response to CNS stress, such as that following trauma, ischemia or infection, where they play a critical but not fully understood role during the neuroinflammatory process (Sofroniew 2015). An activated astrocyte's morphology predominantly involves an increase in size, through the increase of a structural protein, glial fibrillary acidic protein (GFAP), as demonstrated in Figure 1.5. Astrocytes are known to form functional barriers that reduce the spread of immune and inflammatory cells, but can also be neurotoxic and pro-inflammatory by releasing cytokines such as interleukin-1β (IL-1β), interleukin-6 (IL-6) and tumour necrosis factor-α (TNF-α) (Sofroniew 2015; Rana and Musto 2018). Glial cells play an important role during inflammation and their interactions with neurons, effected via cytokines, distinctly govern the transition to seizure states (Diaz Verdugo *et al.* 2019).

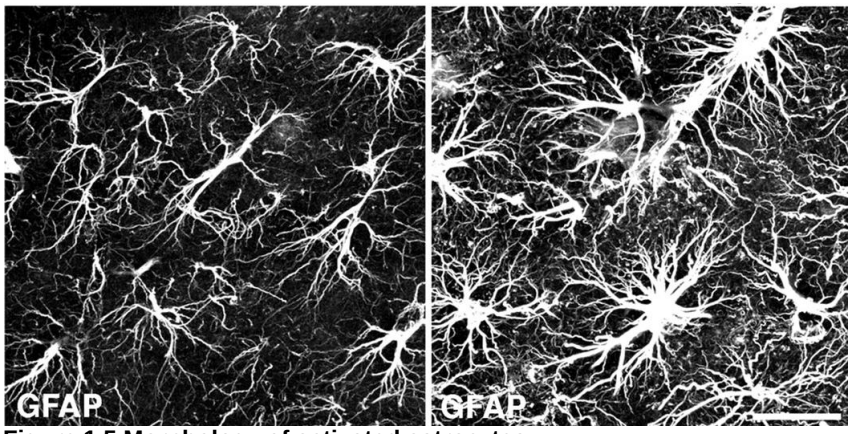

Figure 1.5 Morphology of activated astrocytes.
Astrocytes labelled with an anti-GFAP antibody in lesioned brain tissue (right) and in the non-lesioned contralateral hemisphere (left) demonstrating the morphology changes associated with inflammation and activation. Images taken from Wilhelmsson *et al.* (2006, figure 1). Scale bar 25 µm.

1.5.2 Pro-inflammatory cytokines

Pro-inflammatory cytokine proteins are produced by glial cells and neurons as part of the brain's inflammatory response. Once produced, they go on to stimulate the release of further inflammatory cytokines which can, if not regulated by anti-inflammatory processes, have detrimental effects on CNS function.

IL-1β is a pro-inflammatory cytokine released by classically activated microglia as well as astrocytes and functions to increase neuronal excitability, either by stimulating glutamate release from astrocytes or by increasing calcium influx through neuronal NMDA receptors (Viviani *et al.* 2003; Alyu and Dikmen 2017). IL-1β has also been shown to significantly decrease GABA-signalling in human temporal lobe epilepsy, which further promotes pathological neuronal excitability (Roseti *et al.* 2015). Furthermore, an increase in IL-1β has been found in the brain following seizures (Alyu and Dikmen 2017; Balosso *et al.* 2008) and its inhibition has been shown to reduce seizure propensity (Maroso *et al.* 2011).

TNF-α is another cytokine which plays an important role in neuronal excitation, with differential mechanisms observed in the different glial cell types. When TNF-α is released by activated astrocytes, it reduces neuronal inhibition through the endocytosis of GABA receptors in the dendritic spines of pyramidal neurons (David Stellwagen and Malenka 2006; D. Stellwagen *et al.* 2005). When released by microglia, TNF-α increases excitation by upregulating AMPA receptors (David Stellwagen and Malenka 2006). In addition, TNF-α has been found in the serum of children with febrile seizures at a significantly higher rate than in children that presented with a fever and no accompanying seizures (El Sabbagh *et al.* 2017).

IL-6 is a pro-inflammatory cytokine released by microglia, astrocytes, endothelial cells and neurons and is largely upregulated in response to other cytokines, such as TNF-α and IL-1β (Erta, Quintana, and Hidalgo 2012). It has protective effects, including its essential role in the conversion of innate to adaptive immune responses (Jones 2005). IL-6 also causes gliosis and increased body temperature, which may have neurotoxic effects (Erta, Quintana, and Hidalgo 2012). IL-6 is known to contribute to epileptogenesis through reducing, in particular, effective hippocampal neurotransmission and neurogenesis (Rana and Musto 2018). Furthermore IL-6 production appears to correlate with increased neuronal injury (Ravizza *et al.* 2005).

1.5.3 Blood-brain barrier

BBB permeability is increased by inflammation-induced cytokine release, such as that of IL-1β, TNF-α and IL-6, and allows albumin (not usually found in the brain) to permeate into the parenchymal tissue (Rana and Musto 2018). This has been shown to impair astrocytic buffering of extracellular potassium and glutamate leading to increased neuronal excitability (Van Vliet *et al.* 2007; Seiffert *et al.* 2004).

1.5.4 Link between neuroinflammation and seizures

Inflammation and epilepsy have been shown to be closely linked, with each increasing the likelihood of the other (Vezzani *et al.* 2011). For example, Rasmussen's encephalitis, a disorder in which there is inflammation of the cerebral cortex, is characterised by focal seizures that are often drug-resistant (Varadkar *et al.* 2014). In addition, inflammatory markers, or cytokines, have been found in the excised brain tissue of human epileptic patients (Sheng *et al.* 1994) and experimentally have been found to be elevated after the occurrence of a seizure (Ravizza *et al.* 2005; M. G. De Simoni *et al.* 2000). Experimental seizure models indeed show an upregulation of pro-inflammatory cytokines and inflammation (Balosso *et al.* 2008) and models of inflammation result in, or increase the propensity for, seizures (Cerri *et al.* 2016).

Further evidence shows that inflammation and network excitability are intricately related, which is pertinent to many of the known causes of acquired epilepsies where inflammation

may play a role. This is particularly relevant to NCC because it is still not clear as to whether the mechanism by which NCC leads to seizures involves a substance released by the dying parasite or whether it is the host's inflammatory response to the parasite that leads to seizures, or both.

Live parasites are able to modulate neuroinflammation and can be immunosuppressive (Y. Sun *et al.* 2014). For instance, soluble factors produced by helminths were shown to block the pro-inflammatory effects of lipopolysaccharide (LPS), an endotoxin commonly used experimentally to evoke inflammatory responses (Y. Sun *et al.* 2014). However, even when parasites are able to functionally mask their presence inflammatory markers can often be detected (Nguekam *et al.* 2003; Restrepo *et al.* 2001). Furthermore, the strength of the immune response to helminths seems to correlate with seizure severity (Singhi 2011; Restrepo *et al.* 2001; Herrick *et al.* 2018; Prasad *et al.* 2009). Thus it seems clear that neuroinflammation may play a significant role in the development of seizures in NCC.

1.6 CURRENT MODELS OF NEUROCYSTICERCOSIS

NCC is a complex disease to model because both the tapeworm organism and the host, as well as the interaction between the two, need to be modelled. This adds multiple layers of complexity. In addition, an ideal model would need to capture the fact that humans are accidental intermediate hosts for *T. solium* in the disorder.

1.6.1 Tapeworm species

With regard to the species of tapeworm that can be used to study NCC, there are a large variety that are specialised to infect particular primary and intermediate hosts. The most commonly used species are: *Taenia solium (T. solium)*, which have evolved to infect humans (primary) and pigs (intermediate); *Taenia crassiceps (T. crass.)*, which infects wild canines (primary) and small mammals such as rodents (intermediate); and *Mesocestoides corti (M. corti)*, which has evolved to infect canines and felines (primary) and small mammals, reptiles and birds (intermediate). Working with an organism infective to humans has obvious biosafety concerns, which is why most work on *T. solium* involves observational studies of naturally infected humans or pigs (Lange, Mahanty, and Raimondo 2018). *M.corti* and *T.crass.* have both been used in previous studies to model and study NCC.

M. corti is a popular model for ease of use in the laboratory, as the larval stage can be maintained entirely in culture (Vendelova *et al.* 2016). It is also small enough to allow for relatively easy intracranial inoculation of rodents, which can be a challenge with the other species. There are, however, significant drawbacks to using *M.corti* in models of NCC. For

example, it is not of the same genus as *T. solium* and *T. crass.* which makes it more likely to differ in antigenicity (Matos-Silva *et al.* 2012). Furthermore its natural life cycle never enters the CNS of its host (Lange, Mahanty, and Raimondo 2018) and when injected into the CNS artificially it can proliferate and invade the brain, as opposed to ultimately degenerating and calcifying as is naturally observed in NCC (Matos-Silva *et al.* 2012).

T. crass. is a model organism that is not only similar enough to *T. solium* to be useful, but is also relatively easy to work with in the laboratory. Its antigenic similarity to *T. solium* has been known as far back as the nineties (Sciutto *et al.* 1990) but has recently been further supported by the sequencing of the *T. solium* genome (Tsai *et al.* 2013). *T. crass.* does not usually infect humans (Willms and Zurabian 2010), and interestingly the ORF strain of *T. crass.* has lost the ability to mature into the adult worm stage and therefore does not pose an infection risk to animals. This extensively used ORF strain is also able to asexually divide in the intermediate host by budding off into new larvae, which can be maintained in culture for a few weeks (Willms and Zurabian 2010). This makes it fairly easy to maintain a laboratory colony. The larvae of *T. crass.* are large (roughly the same size as *T. solium*), however, and can be difficult to use with rodent models. Another drawback is that morphological and genetic changes tend to accrue with asexual reproduction as is the case with the ORF strain. A final challenge that occurs when choosing a model species that is different to the one that infects humans (*T. solium*) is the likelihood of species specific immune responses and particular antigens expressed between the parasite and the host. Overall, however, *T. crass.* is the most attractive cestode to use in the laboratory, as it is sufficiently similar to *T. solium* without that organism's biosafety concerns.

1.6.2 *In vivo* models

In order to assess current *in vivo* models of NCC, 57 original research papers found on PubMed were reviewed. Of these, only 11 met the criteria for an *in vivo* model of NCC (see Table 1.1). Only studies that administered the parasitic organism (either *T. solium* or *T. crass.)* in a controlled way, so as to give the cohort a similar base level of infection, were included. This excluded a significant number of studies which used naturally infected pigs, identified by tongue examination. It also excluded all human studies as none provided detail on the number of cysticerci found in each of the patients and therefore it was not possible to determine the original parasite load. Most *in vivo* studies of NCC tend to be observational and exploratory and there is a definitive lack of studies focusing on experimental models of NCC, which is what this thesis aimed to address.

Table 1.1 provides a summary of the 11 *in vivo* studies that met the inclusion criteria. The majority of the studies used parasite material which was injected into the host in the viable

form, which corresponds to when a human host would be asymptomatic. This is with the exception of Robinson *et al.* (2012) and Stringer *et al.* (2003), who intracranially injected rats with homogenised granuloma material, that had been generated in the peritonea of mice. This corresponds to when a host would likely be symptomatic. Focussing on replicating the stage of the disease of interest may be critical as NCC is such a long-term disorder to model, taking years for seizures to develop in the human host.

Further, the time course of each experiment is an important factor to consider and depending on the measured outcomes, this may need to be for a long period in order to capture the full course of the disease. Seizures for example may only manifest during later stages. Interestingly, very few of the models analysed in Table 1.1 investigated seizure occurrence and of the 6 studies that did, a large variation in experimental recording time was found, ranging from hours (Stringer *et al.* 2003; Robinson *et al.* 2012) to months (Saleque *et al.* 1988; Verastegui *et al.* 2015; Agnès Fleury *et al.* 2015) to almost a year (De Aluja *et al.* 1996). In addition, it is important to distinguish the observation of seizures behaviourally from directly measuring electrocorticographic (ECoG) or electroencephalographic activity for evidence of seizures 24 hours a day. Of concern is that the frequency of seizures observed behaviourally may be an underestimate of total seizure burden because, it is typically not possible to observe animals behaviourally 24 hours a day and furthermore seizures may not always generalise, therefore behavioural symptoms may not always be observed during focal seizures. This thesis addresses this issue by developing an *in vivo* model that utilises wireless telemetry to record ECoG continuously over several months, combined with automated seizure detection algorithms to detect seizure activity over this period.

Finally there is the question of modelling NCC *in vivo* in the correct host. In NCC, humans act as both the primary and the accidental intermediate host. There is also a case for using intermediate hosts to model the disorder. For example, Trevisan *et al.* (2016) showed that pigs, which are the intermediate host of *T. solium*, can also develop seizures, suggesting that there might be a similar progression of NCC disease mechanisms in the primary and the intermediate host.

Given the lack of studies that have investigated and modelled NCC *in vivo* this thesis aims to develop an *in vivo* model of NCC (see Aim 3). In addition, this thesis also investigated the effect of *T. crass.* on neurons and network activity *in vitro.*

Table 1.1 A summary of studies meeting my criteria for an *in vivo* model

Experimental Host	Parasite	Parasite material administered	Neurological manifestations / seizures	Length of time studied	Limitations of model	Authors & year of publication	Publication title
Mouse	*T. crass*	Early-stage cysticerci	Unknown	Up to 3 months	Intermediate host No attempt to observe possible seizures, only histopathology	Matos-Silva *et al*, 2012	Experimental encephalitis caused by *Taenia crassiceps* cysticerci in mice
Mouse	*T. crass*	Cysticerci	Unknown	1 month	Intermediate host No attempt to observe possible seizures, only biochemical analysis	Leandro *et al,* 2014	Partial reverse of the TCA cycle is enhanced in *Taenia crassiceps* experimental neurocysticercosis after *in vivo* treatment with anthelminthic drugs
Mouse	*T. crass*	Metacestode fraction (from peritoneal fluid of infected mice)	Unknown	45 days	Intermediate host No attempt to observe possible seizures, only neuro-histopathology Modelling cysticercosis rather than NCC (ip or sc injections)	Zepeda *et al,* 2017	Apoptosis of mouse hippocampal cells induced by *Taenia crassiceps* metacestode factor
Mouse and Rat	*T. crass*	Granuloma homogenate (25µg in 10µl)	**Yes**	6 hours	Intermediate host Granuloma material generated in mouse – concern for cross-species reactivity	Robinson *et al,* 2014	Substance P causes seizures in neurocysticercosis
Rat	*T. crass*	Granuloma homogenate (25µg in 10µl)	**Yes**	1 hour	Intermediate host Granuloma material generated in mouse – concern for cross-species reactivity	Stringer *et al*, 2003	Epileptogenic activity of granulomas associated with murine cysticercosis
Rat	*T. solium*	Activated oncospheres	**Yes**	4 - 6 months	Not natural intermediate host Very low number develop seizures (9%)	Verastegui *et al*, 2015	Novel rat model for neurocysticercosis using *Taenia solium*

Rat	*T. solium*	Postoncospheral form or activated oncospheres	Unknown	4 months	Not natural intermediate host No attempt to observe possible seizures, only immunological analysis	Palma *et al*, 2019	*In vitro* model of postoncosphere development, and *in vivo* infection abilities of *Taenia solium* and *Taenia saginata*
Rat	*T. solium*	Activated oncospheres	Unknown	4 - 5 months	Not natural intermediate host No attempt to observe possible seizures, only neuro-histopathology	Mejia Mazza *et al*, 2019	Axonal swellings and spheroids: a new insight into the pathology of neurocysticercosis
Pig	*T. solium*	Eggs	No	Almost 1 year	Intermediate host No seizures detected (long time period)	De Aluja *et al*, 1996	Experimental *Taenia solium* cysticercosis in pigs: characteristics of the infection and antibody response
Pig	*T. solium*	Eggs + gravid proglottids	Unknown	6 months	Intermediate host No attempt to observe possible seizures, only serology	Nguekam *et al*, 2003	Kinetics of circulating antigens in pigs experimentally infected with *Taenia solium* eggs
Pig	*T. solium*	Activated oncospheres	No	4 months	Intermediate host No seizures or neurological manifestations detected Very low infection efficiency (≤5.4% from a subarachnoid intracranial injection of 1000 activated oncospheres)	Fleury *et al*, 2015	*Taenia solium* : Development of an experimental model of porcine neurocysticercosis
Rhesus monkey	*T. solium*	Eggs	**Yes**	Almost 6 months	Not a natural host (but most similar to humans)	Saleque *et al*, 1988	Induced neurocysticercosis in rhesus monkeys (macaca mulatta) produces clinical signs and lesions similar to natural disease in man

1.6.3 *In vitro* models

In contrast to the few *in vivo* studies in the NCC research field to date, many *in vitro* studies have been performed. Most have focused on immune mechanisms such as changes in the expression of cytokines and chemokines.

In vitro studies of NCC typically rely on blood samples taken from NCC-positive patients and controls. Immune cells, typically lymphocytes, are isolated from the blood and challenged with some form of tapeworm material to see how they respond (Amit *et al.* 2011; Prasad *et al.* 2009). The effects of monocytes that have been stimulated by tapeworm material have been tested on other cell types, including astrocytes, so as to ascertain *Taenia*-induced astrocytic release of chemokines and other immunomodulatory molecules (Uddin *et al.* 2005). In addition, a fair amount of research has been devoted to the analysis of histological preparations of brain tissue from pigs and rodents, as well as humans (Mejia Maza *et al.* 2019; Christensen *et al.* 2016; Matos-Silva *et al.* 2012; Zepeda *et al.* 2017; Robinson *et al.* 2012).

Other common methodologies include using a human or non-human cell line exposed to *T. solium* harvested from the muscle of naturally infected swine (Palma *et al.* 2019; Chile *et al.* 2016) as well as exposing different fractions or components of the parasite material to the cultured cells (Uddin *et al.* 2005, 2010; Amit *et al.* 2011). For example, Amit *et al.* (2011) found that only the cyst fluid antigen elicited a significant immune response.

To the best of my knowledge, no *in vitro* studies to date have investigated the effect of tapeworm material on the functionality of neuronal networks *in situ*. Since previous literature is largely skewed towards analysing the immune response, a further aim of this thesis was to study the electrophysiological properties of neurons in the presence of tapeworm material (see Aim 1 and Aim 2). It is hypothesised that if the acute or relatively sustained presence of *Taenia* larval material were able to alter neuronal membrane properties and ion fluctuations, activate particular neurotransmitter receptors, or modulate network excitability in an intact slice of brain, this would be relevant to the likelihood of seizures developing *in vitro*.

1.6.4 Gaps in the current understanding of NCC

Although a reasonable amount of research has been performed investigating how *Taenia* is able to impact the brain and immune system, there are significant gaps that require further investigation.

NCC has a lengthy disease progression, which is difficult to model. Experimental studies of disease progression or symptom development after the tapeworm larvae have died have been limited as compared to observational studies. In addition, homogenised (dead) *T.crass*. larval material has not been used in any *in vivo* studies to date and has had limited use *in vitro* for

testing the immune response to tapeworm. Therefore in this thesis I almost exclusively utilised homogenised *T.crass*. larvae, to determine what effect the components of freshly killed larvae have on neurons and neuronal networks.

The accurate measurement of seizures in experimental models is another area, which has not been well studied. This is likely due to the difficulty and cost associated with electrophysiological equipment. Of the 6 studies in which the presence or absence of seizures was noted (Table 1.1), only 2 used intracranial electrodes, and in these measurement periods were very short (hours) (Stringer *et al.* 2003; Robinson *et al.* 2012). The 4 other studies simply reported whether seizures were detected, presumably by observation, and few defined phenotypic behaviours for classifying seizures (Verastegui *et al.* 2015; De Aluja *et al.* 1996; Agnès Fleury *et al.* 2015; Saleque *et al.* 1988). Since seizures are the most common symptom of NCC it is of great import to be able to correctly identify and document them.

Finally, while some studies have fractionated *Taenia* homogenate and identified the properties of certain fractions (Uddin *et al.* 2005, 2010; Amit *et al.* 2011), the exact excitatory molecule/s have yet to be elucidated. Identifying the excitatory component, and which neurotransmitter system it is activating, would go some way towards answering how *Taenia* parasites are able to cause seizures in the brain.

In light of the gaps in the literature described above, my research sought to further investigate and characterise neuronal responses in models of NCC by pursuing the following aims and objectives.

1.7 AIMS

Aim 1: Investigate the short-term effect of *Taenia crassiceps* homogenate on neurons *in vitro.*

Aim 2: Investigate the long-term effect of *Taenia crassiceps* homogenate on neurons *in vitro.*

Aim 3: Investigate the chronic effect of *Taenia crassiceps* homogenate *in vivo.*

1.8 OBJECTIVES

1.8.1 Aim 1 Investigate the short term effect of *Taenia crassiceps* homogenate on neurons *in vitro* (chapter 3)

1.1 Establish a colony of tapeworm.

1.2 Determine the acute effect that *T. crassiceps* has on neurons.

1.3 Determine whether the depolarizing effect of *T. crassiceps* is **ionically mediated.**

1.4 Ascertain which **neuronal receptors** mediate the depolarizing effect of *T. crassiceps.*

1.8.2 Aim 2 Investigate the long-term effect of *Taenia crassiceps* homogenate on neurons *in vitro (chapter 4)*

2.1 Investigate the effect of *T. crassiceps* on neuronal **membrane properties.**

2.2 Determine the effect of *T. crassiceps* on the active **firing properties** of neurons.

2.3 Quantify the effect of *T. crassiceps* on **sodium and potassium currents** in neurons.

2.4 Explore the effect of *T. crassiceps* on the **seizure threshold** of neuronal networks *in vitro.*

1.8.3 Aim 3 Investigate the chronic effect of *Taenia crassiceps* homogenate *in vivo (chapter 5)*

3.1 Establish the technology for chronic ECoG recordings in freely moving rats.

3.2 Characterise recorded ECoG activity patterns including induced seizure activity.

3.3 Determine whether *T. crassiceps* results in **seizures/seizure-like activity** *in vivo.*

3.4 Evaluate the effect of *T. crassiceps* on the **seizure threshold** of neuronal networks *in vivo.*

3.5 Determine the effect of *T. crassiceps* on **glial cells** involved in neuroinflammation.

Chapter 2

MATERIALS AND METHODS

Most of the methods detailed below were set up for the first time in Africa and as such required significant optimisation. All reagents used were supplied by Thermo Fischer Scientific, unless otherwise stated.

All animal handling, care and procedures were carried out in accordance with South African national guidelines (*South African National Standard: The Care and Use of Animals for Scientific Purposes* 2008) and with approval from the University of Cape Town Animal Ethics Committee (Protocol No: AEC 015/015, AEC 014/035, AEC 016/005). All animal rooms were maintained between 22 - 24 °C, with a lux of 100 - 300 and food and water available *ad libitum*.

2.1 *TAENIA* MAINTENANCE AND PREPARATION OF WHOLE CYST HOMOGENATE

2.1.1 Intraperitoneal infection

Larvae of *T. crass.* (ORF strain) were donated to us by Dr Siddhartha Mahanty (NIH, Maryland, USA) and propagated *in vivo* by serial intraperitoneal infection of 5 - 8 week old female C57BL/6 mice. Females were used simply because they could be easily group housed without fighting. The small, translucent, motile larvae were selected in phosphate buffered saline (PBS, pH 7.4; Sigma-Aldrich) and injected into 8 mice (20 larvae per mouse) in order to maintain the colony. Every 3 months parasites were harvested by peritoneal lavage, as similarly described by Mahanty, Madrid, and Nash (2013), and washed 6 times in PBS before further processing. This procedure was carried out in an experimental room to which the animals were habituated before the harvesting or injection procedures. The weight of the mice was tracked weekly during the 3 months of infection.

2.1.2 Preparation of homogenate

For the preparation of *T. crass.* whole cyst homogenate, larvae were stored immediately after harvesting at -80 °C. Later these were thawed (thereby lysing the cells) and suspended in PBS (1X) containing a protease cocktail inhibitor (1 % vol / vol, Sigma-Aldrich) at a larval:PBS ratio of 1:3. The larvae were then homogenised on ice using an homogenizer (Polytron, PT 2500E, Kinematica). The resulting mixture was centrifuged (Eppendorf, 5810 R) at 4000 rpm for 20 minutes at 4 °C. The liquid supernatant (between the white floating layer and solid pellet) was collected and filter sterilized through a 0.22 µm size filter (Millex-GV syringe filter, Merck).

This supernatant was then aliquoted and stored at -80 °C until use. To assess whether large or small molecules were responsible for the excitation of neurons, a portion of the whole cyst homogenate was dialysed using a Slide-A-Lyzer™ dialysis cassette (3 kDa MWCO, Separations) in 2l of standard artificial cerebro-spinal fluid (aCSF) at 4° C (see below for composition). The aCSF solution was changed twice over 24 hours. To determine the ionic composition of *T. crass.* whole cyst homogenate a Cobas 6000 analyser (Roche) was used, with ion specific electrodes for K^+ and Na^+. A Mettler Toledo SevenCompact™ pH meter (S210, Merck) was used to determine the pH of the homogenate.

For the preparation of *T. solium* whole cyst homogenate*,* larvae of *T. solium* were harvested from the muscles of a heavily infected, freshly slaughtered pig (performed by Ulrich Fabien Prodjinotho). After extensive washing with sterile PBS (1X), *T. solium* larvae were suspended in PBS containing phenylmethyl-sulphonyl fluoride (5 mM) and leupeptin (2.5 µM) at a larval:PBS ratio of 1:3. Larvae were then homogenised using a sterile hand held homogenizer (T10 Basic Ultra-Turrax, IKA-Werke) at 4 °C. The resulting homogenate was sonicated (Sonopuls HD 2070.2, Bandelin Electronic) (4 x 60 s at 20 kHz, 1 mA, with 30 s intervals) and gently stirred with a magnetic stirrer (Corning PC-420D, Corning) for 2 hours at 4 °C. Thereafter it was centrifuged (Sigma 3-16KL Refrigerated centrifuge, SciQuip Ltd) at 15,000 g for 60 min at 4 °C and the liquid supernatant (between the white floating layer and solid pellet) was collected. The supernatant was filtered through 0.45 µm size filters (Millex GV syringe filter, Merck), aliquoted and stored at -80 °C. All *T. crass.* and *T. solium* larval products were assessed for protein concentration using a BCA protein or Bradford's assay kit, respectively (Merck).

Anja De Lange performed the assessment of daily glutamate production in which both *T. crass. and T. solium* larvae were placed into 12-well plates (±15 per well, of roughly 5 mm length) with 2 ml of culture medium (*Taenia solium* medium: RPMI 1640 (Sigma-Aldrich) with 10 mM HEPES buffer (Sigma-Aldrich), 100 U/ml penicillin (Sigma-Aldrich), 100 µg/ml streptomycin (Sigma-Aldrich), 0.25 µg/ml amphotericin B (Sigma-Aldrich) and 2 mM L-glutamine (Whitehead Scientific); *Taenia crassiceps* medium: Earles Balanced Salt Solution (EBSS, Sigma-Aldrich) with 100 U/ml penicillin, 100 µg/ml streptomycin, 11.4 U/ml nystatin (Sigma-Aldrich), and 2 mM glutamax). Every 24 hours 1ml of culture media was collected from each well, stored at -80 °C, and replaced with fresh culture medium. The concentration of glutamate was measured using a glutamate assay kit according to the supplier's instructions (Sigma-Aldrich).

2.2 HIPPOCAMPAL BRAIN SLICE PREPARATION

Organotypic brain slices were prepared using 6 - 8 day old male Wistar rats and C57BL/6 mice following the protocol originally described by Stoppini *et al.*, (1991). Males were used to exclude any possible variable effect of the oestrus cycle on results. Rats and mice were transported to the tissue culture laboratory in the afternoon and allowed to habituate before the procedure. Brains were extracted and swiftly placed in cold (4 °C) dissection media consisting of EBSS supplemented with 6.1 g/l of HEPES, 6.6 g/l of D-glucose and 200 µl of saturated sodium hydroxide (all from Sigma-Aldrich). The hemispheres were separated and individual hippocampi were removed and immediately cut into 350 µm slices using a McIlwain tissue chopper (Brinkmann, Mickle). Cold dissection media was used to rinse the slices before placing them onto Millicell-CM membranes (Sigma-Aldrich). Slices were maintained in culture medium consisting of (vol / vol); 23 % EBSS, 50 % MEM with glutamax, 25 % heat-inactivated horse serum (Biochrom), 2 % B27 and 6.5 g/l glucose (all from Sigma-Aldrich unless otherwise stated). For some experiments *T. crass.* (50 µg/ml) or LPS (10 µg/ml) was added to the media for 24 hours. Slices were incubated in a 5 % carbon dioxide (CO_2) humidified incubator at between 35 – 37 °C. Recordings were made after 6 - 14 days in culture, as this is the ideal time for the slice to have recovered from the slicing procedure (the tissue debris have cleared) but it is not so old that recurrent connections are common, which may result in the slice being more excitable (A. De Simoni and Yu 2006). I elected to use slices from the hippocampus for the *in vitro* experiments because of the reliability of the hippocampal organotypic brain slice culture preparation and because the hippocampus is often involved in the development of seizures (A. De Simoni and Yu 2006).

2.3 ELECTROPHYSIOLOGY

2.3.1 *In vitro* patch-clamp recordings

Brain slices were transferred to a submerged recording chamber on a patch-clamp rig, which was maintained at a temperature between 28 and 30 °C, and were continuously superfused with standard aCSF bubbled with carbogen gas (95 % O_2: 5 % CO_2) using peristaltic pumps (102R, Watson-Marlow Fluid Technology Group). The standard aCSF was composed of: NaCl (120 mM); KCl (3 mM); $MgCl_2$ (2 mM); $CaCl_2$ (2 mM); NaH_2PO_4 (1.2 mM); $NaHCO_3$ (23 mM) and D-Glucose (11 mM) in deionised water with pH adjusted to between 7.35 - 7.40 using 0.1 mM NaOH (Sigma-Aldrich). Neurons in the CA3 region of the hippocampus were visualized using a Zeiss Axioskop or Olympus BX51WI upright microscope using 20x or 40x water-immersion objectives and targeted for recording. Micropipettes were prepared (tip

resistance between 3 and 7 MΩ) from borosilicate glass capillaries (outer diameter 1.2 mm, inner diameter 0.69 mm, Harvard Apparatus Ltd) using a horizontal puller (Sutter). Recordings were made in current clamp mode using Axopatch 200B amplifiers (Axon Instruments) and data acquired using WinWCP (University of Strathclyde) or Igor (Markram Laboratory, Ecole polytechnique fédérale de Lausanne). Traces were analysed using custom scripts in Matlab (R2015b, MathWorks). Two internal solutions were used: a "standard" internal solution (K-gluconate (126 mM), KCl (4 mM), HEPES (10 mM) Na_2ATP (4 mM), NaGTP (0.3 mM) and Na_2-phosphocreatine (10 mM); Sigma-Aldrich) and a "caesium" internal solution (CsOH (120 mM), Gluconic acid (120 mM), HEPES (40 mM), Na_2ATP (2 mM), NaGTP (0.3 mM) and NaCl (10 mM); Sigma-Aldrich).

In addition to the patch pipette, for puffing experiments a secondary "puffer" pipette was pulled with the same tip resistance as the patch pipette. Experimental substances were then puffed onto neurons using an OpenSpritzer, a custom made pressure ejection system (Forman *et al.* 2017). For these experiments current was injected if required to ensure a neuronal resting membrane potential within 2 mV of -60 mV. In all puffing experiments each data point represents the mean peak puff-induced change in membrane potential from 10 sweeps. In some experiments tetrodotoxin (TTX, 2 µM) was added to the aCSF to block voltage-gated sodium channels.

To test intrinsic properties of slices treated for 24 hrs with *T. crass.* homogenate or LPS (see Chapter 4), whole-cell current clamp and voltage clamp recordings were made using the standard internal solution and aCSF.

Pharmacological manipulations were performed by bath application of drugs using a perfusion system. Mecamylamine hydrochloride (10 µM, #2843, WhiteSci), Amiloride hydrochloride hydrate (2 mM, #A7410, Sigma-Aldrich), D-AP5 (50 µM, #010610, WhiteSci) and CNQX disodium (10 µM, #1045, WhiteSci) were purchased from Tocris. Kynurenic acid was acquired from Sigma-Aldrich. As Substance P has no known blocker it was applied directly onto the recording cell using the OpenSpritzer (100 µM, #S-6883, Sigma-Aldrich).

2.3.2 Calcium imaging

For calcium imaging, organotypic hippocampal mouse brain slices were virally transfected with a genetically-encoded Ca^{2+} reporter (GCAMP6s under the synapsin promoter, AAV1.Syn.GCaMP6s.WPRE.SV40) one day post culture using the OpenSpritzer and imaged 5 days later using an Olympus BX51WI microscope, 20x water-immersion objective, CCD camera (CCE-B013-U, Mightex) and 470 nm LED (Thorlabs). Images were collected using µManager (Edelstein *et al.* 2010) and analysed using Caltracer3 beta scripts in Matlab.

2.3.3 *In vivo* wireless telemetry

Stereotaxic surgery was performed on 14 male Wistar rats (4 of which were a pilot study) weighing between 400 and 450 g, as described by (Snowball *et al.* 2019). Anaesthetised rats (isoflurane in oxygen; Induction: 5 % at 2 l/min, maintenance 2.5 - 1.5 % at 1.5 l/min, Safeline) were placed in the stereotaxic frame (Kopf) and burr holes were drilled at the following locations relative to bregma; X: +3 mm, Y: -7 mm for the recording electrode, X: -2.60 mm, Y: -4.44 mm for the reference electrode and X: +2 mm, Y: -0.8 mm for the fixing screw. Thereafter an Open Source Instruments (OSI) A3028E ECoG transmitter was implanted subcutaneously over the dorsum with the attached wires extending subcutaneously up to the cranium where the recording and reference electrodes were positioned through each burr hole approximately 0.5 mm into the brain parenchyma. Each electrode was secured in place with either a screw or a cannula (Plastics One), to allow for the intracranial injections beginning after 2 weeks of baseline recording. The screws and cannulae were fixed in place with dental cement (Ivodent) forming a small, circular headpiece and the dorsum was closed with nylon suture material (Ethicon). Post-operative medication and pain management included a second Buprenorphine dose (8 hours following the pre-surgery dose), Meloxicam (Boehringer Ingelheim, 1mg/kg) administered subcutaneously for 3 days, EMLA cream (AstraZeneca) for the dorsum incision, 2ml saline (VetServ) subcutaneously and eye gel (Aspen, also used throughout the surgery). The room where the surgical procedures were performed was separated from the room in which the rats' were housed by a connecting room in which the preparation for the surgery took place (injections, weighing etc.). Rats were habituated to the procedure room and were transferred to the surgery room once anaesthetised. After the surgery, whilst recovering from anaesthesia they were kept under a warming light in the procedure room until they could be returned to their home cage.

Rats were individually housed (2 cages side-by-side) in custom built Faraday cages to facilitate recording. Welfare monitoring was conducted twice per day for 7 days, thereafter once daily. Rats were weighed daily for 4 days, thereafter weekly. One rat was euthanased 8 weeks into the experiment as he had damaged his headpiece irreparably.

2.3.3.1 Injections

After two weeks of baseline ECoG recording, animals were injected via the guide cannula with either *T. crass.* homogenate or saline (with 15 endotoxin units, equivalent to the *T. crass.* sample). Rats were anaesthetised and injected in the same procedure and surgery rooms as used previously. Injections were made into the right hemisphere V1 cortex (X +3 mm and Y -7 mm relative to bregma, Z -1 mm from the pia) for all 10 rats and for half of the rats an additional 2 injection sites (dorsal hippocampus and V2 cortex) in the left hemisphere (X -2.6 mm and Y -4.44 mm relative to bregma, Z -3.2 mm and Z -1 mm from the pia) as shown in Table 2.1.

In practicality the z co-ordinates had an additional 8 mm (the length of cannula above the skull) as they were counted from when the needle first entered the cannula. Once the needle was lowered to each injection site it was left in place for 2 minutes. Thereafter 3 injections of 200 nl each were made, at approximately 100nL/min, with a 1 minute wait in between, a 5 minute wait at the end and an additional 5 minute wait once the needle had been raised to the position of the bottom of the cannula. As each injection site was to receive 3x 200 nl, the injections were made at 3 micro-locations around the site. For example, for the V1 site (Z-1 mm) the injections were made at 1.1, 1.0 and 0.8 mm down into the brain. This was to ensure an even delivery and better diffusion of the *T. crass.* or saline from the needle tip. Each rat had 3 intracranial injection sessions, for which the animal was anesthetised, every 2 weeks (Figure 2.1). For the third intracranial injections, the injection volume was doubled. During the first intracranial injection all rats (*T. crass.* injected and saline injected) also received an intradermal injection of 100 µl of *T. crass.* homogenate in Freund's incomplete adjuvant (1:1) into each hind limb. The Freund's incomplete adjuvant allows the antigen of interest (in this case *T. crass.* homogenate) to be gradually released in order to facilitate a peripheral immune response.

24 hours prior to sacrifice a seizure threshold test was performed in which each rat was lightly anesthetised and was injected with 400 nl of 10 µM picrotoxin, a known pro-convulsant, into the visual cortex of the right hemisphere. They were monitored closely both visually and via their ECoG for several hours. The picrotoxin dose was intentionally low in order to determine if our experimental interventions may have made the animals more vulnerable to picrotoxin induced seizures. Of the 10 rats in the experiment, one was lost prior to the endpoint and was not included in the seizure threshold test.

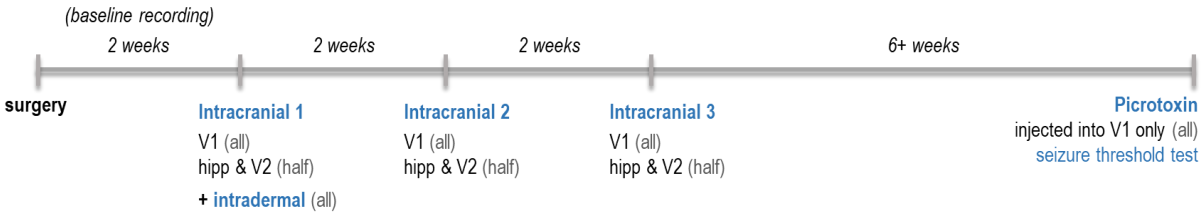

Figure 2.1 Experimental timeline of the investigation into the chronic effects of *T. crass.*
Injection areas are the V1 cortex ('V1'), the hippocampus ('hipp') and the V2 cortex ('V2').

Table 2.1 Treatment conditions of rats in the *in vivo* experiment.

Rat	Treatment	Injection into V1 cortex of right hemisphere (x3)	Injection into hippocampus and V2 cortex of left hemisphere (x3)	Extra notes
1	saline	yes	no	
2	saline	yes	no	
3	*T. crass.*	yes	no	
4	*T. crass.*	yes	no	
5	*T. crass.*	yes	no	
6	*T. crass.*	**yes**	**yes**	
7	*T. crass.*	**yes**	**yes**	Excluded from immunohistochemical analysis
8	saline	**yes**	**yes**	
9	saline	**yes**	**yes**	Excluded from seizure threshold test
10	*T. crass.*	**yes**	**yes**	

2.3.3.2 ECoG acquisition and analysis

The rats were housed in Faraday cages with aerials to collect the ECoG signals. Signals from the subcutaneous transmitters (A3028E, OSI), were continuously recorded from the freely moving rats using Neuroarchiver software (OSI) for up to 12 weeks (0.3–160 Hz, 512 samples / s). The raw ECoG was observed and analysed during playback of the archived files alongside the 'Event Classifier' application in Neuroarchiver. For automated seizure / ictal-like event detection, video-ECoG matching was used to identify ECoG events of interest associated with an observed behaviour / seizure in order to create an 'Event library'. The Event Classifier application (OSI) was used to do this by classifying 1 s segments of ECoG according to several metrics (coastline, intermittency, coherence and spikiness) enabling similar events (*e.g.* chewing artefact, ictal events) to cluster together when plotted according to the metrics. My event library was made with at least 50 examples of each type of event (ictal, chewing artefact, baseline, scratching headpiece) from at least 8 animals. Definitive ictal activity recorded following picrotoxin injection was used to define the ictal event type. This then allowed for unbiased identification and quantification of ECoG events recorded over the 12 week period by automated comparison to the event library (see http://www.opensourceinstruments.com/Electronics/A3018/Seizure_Detection.html for further details). I compared the number of ictal-like events between *T. crass.* treated rats and controls. A seizure was defined as at least 5 consecutive ictal-like events (*i.e.* lasting more than 5 s). Each seizure was visually confirmed. Data was quantified using Microsoft excel v14 and Graphpad Prism 5.

2.4 IMMUNOHISTOCHEMISTRY

2.4.1 Perfusion

After 12 weeks rats were anesthetized (Halothane, Safeline) and transcardially perfused with PBS followed by paraformaldehyde (4 %) (Sigma-Aldrich). Briefly, the thorax was opened and the heart exposed so that a blunted 18-gauge needle (through which PBS and then fixative would be pumped) could be inserted into the left ventricle, just lateral to the, being careful not to pierce the septum. The right atrium of the heart was punctured, allowing blood to spill out of the heart and drain away. The perfusion was judged to be adequate based upon the presence of fasciculation in the body and the brain being very white in colour. All perfusions were carried out in the morning in a laboratory to which the rats were habituated before the procedure began. Brains were post-fixed for 24 hours and then transferred to 30 % sucrose (in dH_2O), all at 4 °C. Once the brains were fully cryoprotected, judged by an increased density *i.e.* sinking to the bottom of the sucrose solution, they were frozen in Optimal Cutting Temperature reagent (Jung) and stored at -80°C until slicing.

2.4.2 Slicing

The right hemisphere of each brain was marked in an area of non-interest with a needle. Brains were sectioned at -20 °C on a Leica CM 1850 cryostat microtome into 50 µm coronal sections. Each brain was sectioned in a posterior to anterior direction using landmarks identified with the Paxinos and Watson (2007) rat brain atlas and slices were collected free-floating into PBS at 4 °C. The two slices which best showed the electrode tract were chosen to be stained for each rat, along with 2 more slices from each rat to serve as controls against endogenous tissue fluorescence and non-specific antibody binding.

2.4.3 Staining

Slices were first permeabilized in PBS containing 3 % triton X-100 (Sigma-Aldrich) for 3x 10 minutes before blocking for 1 hour (PBS with 1 % triton x-100 and 2 % bovine serum albumin). Slices were incubated overnight at room temperature in PBS with 3 % Triton X-100 and primary antibodies: mouse anti-GFAP (diluted 1:1000; #G3893, Sigma-Aldrich) and goat anti-Iba1 (diluted 1:500; #ab107159, Abcam). After 3x 10 minutes washes in PBS-triton slices were incubated at room temperature for 5 hours with PBS-triton and secondary antibodies: donkey anti-mouse Alexa 488 (diluted 1:500; #715-546-150, Jackson ImmunoResearch) and donkey anti-goat Cy3 (diluted 1:1000; #705-166-147, Jackson ImmunoResearch). After a further 3x 10 minutes of washing slices were incubated with PBS containing Hoechst nuclear stain (1:1000; #H1399, Thermo Fischer Scientific) for 15 minutes in the dark and then washed

for a final 10 minutes in PBS. Slices were mounted using Mowiol mounting medium with anti-fade (Sigma-Aldrich) and cover-slipped (B&M Scientific). All slices from all 9 rats were stained in the same session.

Table 2.2 Antibodies used in immunohistochemistry experiment.

Antibody	Dilution in blocking solution	Fluorescent channel	Manufacturer
Primary Antibodies:			
Iba1 (goat polyclonal)	1:500	Red (changed to magenta during analysis for better visibility)	Abcam
GFAP (mouse monoclonal)	1:1000*	Green	Sigma-Aldrich
Secondary Antibodies:			
Donkey anti-goat Cy3	1:1000*	Red (changed to magenta during analysis for better visibility)	Jackson ImmunoResearch
Goat anti-mouse ALEXA 488	1:500*	Green	Jackson ImmunoResearch
Other: Hoechst nuclear marker	1:1000*	Blue	Thermo Fischer Scientific
*antibodies in 50% glycerol, halve the dilution if using pure antibody.			

2.4.4 Imaging

Imaging was initially performed using a LSM510 Meta NLO model confocal microscope (Carl Zeiss, Zen 2009 software) and a AxioCam MRm camera with a 20x objective (Zeiss) in order to acquire a detailed tile, z-stack image of the area just below the electrode tract and corresponding area (with the exact same settings) in the adjacent hemisphere. Some qualitative images were obtained using a 40x water immersion objective.

A LSM 880 airyscan confocal microscope (Carl Zeiss, ZEN SP 2 software) with 20x and 63x objectives (Zeiss) was used to acquire images for the microglial activation investigation. To quantify microglial cell numbers, the 20x objective was used to acquire tiled z-stacks of the area immediately surrounding the electrode tract in the right hemisphere. In order to be able to quantify microglial morphology, high resolution images were obtained of individual microglia (Iba1) using the 63x objective.

The non-specific binding control and the endogenous fluorescence controls showed no staining. A total of 8 rats were included in the immunohistological analysis, as one rat was lost prior to the endpoint and for another slice sectioning was incorrectly performed.

2.4.5 Quantification

All image processing and quantification was performed using Zen Black 2.3 (Carl Zeiss) and Image J 1.52a (NIH). To assess the extent of GFAP (astrocytes) and Iba1 (microglia) labelling surrounding the right hemisphere electrode tract, collapsed z-stack tile images were used to measure average fluorescence and the average number of pixels above a threshold. To quantify the number of pixels above a threshold, a mask tool which removes low level background fluorescence in Zen, as shown in Figure 2.2, was used. These measurements provide a general indication of the number of each cell type or the size of the cells. Right hemisphere measurements were normalised using images from the corresponding left hemisphere (where no electrode had been present) in order to correct for absolute differences in fluorescence arising during the staining protocol. Two slices (including left and right hemispheres) were analysed for each rat.

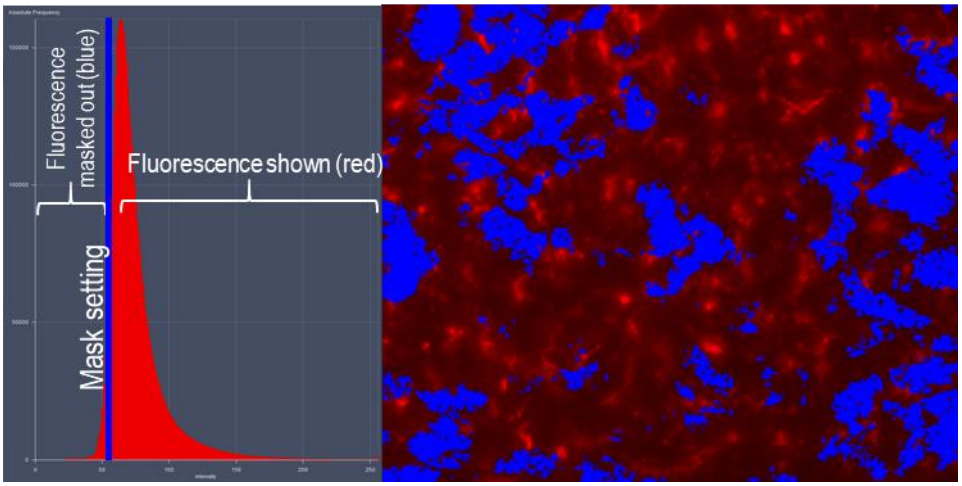

Figure 2.2 Mask tool in Zen to remove low-level background fluorescence and set a threshold.

Further higher resolution camera images of microglial cell bodies, labelled for Iba1, were captured and qualitatively assessed, to compare between *T. crass.* treated and control slices. Features such as the length of the microglial processes and size of cell body were broadly compared and informed the need for further, more extensive and quantifiable analysis of the microglia.

Measurements of microglial density, clustering and spacing were performed on collapsed z-stack images taken using a confocal microscope, tile images taken of the area surrounding the recording electrode, in a manner blind to the condition of the animal, as previously described by Hui *et al.* (2019). One image was analysed for each rat. Each Iba1-labelled microglial cell body was marked in its centre with dot in Image J and the number of cells automatically generated using the 'analyze particles' function. The 'nearest neighbour' distance plugin was used to determine the shortest distance to any other cell, for every cell.

Cellular density was calculated by dividing the total number of cells by the surface area of the image (measured in mm^2). The spacing index is reported as the (average nearest neighbour distance)^2 multiplied by the density.

To assess microglia morphology 20 high resolution confocal images, taken with the 63x oil immersion objective of the area surrounding the electrode tract on both sides, were analysed per rat. For accuracy, these collapsed z-stack images were only of cells in which the entire Iba1-labelled cell body and proximal processes were clearly visible. For each cell, the area of the soma was determined using the freehand selection tool in Image J to trace around its borders. The polygon tool was used to determine the arbourisation area by joining the tips of distal processes. Inputting the length of the scale bar into the 'set scale' feature in Image J meant the number of pixels could be converted to actual distances. The arbourisation circularity index was calculated, from the same drawn polygon, to give an indication of how evenly the distal processes extended from the cell body. The morphological index is reported as the soma area divided by the arbourisation area. This measurement was of particular interest to assess the 'activation state' of the cells as microglia in an inflammatory environment, for example, are known to shorten their processes and show enlarged cell bodies, which would give them a larger morphological index.

2.5 DATA ANALYSIS AND STATISTICS

Data was graphed and analysed using Matlab R2015b, Microsoft excel v14 and GraphPad Prism v5. Adobe Illustrator vCS6 was used to create all figures.

All data was subjected to a Shapiro-Wilk test for normality and found to be parametric or non-parametric.

2.5.1 Parametric statistical analysis

The student's t-test (either paired or unpaired) was used when comparing the means of two groups. When comparing multiple groups a one-way analysis of variance (ANOVA) or repeated measures ANOVA was used as appropriate. If significant ($p < 0.05$), this was followed with a Tukey's post hoc test. Data presented as mean and standard error of the mean (SEM).

2.5.2 Non-parametric statistical analysis

Non-parametric data comparing two groups underwent a Mann Whitney U test if unpaired and a Wilcoxin signed ranked pairs test if paired. For multiple comparisons of independent data a

Kruskal-Wallis ANOVA was done. For multiple comparisons of paired data a Friedman test was performed. If significant ($p < 0.05$), in either case, this was followed with a Dunn's Multiple Comparison test. Data presented as median and interquartile range (IQR).

Chapter 3

THE ACUTE EFFECTS OF *TAENIA CRASSICEPS* ON NEURONS *IN VITRO*

3.1 INTRODUCTION

In endemic areas, approximately 29 % of people with epilepsy have NCC (Ndimubanzi *et al.* 2010). Despite the impact of NCC, compared to other causes of epilepsy, there are a paucity of studies investigating the seizure mechanisms involved (Lange, Mahanty, and Raimondo 2018). As a result, precisely how cestode larvae cause recurrent seizures is still relatively poorly understood.

In NCC seizures may occur at any stage following initial infection (Garcia and Del 2017). It is thought that inflammatory processes in the brain can play an important role in the development of recurrent seizures (Vezzani *et al.* 2016). Therefore, previous work exploring seizure development in NCC has typically focused on how the host neuroinflammatory response to larvae might precipitate seizures (Nash *et al.* 2015; Lange, Mahanty, and Raimondo 2018). For example, Robinson *et al.* (2012) have shown that production of the inflammatory molecule and neurotransmitter, Substance P, in peritoneal cestode granulomas can precipitate acute seizures. In addition to substances (such as Substance P) produced by the host response, cestodes themselves are known to excrete or secrete various products. For example cestode larvae derived factors are known to modulate the activation status of immunocytes such as microglia and dendritic cells (Y. Sun *et al.* 2014; Emilia Vendelova *et al.* 2016). However, comparatively little is known about how factors contained in, or secreted by, cestode larvae might affect neurons and neuronal networks directly, including whether these may have pro-seizure effects.

To address this, whole-cell patch-clamp recordings and calcium imaging in rodent hippocampal organotypic slice cultures was used to explore the direct effects of cestode larval products on neuronal activity. I found that the whole homogenate products of *Taenia crassiceps* larvae have a strong, acute, excitatory effect on neurons. This was sufficient to trigger seizure-like events *in vitro*. *T. crass.* larval dependent neuronal depolarization was mediated by glutamate receptor activation and not nicotinic acetylcholine receptors, acid-sensing ion channels nor Substance P. Direct measurement of glutamate concentration

revealed that the homogenate of both *T. crass.* and *T. solium* larvae contain high levels of glutamate. Finally, we found that larvae of both species produce and release this excitatory neurotransmitter into their immediate environment. My findings are relevant for the understanding of seizure generation in neurocysticercosis.

3.2 *TAENIA CRASSICEPS* HOMOGENATE EXCITES NEURONS AND CAN ELICIT EPILEPTIFORM ACTIVITY.

To investigate the potential acute effects of *T. crass.* larvae on neurons, *T. crass.* larval homogenate was prepared using larvae harvested from the peritonea of mice which were freeze-thawed and homogenized (Figure 3.1 A). Whole-cell patch-clamp recordings were made from CA3 pyramidal neurons in rodent hippocampal organotypic brain slice cultures and pico-litre volumes of *T. crass.* homogenate were directly applied to the soma of neurons using a custom built pressure ejection system (Figure 3.1 A) (Forman *et al.* 2017). Application of the homogenate (20 ms puff) elicited immediate, transient depolarization of the membrane voltage in recordings from both rat and mouse neurons (Figure 3.1 B). Increasing the amount of homogenate delivered by increasing the pressure applied to the ejection system resulted in increasingly large membrane depolarization, which could trigger single or multiple action potentials (Figure 3.1 B - C). Similar puffs of artificial cerebrospinal fluid (aCSF) did not affect the neuronal membrane potential excluding the possibility that mechanical effects might account for the homogenate-induced depolarization I observed.

To further explore the acute excitatory effect of *T. crassiceps* on neurons, neuronal networks and the propagation of network activity, Dr Raimondo and I performed fluorescence Ca^{2+} imaging in mouse hippocampal organotypic brain slice cultures. Neurons were virally transfected with the genetically-encoded Ca^{2+} reporter, GCAMP6s, under the synapsin promoter and imaged using widefield epifluorescence microscopy (Figure 3.1 D). To simulate a pro-ictal environment, a low Mg^{2+} aCSF was used (0.5 mM Mg^{2+}) and neurons in the dentate gyrus were imaged whilst small, spatially restricted puffs of *T.crass*. homogenate were delivered every 15 ms using a glass pipette (Figure 3.1 D). The cells within the direct vicinity of the puffing pipetted showed a sharp increase in fluorescence immediately following the delivery of *T. crass.* homogenate (Figure 3.1 E t_1) for all 3 puffs, indicating Ca^{2+} entry following membrane depolarization and action potential generation. Interestingly, cells in the periphery showed notable increases in fluorescence at a delayed interval following some (but not all) puffs (Figure 3.1 E t_2). The excitation of these cells could only be as a result of being synaptically connected to the cells that were exposed to the puff itself, as they were not

positioned close enough to the puffer pipette to be directly excited by the homogenate. Indeed a current-clamp recording from a neuron in the same slice (Figure 3.1 E inset) indicates that a single, spatially restricted puff of *T. crass.* homogenate is able to elicit the onset of a regenerative seizure-like event lasting far longer than the puff itself. Together this indicates that *T. crass.* homogenate results not just in a transient depolarization of cells in the immediate vicinity of application, but can trigger a wave of excitation that propagates through the brain slice in both space and time. This demonstrates that *T. crass.* homogenate can initiate seizure-like activity under suitable conditions.

3.3 POTASSIUM CONTRIBUTES MODESTLY TO *TAENIA CRASSICEPS* INDUCED NEURONAL DEPOLARIZATION.

The extracellular concentration of K^+ ($[K^+]_e$, typically 3 - 4 mM) is considerably lower than the intracellular concentration of K^+ ($[K^+]_i$, typically 100 mM) within neurons (Jiang and Haddad 1991), which means that even small changes in $[K^+]_e$ result in relatively large changes to the transmembrane K^+ gradient and consequently the reversal potential for K^+ (E_{K+}). Due to the fact that constitutively activated K^+ conductances, or K^+ "leak" channels (Lesage 2003), are the major contributor to the resting membrane potential, addition of extracellular K^+ and accompanying changes to E_{K+} result in membrane depolarization.

As all cells have a high $[K^+]_i$, it is conceivable that the *T. crass.* homogenate could have a high K^+ concentration, which would then account for its depolarizing and excitatory effects on neurons. To address this, we first directly measured the ionic composition of the *T. crass.* homogenate using a Roche Cobas 6000. The K^+ concentration of the *T. crass.* homogenate was 11.39 mM as compared to 3.0 mM in our standard aCSF. The *T. crass.* homogenate Na^+ concentration was 123.9 mM and 144.2 mM for the aCSF. Although the K^+ concentration is higher in the homogenate than the aCSF, the ionic composition more closely reflects that of the extracellular as opposed to intracellular compartment. Nonetheless, we set out to determine what effect application of 11.39 mM K^+ would have on neurons in our system. Whole-cell patch-clamp recordings in current clamp mode using a standard internal solution and aCSF were made from CA3 pyramidal neurons in rat hippocampal organotypic brain slice cultures. If necessary, current was injected to ensure that the baseline membrane potential was within 2 mV of -60 mV. To remove membrane potential fluctuations due to synaptic noise, and to prevent regenerative Na^+ conductances due to voltage-gated sodium channels, 2 µM

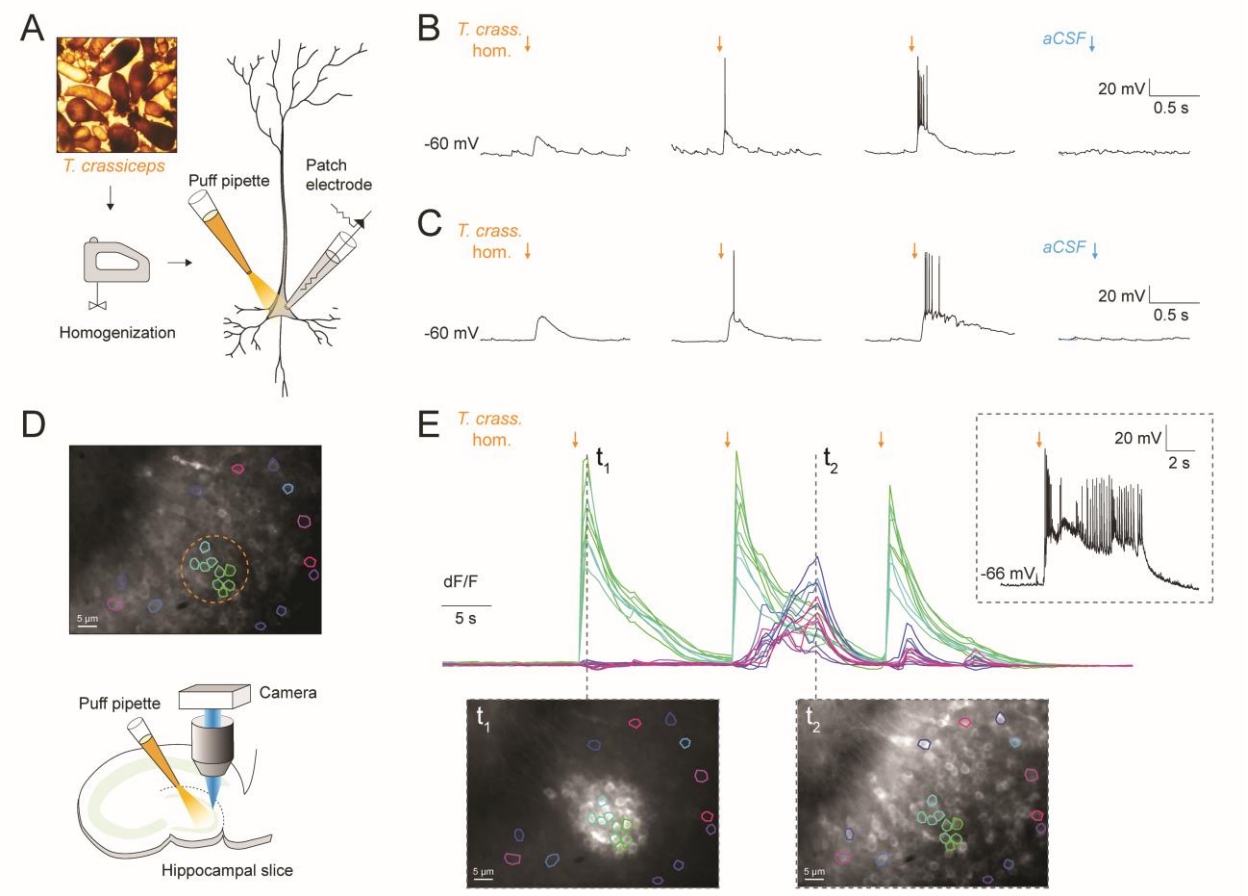

Figure 3.1 *Taenia crassiceps* homogenate excites neurons and can elicit epileptiform activity.
A) Schematic showing the experimental set up in which whole-cell patch-clamp recordings were made from CA3 hippocampal pyramidal neurons in rodent organotypic slice cultures while a puffer pipette delivered pico-litre volumes of homogenised *Taenia crassiceps* larval homogenate (*T. crass.* hom.) targeted at the cell soma. B) Current clamp recording from a rat pyramidal neuron while increasing amounts of *T. crass.* homogenate was applied via the puff pipette (left to right, orange arrows). Small amounts of *T. crass.* homogenate resulted in depolarization (left), increasing amounts elicited single (middle left) or even bursts of action potentials (middle right) whilst a similar puff of aCSF had no effect on the neuronal membrane potential (right, blue arrow), showing that potential mechanical disruption of the cell by a puff is not sufficient to depolarise it. C) As in 'B', identical effects of *T. crass.* homogenate could be elicited in current clamp recordings from a CA3 hippocampal pyramidal neuron in a mouse organotypic brain slice culture. D) Top: widefield fluorescence image of neurons in the dentate gyrus of a mouse hippocampal organotypic brain slice culture expressing the genetically-encoded Ca^{2+} reporter GCAMP6s under the synapsin promoter in aCSF containing 0.5 mM Mg^{2+}. A subset of neurons used to generate the Ca^{2+} traces in 'E' are indicated by different colours. The orange dotted circle indicates where *T. crass.* homogenate was delivered using the puff pipette. Bottom, schematic of the experimental setup including puffer pipette and CCD camera for Ca^{2+} imaging using a 470 nm LED. E) Top, dF/F traces representing Ca^{2+} dynamics from the GCAMP6s expressing neurons labelled in 'D' concurrent with 3 puffs (30 ms duration) of *T. crass.* homogenate 15 s apart. Bottom: two images of raw Ca^{2+} fluorescence at two time points; t1 and t2. Note how at time point t2 neurons distant to the site of *T. crass.* homogenate application are also activated, indicating spread of neuronal activity. Inset, top-right: current clamp recording from a neuron demonstrates that *T. crass.* homogenate application was able to evoke a seizure-like event.

TTX was added to the aCSF. Puffs of aCSF containing 11.39 mM K^+ were directed toward the soma of recorded neurons. Whilst this did cause a depolarization of the membrane potential, the effect was modest resulting in a mean positive shift of 0.72 mV (IQR 0.51 - 1.04 mV, N = 8) in the membrane potential, which was significantly less than the depolarization caused by puffs of *T. crass.* homogenate (median 10.12 mV, IQR 9.93 - 12.49 mV, N = 5, p = 0.0016, Mann-Whitney U test, Figure 3.2 A, B, D). Next, to isolate *T. crass.* homogenate induced depolarization, which was not mediated by K^+, we performed whole-cell patch-clamp recordings using a caesium based internal solution (see Materials and Methods page 26), which blocks K^+ channels. The addition of caesium did not greatly change the positive shift in membrane potential caused by *T. crass.* homogenate (median 13.76, IQR 10.87 - 17.24 mV, N = 49, p ≤ 0.0489, Mann-Whitney U test, Figure 3.2 C, D). Together, this indicates that although K^+ in the *T. crass.* homogenate does contribute to membrane depolarization, the majority of the effect is mediated by a different component.

3.4 *TAENIA CRASSICEPS* HOMOGENATE INDUCED NEURONAL DEPOLARIZATION IS MEDIATED BY A SMALL MOLECULE.

Next, to determine the fraction of the *T. crass.* homogenate, which underlies the acute excitatory effect on neurons we observed, we used a dialysis membrane to separate the fraction of the homogenate bigger than 3 kDa from the total homogenate. To do so we used a 3 kDa dialysis cassette incubated overnight in standard aCSF. This effectively removed molecules smaller than 3 kDa from the homogenate. When this dialysed *T. crass.* homogenate containing only the fraction bigger than 3 kDa was puffed onto the cells in the same recording conditions as in Figure 3.2 B and C, the depolarizing response was greatly reduced (p ≤ 0.0003, Mann-Whitney U test, Figure 3.3 A - C). The median positive shift in membrane potential for dialysed *T. crass.* homogenate was only 0.27 mV (IQR 0.20 - 0.85 mV, N = 5) as compared to a median of 13.76 mV (IQR 10.87 - 17.24 mV, N = 49) for the total homogenate (Figure 3.3). This indicates that the excitatory component of the *T. crass.* homogenate is a molecule smaller than 3 kDa.

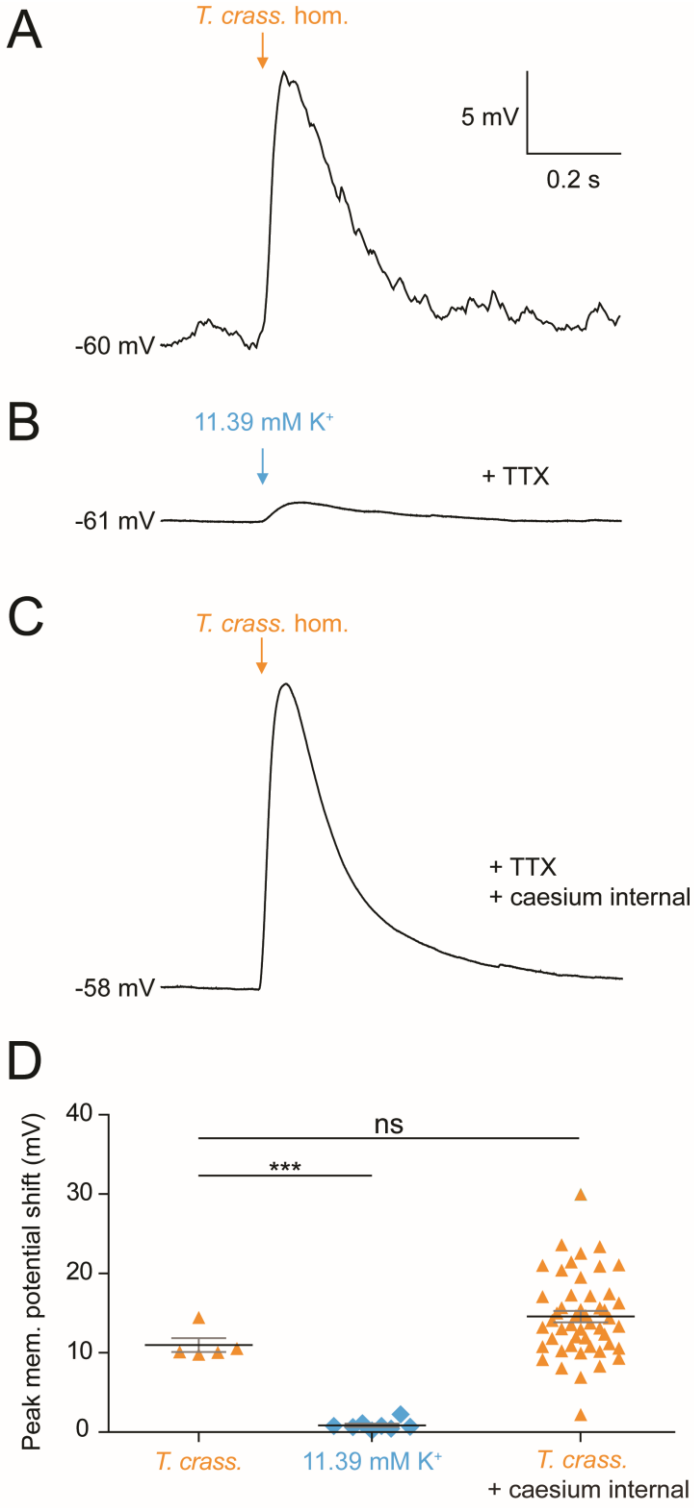

Figure 3.2 Potassium contributes modestly to *Taenia crassiceps* induced neuronal depolarization. (A) Whole-cell patch-clamp recording using a standard internal in current clamp mode from a CA3 pyramidal neuron in a rat organotypic hippocampal slice culture. A 20 ms puff of T. crassiceps homogenate (*T. crass.* hom.) (orange arrow) directed at the cell soma is delivered via a puffer pipette, causing depolarization. B) As in 'A' but puffing aCSF containing 11.39 mM K^+ (equivalent to the K^+ concentration of *T. crass.* homogenate) caused modest depolarization. 2 µM TTX was added to the aCSF to reduce synaptic noise in the voltage trace. C) As in 'A' but with a caesium based internal electrode solution to block K^+ channels and 2 µM TTX in the aCSF. Puffs of *T. crass.* homogenate (orange arrow) resulted in sizeable depolarization. D) Population data showing that the response from the 11.39 MM K^+ puff was significantly smaller than the *T. crass.* homogenate (with and without caesium internal). Values with means ± SEM; *** $p \leq 0.001$, each data point represents a cell.

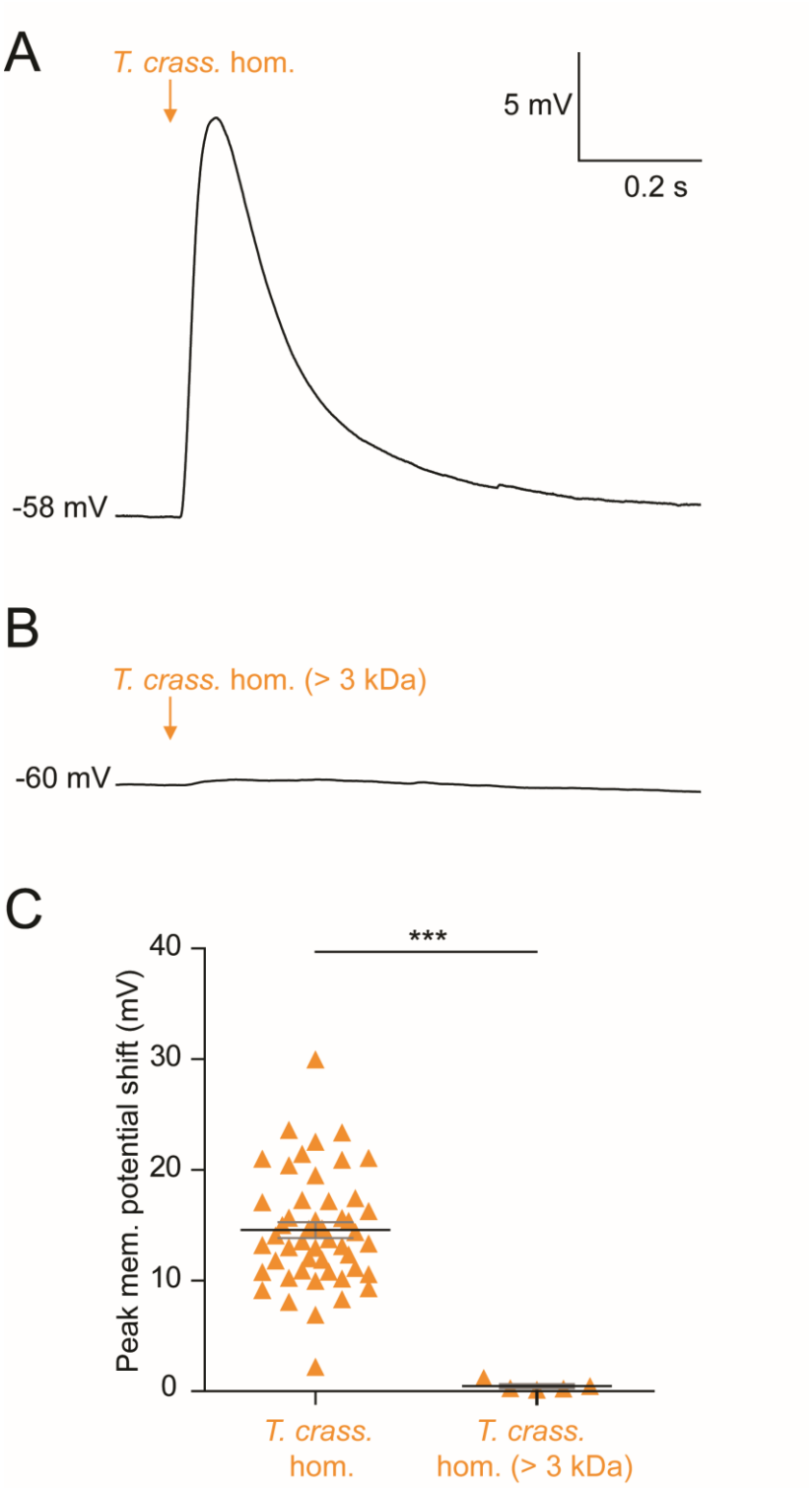

Figure 3.3 *Taenia crassiceps* homogenate induced neuronal depolarization is mediated by a small molecule.
Whole-cell patch recordings in current clamp mode were made from CA3 pyramidal neurons in rat organotypic hippocampal slice cultures using a caesium based internal in the presence of 2 µM TTX. A) Delivery of a puff of *T. crassiceps* homogenate *(T. crass.* hom.*)* caused a depolarizing shift in membrane potential. B) The depolarizing response to *T. crass.* homogenate was largely abolished by dialysing out all molecules smaller than 3 kDa. C) Population data demonstrating that the *T. crass.* homogenate response is significantly reduced by dialysis, indicating that the excitatory component is a small molecule (< 3 kDa). Values with means ± SEM; *** $p \leq 0.001$, each data point represents a cell.

3.5 *TAENIA CRASSICEPS* HOMOGENATE INDUCED NEURONAL DEPOLARIZATION IS NOT MEDIATED BY NICOTINIC ACETYLCHOLINE RECEPTORS, ASIC RECEPTORS, OR SUBSTANCE P.

Our results demonstrate that the *T. crass.* derived small molecule induces neuronal depolarization very rapidly (within ms), as such, it is highly likely that this molecule is an agonist of a neuronal ionotropic receptor. Therefore, we utilized pharmacological methods to determine the ionotropic receptor system via which the *T. crass.* derived small molecule acts.

Nicotinic acetylcholine receptors (nAchRs) are well described ionotropic receptors in the nervous system, which mediate depolarization via a mixed Na^+, K^+ conductance (Bear, Connors, and Paradiso 2007). Again, using a caesium based internal solution in the presence of TTX in the aCSF, CA3 neurons were whole-cell patched and the peak voltage during *T. crass.* homogenate induced neuronal depolarisation measured before, during and after bath application of the non-competitive nicotinic acetylcholine receptor antagonist mecamylamine hydrochloride (10µM) to block nAchRs (Figure 3.4 A). The blockade of nAchRs did not significantly alter the *T. crass.* homogenate induced depolarisation. The median *T. crass.* homogenate induced depolarization was 16.28 mV (IQR 13.54 - 23.63 mV) during baseline, 16.58 mV (IQR 11.21 - 24.50 mV) in the presence of mecamylamine hydrochloride and 13.20 mV (IQR = 10.37 - 23.48 mV) following washout ($N = 5$, $p > 0.05$, Friedman test, Figure 3.4 A, B).

Acid-Sensing Ion Channels (ASICs) are proton-gated sodium channels known to be expressed by hippocampal neurons and result in neuronal depolarization when activated. We therefore considered that the pH of the *T. crass.* homogenate may be important as acidic conditions could activate ASICS and cause neuronal depolarization. We measured the pH of the *T. crass.* homogenate (mean = 7.99), which was too alkaline to activate ASICs, activated maximally at a pH of 5 (Weng *et al.* 2004). However, certain compounds can activate ASICs directly (Osmakov *et al.* 2017). Therefore, to determine whether activation of ASICs could underlie *T. crass.* homogenate induced depolarization we used the non-specific ASIC blocker amiloride (2 mM). The presence of amiloride did not significantly attenuate the effect of the homogenate (Figure 3.4 C), with the mean *T. crass.* homogenate induced depolarization being 14.55 mV (SEM 1.41 mV) during baseline, 12.12 mV (SEM 2.25 mV) in the presence of amiloride and 17.06 mV (SEM 2.20 mV) following washout ($N = 10$, $p > 0.05$, repeated measures ANOVA, Figure 3.4 C, D).

A further possible candidate for our excitatory small molecule was Substance P, an abundant neuropeptide and neurotransmitter (Liu *et al.* 2002; Harrison and Geppetti 2001). Robinson *et al* (2012) have found Substance P in close vicinity to human NCC granulomas. Garza *et al.*

(2010) found that Substance P signalling contributes to granuloma formation and Substance P enhanced NMDA channel function (Lieberman and Mody 1998). We therefore investigated whether Substance P could elicit a similar neuronal depolarizing response to that of *T. crass.* homogenate. However, we found that 100 µM Substance P had no acute effect on the membrane potential of CA3 hippocampal pyramidal neurons (0.08 mV, IQR 0.01 – 0.12 mV, N = 5, p > 0.05, Wilcoxon signed rank test with theoretical median = 0.00, Figure 3.4 E, F). Together this data indicates that *T. crass.* homogenate induced neuronal depolarization is not mediated by nicotinic acetylcholine receptors, ASIC receptors, nor Substance P.

3.6 THE DEPOLARIZING EFFECTS OF *TAENIA CRASSICEPS* ARE MEDIATED BY GLUTAMATE RECEPTOR ACTIVATION.

The predominant excitatory neurotransmitter in the nervous system is glutamate (Bear, Connors, and Paradiso 2007). Glutamate activates a number of ionotropic glutamate receptors (GluRs) including AMPA, Kainate and NMDA receptors (Bear, Connors, and Paradiso 2007), therefore it is likely that *T. crass.* homogenate could cause neuronal depolarization by activation of GluRs. To test this possibility we again made whole-cell current clamp recordings from CA3 hippocampal pyramidal cells using a caesium based internal in the presence of TTX to block voltage-gated sodium channels. *T. crass.* homogenate induced neuronal depolarization was measured before, during and after the application of 10µM CNQX, 50µM D-AP5 and 2mM kynurenic acid to block all three classes of GluRs. I found that GluR blockade significantly reduced the mean *T. crass.* homogenate induced neuronal depolarization from 14.72 mV (IQR 13.39 - 15.68 mV) to 1.90 mV (IQR 1.09 - 2.21 mV, N = 9, p ≤ 0.01, Friedman test with Dunn's multiple comparison test, Figure 3.5 A, B), which recovered to a median value of 14.37 mV (IQR 7.32 - 16.38 mV) following washout (N = 9, *p* ≤ 0.01, Friedman test with Dunn's multiple comparison test, Figure 3.5 A, B). This indicated that activation of GluRs is the primary mediator of the depolarizing effect of *T. crass.* homogenate I observed.

3.7 *TAENIA CRASSICEPS* AND *TAENIA SOLIUM* LARVAE CONTAIN AND PRODUCE GLUTAMATE.

Glutamate is the major excitatory neurotransmitter in the brain and the prototypical agonist of GluRs (Bear, Connors, and Paradiso 2007). Together with a fellow doctoral student in the lab,

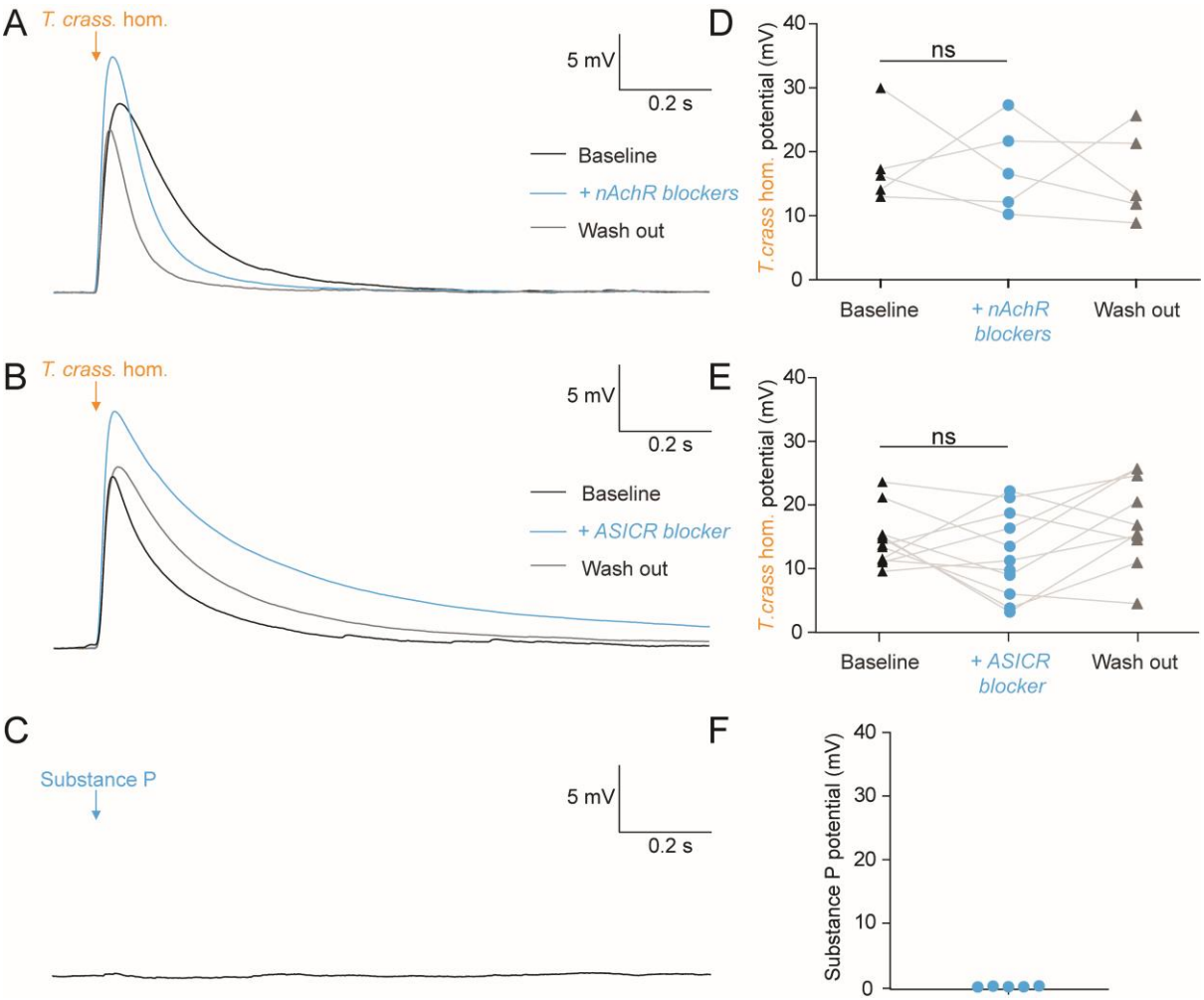

Figure 3.4 *Taenia crassiceps* homogenate induced neuronal depolarization is not mediated by nicotinic acetylcholine receptors, ASIC receptors, or Substance P.
Whole-cell patch recordings were made from CA3 pyramidal neurons in rat organotypic hippocampal slice cultures using a caesium based internal in the presence of 2 µM TTX. If necessary, current was injected to maintain the membrane potential within 2 mV of -60 mV. A) The depolarizing response to a *T. crassiceps* homogenate *(T. crass.* hom.*)* puff (orange arrow) before (black trace), during (blue trace) and after (grey trace) the addition of a nicotinic acetylcholine receptor (nAchR) blocker (mecamylamine hydrochloride, 10µM). B) Population data demonstrating that nAchR blockade has no significant effect on the *T. crass.* homogenate induced depolarization. C) The depolarizing response to a *T. crass.* homogenate puff (orange arrow) before (black trace), during (blue trace) and after (grey trace) the addition of an ASIC receptor blocker (amiloride, 2 mM) D) Population data demonstrating that ASIC receptor blockade has no significant effect on the *T. crass.* homogenate induced depolarization. E) Current clamp trace showing that a puff of 100 µM Substance P (blue arrow) does not affect the membrane potential of CA3 pyramidal neurons. F) Population data for Substance P application. ns = not significant, $p > 0.05$, each data point represents a cell.

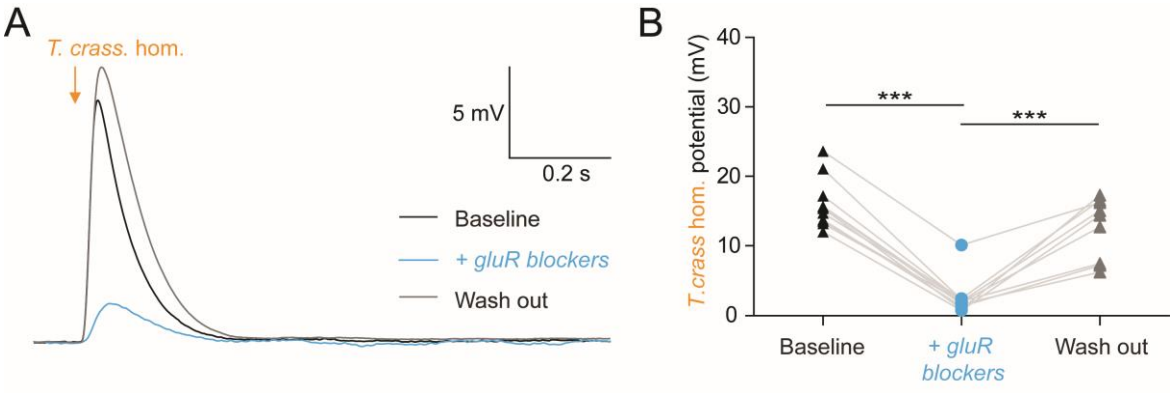

Figure 3.5 The depolarizing effects of *Taenia crassiceps* are mediated by glutamate receptor activation.
A) Whole-cell current clamp recording from a rat CA3 pyramidal neuron in a hippocampal organotypic slice culture. Neuronal membrane potential in response to a 20 ms puff of *T. crassiceps* homogenate *(T. crass.* hom.*)* (orange arrow) before (black trace), during (blue trace) and following wash out (grey trace) of a pharmacological cocktail to block glutamate receptors (10µM CNQX, 50µM D-AP5 and 2mM kynurenic acid). B) Population data shows that the depolarization response to *T. crass.* homogenate is significantly reduced in the presence of glutamate receptor blockers and returns upon wash out. Values with means ± SEM; ****p* ≤ 0.001, each data point represents a cell.

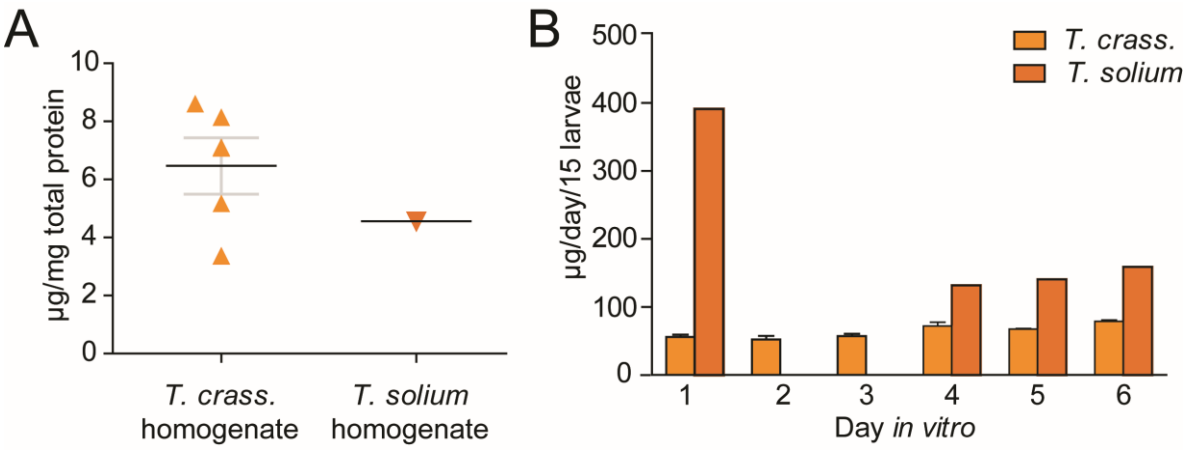

Figure 3.6 *Taenia crassiceps* and *Taenia solium* larvae contain and produce glutamate.
A) Glutamate levels in whole cyst homogenate of *T. crassiceps (T. crass)* and *T. solium* larvae. B) Glutamate production per day per 15 larvae for 6 days *in vitro* for *T. crass.* and *T. solium* larvae. Note that both species of larvae produce glutamate *de novo*, particularly on days 4 – 6.

Anja de Lange, we directly measured the concentration of glutamate in the *T. crass.* homogenate we had been puffing onto neurons using a glutamate assay (see Materials and Methods page 24). We found that the mean concentration of glutamate in the *T. crass.* homogenate was 6.47 µg/mg (SEM 0.97 µg/mg, N = 5, Figure 3.6 A) – corresponding to approximately 112 µM for puffing experiments. Glutamate at this concentration robustly activates GluRs in hippocampal pyramidal neurons (Forman *et al.*, 2017). *T. crass.*, whilst a closely related species to *T. solium*, is not the causative pathogen in humans. We therefore also measured the glutamate concentration in homogenate prepared from larvae of *T. solium*, the predominant pathogen responsible for human NCC. We recorded a glutamate concentration of 4.56 µg/mg (N = 1), which indicates that the concentration of this excitatory neurotransmitter is also high within larvae of *T. solium* (Figure 3.6 A).

Whilst glutamate is a neurotransmitter in the CNS, it is also an ubiquitous metabolite present in the cytoplasm of the majority of cells (Newsholme *et al.* 2002). Therefore it is possible that the *T. crass.* and *T. solium* homogenate only contains glutamate due to cell lysis during homogenate preparation. To determine whether larvae of both these cestodes actively produce and excrete or secrete glutamate into their environments we measured the *de novo* daily production of glutamate by larvae following harvest of live larvae from the intermediate host (mice for *T. crass.* and pigs for *T. solium* , see Materials and Methods page 24). Both species of larvae were observed to generate glutamate *de novo* and release this into the culture media (Figure 3.6 B). *T. crass.* larvae released a relatively constant daily amount of glutamate (mean 64.07 µg/15 larvae per day, SEM 4.31 µg/15 larvae per day, N = 3, Figure 3.6 B). *T. solium* larvae released a large amount of glutamate on the first day post-harvest, none on the 2nd and 3rd day *in vitro,* but again begin to produce large amounts of glutamate on days 4, 5 and 6 (mean 137.06 µg/15 larvae per day, SEM 58.49 µg/15 larvae per day, N = 1, Figure 3.6 B). Collectively these results demonstrate that larvae of both *T. crass.* and *T. solium* contain and release glutamate into their immediate surroundings.

3.8 DISCUSSION

In this chapter I investigated the acute effects of *T. crass.* larval homogenate on pyramidal neurons in the CA3 region of the hippocampus in cultured organotypic rodent brain slices. To do this I performed patch-clamp recordings of neuronal voltage whilst applying puffs of tapeworm homogenate onto the cells.

In the first experiment I showed that, indeed*, T. crass.* homogenate is able to depolarise the membrane voltage of a cell, and that the more homogenate that is applied, the more excitable the cell became, producing multiple action potentials. The mechanical effect of the puffs from

the OpenSpritzer were controlled for by applying aCSF onto cells, with no measurable response. Furthermore we were able to show, with the use of calcium imaging, that excitation from an application of *T. crass.* was able to propagate to neurons out of the proximity of the puff of homogenate, and was even able to generate epileptiform activity.

Next I measured the ionic components of the larval homogenate and found the K^+ concentration to be somewhat raised compared with that found extracellularly in the CSF (11.39 mM). This was somewhat expected as the homogenate was made by lysing the larvae, and given that the typical concentration of K^+ within cells is very high (±100 mM) one might have expected a much higher K^+ concentration of the homogenate. The comparatively low homogenate K^+ concentration suggests that the larval cystic fluid must make up a large proportion of the total larval fluid, and that this cystic fluid has a relatively low K^+ concentration. Never-the-less, the slightly raised concentration of K^+ in the homogenate, when applied extracellularly to neurons, is predicted to reduce the flow of K^+ ions out of the neuron, resulting in more positive charge remaining inside and thus raising the membrane voltage closer to the spike threshold. Indeed, when a solution of aCSF with the equivalent concentration of K^+ (11.39 mM) to the homogenate was puffed onto neurons it resulted in a modest (approximately 2 mV) increase in membrane voltage. This therefore likely contributed to, but did not completely account for, the marked depolarising effect that the larval homogenate has on neurons. Wang *et al.* (2016) have noted that when the aCSF extracellular K^+ is raised to 9 mM it can have significant pro-seizure effects (greater seizure duration, shortened interictal intervals etc.) but that at concentrations higher than this neurons went into depolarisation-block. Our model is unlikely to show such a strong effect as we were only altering the extracellular K^+ concentration in a localised position, by puffing the high K^+ aCSF onto our recording cell. In order to exclude the depolarizing contribution of raised K^+ within the homogenate, a caesium internal solution was used for the remaining experiments in the chapter to block the K^+ channels and thus exclude this effect.

Thereafter I separated the homogenate by size using a 3 kDa membrane and found that once all molecules smaller than 3 kDa had dialysed out of the homogenate it no longer had a depolarising effect on the neuronal membrane potential. I then wanted to identify which small molecule was having the excitatory effect or at least which neurotransmitter system it was having an effect on. To do this I performed a series of experiments utilising blockers of acetylcholine (mecamylamine hydrochloride) or ASICs (amiloride) and by applying Substance P directly to compare the effect. None of these neurotransmitter systems explained the *T. crass.* effect. I then utilised a cocktail of glutamate blockers (kynurenic acid, CNQX and D-AP5) which were successful in abolishing the excitatory response. I could therefore

conclude that the larval homogenate was generating its effect by binding to glutamate receptors.

In order to ascertain whether the larval homogenate contained glutamate itself or a glutamate agonist my colleague, Anja de Lange, performed assays to determine the amount of glutamate in the homogenate of *T. crass.* and *T. solium*, as well as the amount of glutamate produced by viable *T. crass.* and *T. solium* larvae. This is the first time, to my knowledge, that it has been conclusively known that *T.crass.* and *T. solium* larvae both produce and contain glutamate, which is able to depolarise pyramidal neurons and even cause epileptiform-type activity.

The limitation is that only the most acute response is investigated using these methods. Glutamate, being the main excitatory transmitter in the brain, is very tightly buffered by neurons and astrocytes and so the additional extracellular glutamate may be quickly removed in a less acute model. Thus in chapter 4 I investigated how 24 hour treatment of organotypic mouse brain slices with *T. crass.* homogenate affected the intrinsic properties of neurons and the excitability of the slices.

Chapter 4

THE SHORT-TERM EFFECTS OF *TAENIA CRASSICEPS* ON NEURONS *IN VITRO*

4.1 INTRODUCTION

In the previous chapter I explored the acute, very immediate (*i.e.* millisecond to second) effects of *T. crass.* larval products on neurons, which would reflect direct effects on receptors and ion channels. To explore potential longer-term effects driven by processes which might require longer time scales (*i.e.* second messenger cascades, phosphorylation, innate immunity or gene expression) I treated organotypic brain slices for 24 hours with *T. crass.* larval homogenate.

Inflammatory markers have been found in the brains of patients with NCC (Restrepo *et al.* 2001; Sheng *et al.* 1994), and have been shown to be released by glia in the presence of tapeworm homogenate within hours, usually peaking by 24 hours (Uddin *et al.* 2005). Inflammation also impairs glutamate buffering by astrocytes (Van Vliet *et al.* 2007; Seiffert *et al.* 2004). In turn, a build-up of glutamate can enhance neuronal excitability. Therefore, the addition of an external source of glutamate such as from *T. crass.* or *T. solium* larvae/homogenate (the finding from Chapter 3) could possibly change the intrinsic properties of neurons (Hamlet and Lu 2016) or the excitability of the network (DeLorenzo, Pal, and Sombati 1998). Beyond this, it is also possible that hitherto unidentified factors within the *T. crass.* larval homogenate could modify the properties of neuronal circuits within brain slices on a longer timescale than that explored in the previous chapter.

Thus I treated brain slices with tapeworm homogenate for 24 hours. Beside the negative control of standard growth media I also included a "positive control" group treated with lipopolysaccharide (LPS). LPS is a component of the cell wall of gram negative bacteria and is strongly pro-inflammatory through its activation of microglial Toll-like Receptors (Lively and Schlichter 2018) and the subsequent release of cytokines such as IL-1β, TNF- α and IL-6 (Papageorgiou *et al.* 2016). Furthermore, LPS treatment has been shown to exert electrophysiological changes on hippocampal neurons *in vitro* (Hellstrom *et al.* 2005). I utilised whole-cell patch-clamp recordings of pyramidal cells in mouse hippocampal sections to investigate possible differences in neuronal firing properties, ion currents and seizure

threshold. I found that 24 hours of *T. crass.* homogenate exposure had no effect on the membrane properties, active firing properties, sodium or potassium currents of neurons nor on network excitability. In contrast LPS exposure did increase the spiking threshold of neurons.

4.2 SUSTAINED EXPOSURE TO *TAENIA CRASSICEPS* HOMOGENATE DOES NOT AFFECT BASIC NEURONAL MEMBRANE PROPERTIES.

Mouse hippocampal organotypic brain slice cultures were prepared and maintained with standard growth media until day 6 or 7 when they were treated for 24 hours with either; standard growth media or media containing *T. crass.* homogenate (50 µg/ml) or LPS (10 µg/ml). Whole-cell patch-clamp recordings were then made from hippocampal pyramidal neurons and used to assess how the various treatment conditions might have affected the intrinsic properties of the neurons (Figure 4.1 A). Standard growth media was used as a negative control. LPS was used as a potential positive control in order to drive an innate inflammatory response in the slices. Sun *et al.* (2014) found high concentrations of cytokines produced by microglia in response to a 24 hour treatment with helminth soluble factors. Since this timeframe was enough to evoke an immune response, we wondered whether we might also see electrophysiological changes during this same time period.

The quality of each patch was determined by calculating the access resistance (Ra), which determines how effective the electrical access (conductance) is to the cell. Only cells with a Ra under 30 mOhm were chosen to ensure optimal recordings were achieved. The mean Ra for the *T. crass.*, LPS and media groups were 17.18 mOhm (SEM 1.66 mOhm, N = 14), 18.54 mOhm (SEM 1.53 mOhm, N = 9) and 13.66 mOhm (SEM 1.05 mOhm, N = 11), respectively and were not significantly different from one another ($p > 0.05$, One-way ANOVA, data not shown in figure). This ensured that recording conditions were equivalent between treatment groups.

Thereafter I first measured the resting membrane potential, membrane resistance and capacitance, which comprise the basic membrane properties and fundamentally modulate neuronal signalling. Resting membrane potential is the measurement of the voltage across the membrane under baseline conditions. An alteration in this intrinsic property could result in a more excitable neuron. The mean resting membrane potential for the *T. crass.*, LPS and media groups were -64.72 mV (SEM 5.88 mV, N = 14), -61.82 mV (SEM 8.26 mV, N = 9) and -64.43 mV (SEM 3.96 mV, N = 11), respectively and were not significantly different from one another ($p > 0.05$, One-way ANOVA, Figure 4.1 B).

Membrane resistance reflects how easily ions can flow through the cell membrane and thus is an indicator of the number of ion channels, particularly K^+ leak channels in the neuronal membrane. The mean membrane resistance for the *T. crass.*, LPS and media groups were 200.30 mOhm (SEM 95.99 mOhm, N = 15), 185.30 mOhm (SEM 89.70 mOhm, N = 10) and 193.30 mOhm (SEM 61.79 mOhm, N = 12), respectively and were not significantly different from one another ($p > 0.05$, One-way ANOVA, Figure 4.1 C).

Membrane capacitance represents the size of the lipid membrane and the charge it is able to store across it. It also determines how quickly a cell's membrane potential can respond to a change in current. The median capacitance for the *T. crass.*, LPS and media groups were 182.2 mμF (IQR 131.9 – 250.0 mμF, N = 14), 169.4 mμF (IQR 163.1 – 220.5 mμF, N = 9) and 186.8 mμF (IQR 174.2 – 249.6 mμF, N = 11), respectively and were not significantly different from one another ($p > 0.05$, Kruskal-Wallis test, Figure 4.1 D).

Together the membrane resistance and membrane capacitance determine the membrane time constant which sets the integrative properties of a neuron. My data showed that slice incubation for 24 hrs with neither *T. crass.* homogenate nor LPS had any significant effect on the basic membrane properties of hippocampal pyramidal cells.

4.3 SUSTAINED EXPOSURE TO *TAENIA CRASSICEPS* HOMOGENATE DOES NOT AFFECT THE ACTIVE FIRING PROPERTIES OF NEURONS.

The intrinsic excitability of a neuron is largely determined by how readily and at what rate it can generate action potentials. Changes in the active firing properties of neurons have been demonstrated in a number of epilepsy syndromes (Avanzini and Franceschetti 2003). Therefore to determine whether longer-term exposure of *T. crass.* homogenate affected the active firing properties of neurons I measured; spike threshold, current threshold density, maximum spike rate, absolute maximum spike rate, current and current threshold density which evoke the maximum spike rate in neurons in the same three treatment conditions.

I first calculated the spike threshold by performing a series of current steps, which increased the membrane voltage until the first action potential was generated. The spike threshold was determined as the voltage at which the first action potential was generated (Figure 4.2.1 A). The spike threshold essentially shows how excitable a cell is as a more negative spike threshold would mean that relatively little depolarising synaptic input is required for that cell to spike. The median spike threshold for each of the *T. crass.*, LPS and media groups were -34.13 mV (IQR -34.99 – -32.74 mV, N = 14), -31.55 mV (IQR -32.76 – -30.60 mV, N = 9)

and -33.64 mV (IQR -34.12 – -33.04 mV, N = 11). No difference was seen between *T. crass.* and control or between LPS and control groups, but the LPS group had a significantly higher

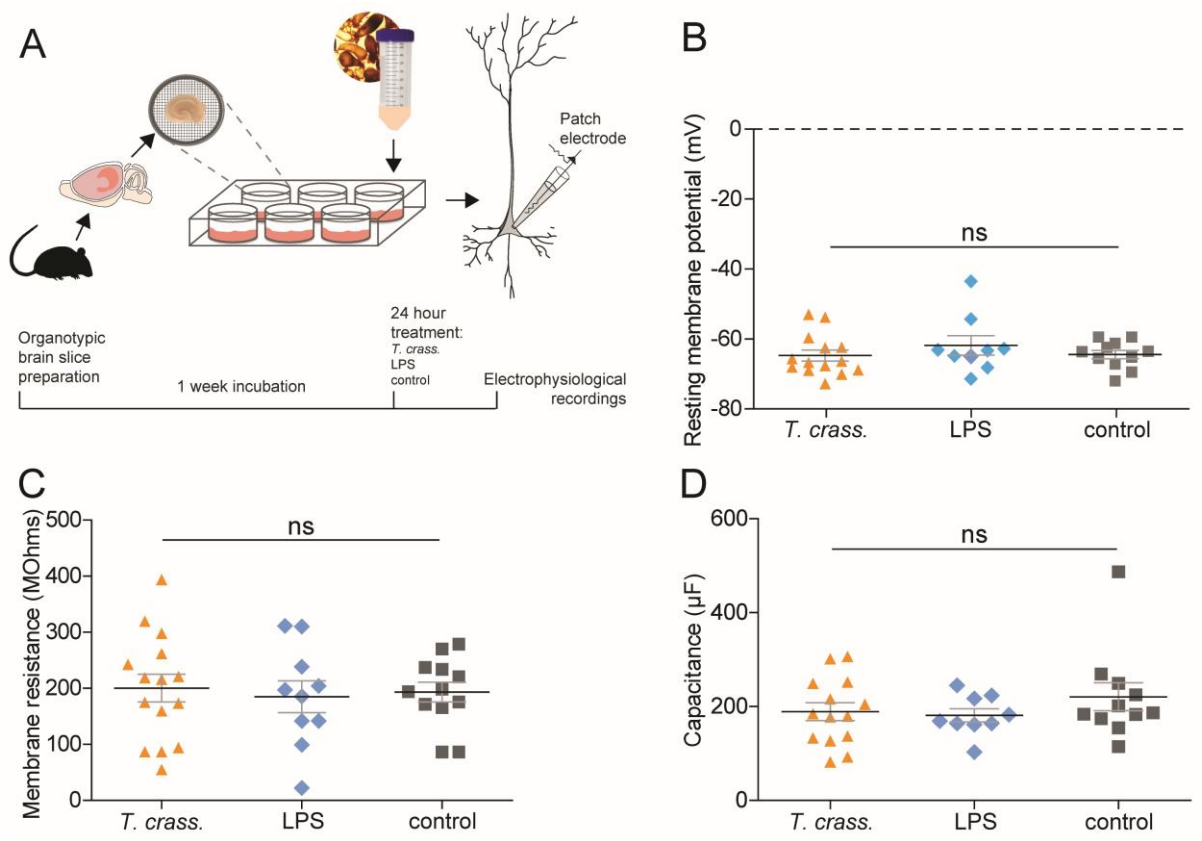

Figure 4.1 Sustained exposure to *Taenia crassiceps* homogenate does not affect neuronal membrane properties.
A) Whole–cell patch-clamp recordings were made from CA3 pyramidal neurons in mouse hippocampal organotypic slice cultures. Slices were treated for 24 hours pre-electrophysiological recording with either; 50 µg/ml *Taenia crassiceps* homogenate, 10 µg/ml LPS or standard growth media. B) There was no significant difference between any of the groups for the resting membrane potential of the cells. C) The membrane resistance also did not differ significantly between groups. D) There was no significant difference in the capacitance between any of the groups. Values with means ± SEM; ns = not significant, each data point represents a recording from one cell.

spike threshold than the *T. crass.* group ($p = 0.0098$, Kruskal-Wallis test with Dunn's multiple comparison test, Figure 4.2.1 B) meaning LPS treatment makes cells less excitable.

Current threshold density is the amount of current a cell requires to fire its first action potential normalised by the cell's capacitance, which accounts for the size of the cell and is a more finely tuned way of measuring excitability. The median current threshold density for each of the *T. crass.*, LPS and media groups were 0.74 pA/pF (IQR 0.55 – 1.19 pA/pF, N = 14), 0.85 pA/pF (IQR 0.48 – 1.07 pA/pF, N = 9) and 0.85 pA/pF (IQR 0.45 – 0.98 pA/pF, N = 11), respectively and were not significantly different from one another ($p > 0.05$, Kruskal-Wallis test, Figure 4.2.1 C).

The maximum spike rate is a metric of how rapidly a cell can send signals by measuring the maximum number of action potentials it can generate in a given time. The maximum spike rate is calculated using a series of current steps, which increase the membrane voltage such that a cell is generating as many action potentials as possible (Figure 4.2.2 A). The number is counted for the first 500 ms of the current step recording thus resulting in a spike rate denoted in Hz. The maximum spike rate for each of the *T. crass.*, LPS and media groups were 23.00 Hz (SEM 1.24 Hz, N = 14), 19.33 Hz (SEM 2.11 Hz, N = 9) and 22.36 Hz (SEM ± 1.23 Hz, N = 11), respectively and were not significantly different from one another ($p > 0.05$, One-way ANOVA, Figure 4.2.2 B).

The absolute maximum spike rate was calculated as the shortest time between spikes and shows the absolute fastest a cell could send signals, theoretically as it would be unlikely to sustain this speed. The median absolute maximum spike rate for each of the *T. crass.*, LPS and media groups were 41.45 Hz (IQR 34.71 – 51.62 Hz, N = 14), 40.00 Hz (IQR 32.80 - 55.62 Hz, N = 9) and 45.98 Hz (IQR 40.40 – 63.49, Hz, N = 11), respectively and were not significantly different from one another ($p > 0.05$, Kruskal-Wallis test, Figure 4.2.2 C).

Since I did not observe any differences between the *T. crass.* and control groups in terms of their active firing properties I next wanted to ensure I wasn't missing a potential difference whereby cells could achieve the same maximum spike rate but might require different amounts of input current to do so. I therefore calculated the mean current which evokes the maximum spike rate for each of the *T. crass.*, LPS and media groups, which were 637.40 pA (SEM 90.08 pA, N = 14), 535.80 pA (SEM 92.54 pA, N = 9) and 753.20 pA (SEM 99.50 pA, N = 11), respectively and were not significantly different from one another ($p > 0.05$, One-way ANOVA, Figure 4.2.2 D). Performing the same analysis but normalising for cell size; the mean current threshold density which evokes the maximum spike rate for each of the *T. crass.*, LPS and media groups were 3.29 pA/pF (SEM 0.31 pA/pF, N = 14), 2.98 pA/pF (SEM 0.48 pA/pF,

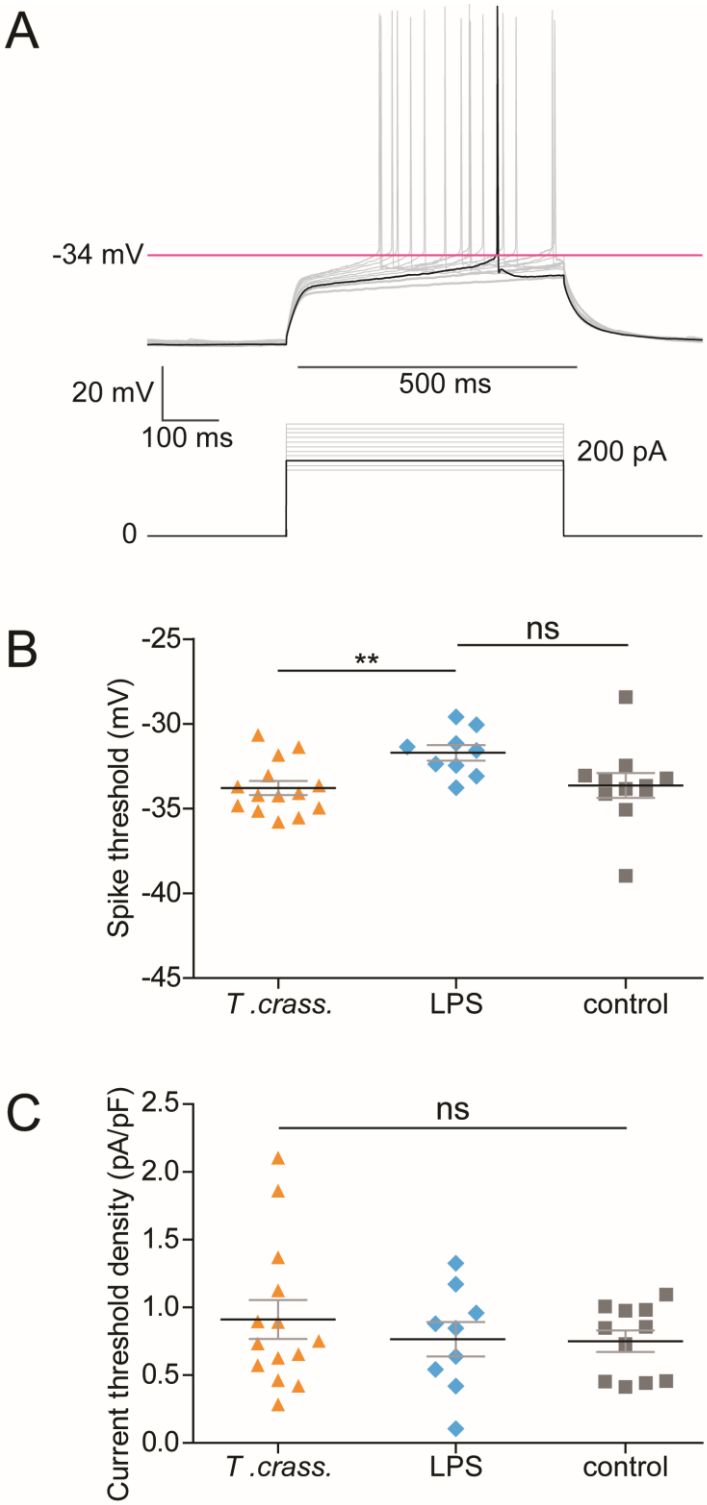

4.2.1 Sustained exposure to *Taenia crassiceps* homogenate does not affect the active firing properties of neurons; including the spike threshold and current threshold density.

Whole–cell patch-clamp recordings were made from CA3 pyramidal neurons in mouse hippocampal organotypic slice cultures. Slices were treated for 24 hours pre-electrophysiological recording with either; 50 µg/ml *Taenia crassiceps* homogenate, 10 µg/ml LPS or standard growth media. A) Example trace showing the current required to raise the membrane voltage high enough for the cell to fire an action potential, with the pink line indicating the spike threshold or the voltage at which the first action potential is fired. B) The spike threshold significantly differs only between the *Taenia crassiceps* and LPS groups. C) There were no differences between the any of the groups for the current threshold density. Values with means ± SEM; **p < 0.01, ns = not significant, each data point represents a cell.

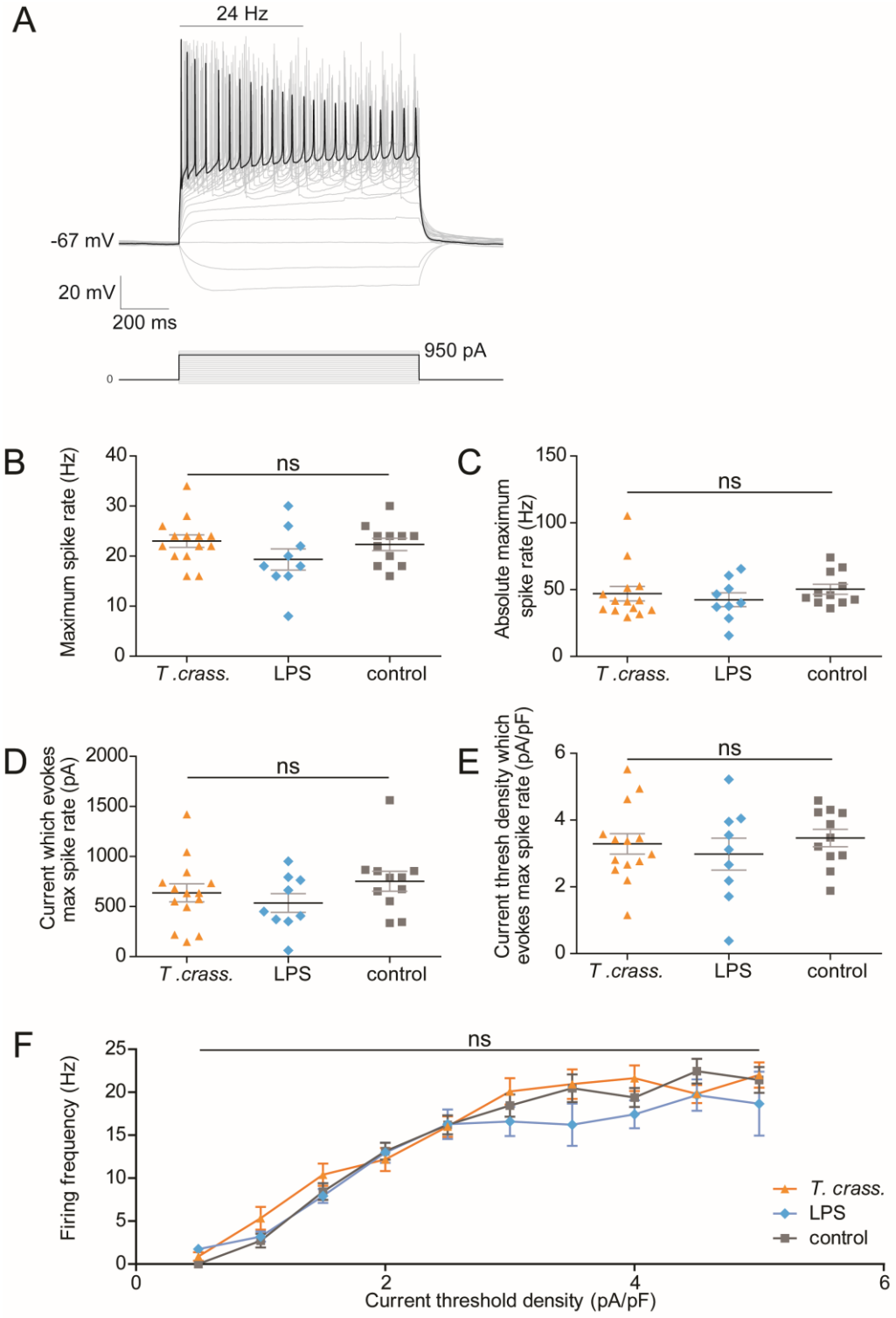

4.2.2 Sustained exposure to *Taenia crassiceps* homogenate does not affect the active firing properties of neurons; including the maximum spike rate and its relationship to current threshold density.
Whole–cell patch-clamp recordings were made from CA3 pyramidal neurons in mouse hippocampal organotypic slice cultures. Slices were treated for 24 hours pre-electrophysiological recording with either; 50 µg/ml *Taenia crassiceps* homogenate, 10 µg/ml LPS or standard growth media. A) Example trace showing the maximum number of spikes that can be elicited from a cell in order to determine the max spike rate and absolute max spike rate for each of the experimental conditions. B & C) Neither the maximum spike rate nor the absolute maximum spike rate differed significantly between the groups. D & E) Both the current and the current threshold density required to evoke the max spike rate also did not differ significantly between the groups. F) Furthermore, the relationship between the firing frequency and current threshold density did not differ between the groups. Values with means ± SEM; ns = not significant, each data point represents a cell.

N = 9) and 3.46 pA/pF (SEM 0.26 pA/pF, N = 11), respectively and were not significantly different from one another ($p > 0.05$, One-way ANOVA, Figure 4.2.2 E).

I then wondered if perhaps a difference would exist below the level of the maximum spike rate and so analysed the firing frequency at increasing current threshold densities. The relationship between the firing frequency and current density did not differ significantly between the groups ($p > 0.05$, Friedman test, Figure 4.2.2 F). Although it was not statistically significant, for the above metrics of active firing properties, the LPS condition tended to be slightly less excitable. The *T. crass.* condition however, was almost indistinguishable from the control group, which demonstrated that 24 hrs of *T. crass.* homogenate application had no observable effect on the active firing properties of hippocampal pyramidal neurons.

4.4 SUSTAINED EXPOSURE TO *TAENIA CRASSICEPS* HOMOGENATE DOES NOT AFFECT THE SIZE OF VOLTAGE-GATED SODIUM CURRENTS IN NEURONS.

Ion flux across the membrane determines changes in membrane voltage. Na^+ flux through voltage-gated Na^+ channels underlies the membrane depolarization, which constitutes the neuronal action potential. An example trace in voltage clamp demonstrates the Na^+ current that is generated when voltage-gated Na^+ channels are opened following a voltage step to a more positive potential (10 mV) (Figure 4.3 A).

The mean absolute maximum voltage-gated Na^+ current for each of the *T. crass.*, LPS and media groups were -5573 pA (SEM 455.3 pA, N = 14), -4732 pA (SEM 467.7 pA, N = 9) and -6202 pA (SEM 337.7 pA, N = 11), although there was a trend for the size of currents in the LPS treated condition to be smaller, there was no significant difference between any of the conditions ($p > 0.05$, One-way ANOVA, Figure 4.3 B).

4.5 SUSTAINED EXPOSURE TO *TAENIA CRASSICEPS* HOMOGENATE DOES NOT AFFECT THE MAXIMUM SIZE OF POTASSIUM CURRENTS IN NEURONS.

The movement of K^+ out of the cell is responsible for the repolarisation of the membrane and is also essential to a cell's ability to send signals rapidly. An example trace in the voltage clamp recording configuration demonstrates the current generated when K^+ channels are open at a depolarised potential (30 mV) (Figure 4.4 A).

The median maximum K^+ current for each of the *T. crass.*, LPS and media groups were 2947 pA (IQR 2382 – 4483 pA, N = 11), 2500 pA (IQR 2068 - 3682 pA, N = 8) and 4338 pA (IQR

2633 - 4626 pA, N = 9), respectively and were not significantly different from one another (p > 0.05, Kruskal-Wallis test, Figure 4.4 B).

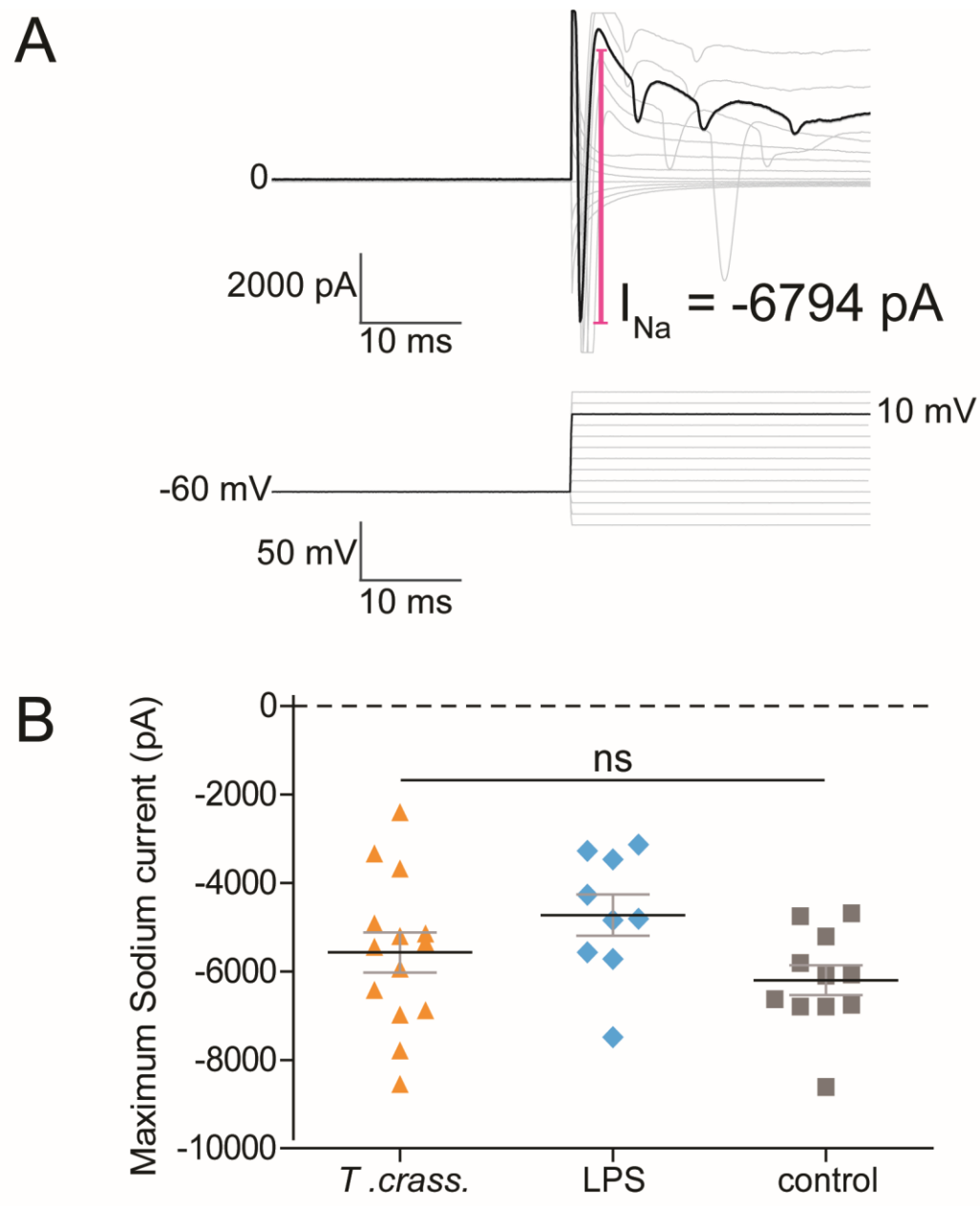

4.3 Sustained exposure to *Taenia crassiceps* homogenate does not affect the maximum size of voltage-gated sodium currents in neurons.
Whole–cell patch-clamp recordings in voltage clamp mode were made from CA3 pyramidal neurons in mouse organotypic slice cultures. Slices were treated for 24 hours pre-electrophysiological recording with either; 50 µg/ml *Taenia crassiceps* homogenate, 10 µg/ml LPS or standard growth media. A) Example trace showing the measurement of the absolute maximum voltage-gated sodium current elicited following positive voltage steps. B) The mean maximum sodium current was not significantly different between the groups. Values with means ± SEM; ns = not significant, each data point represents a cell.

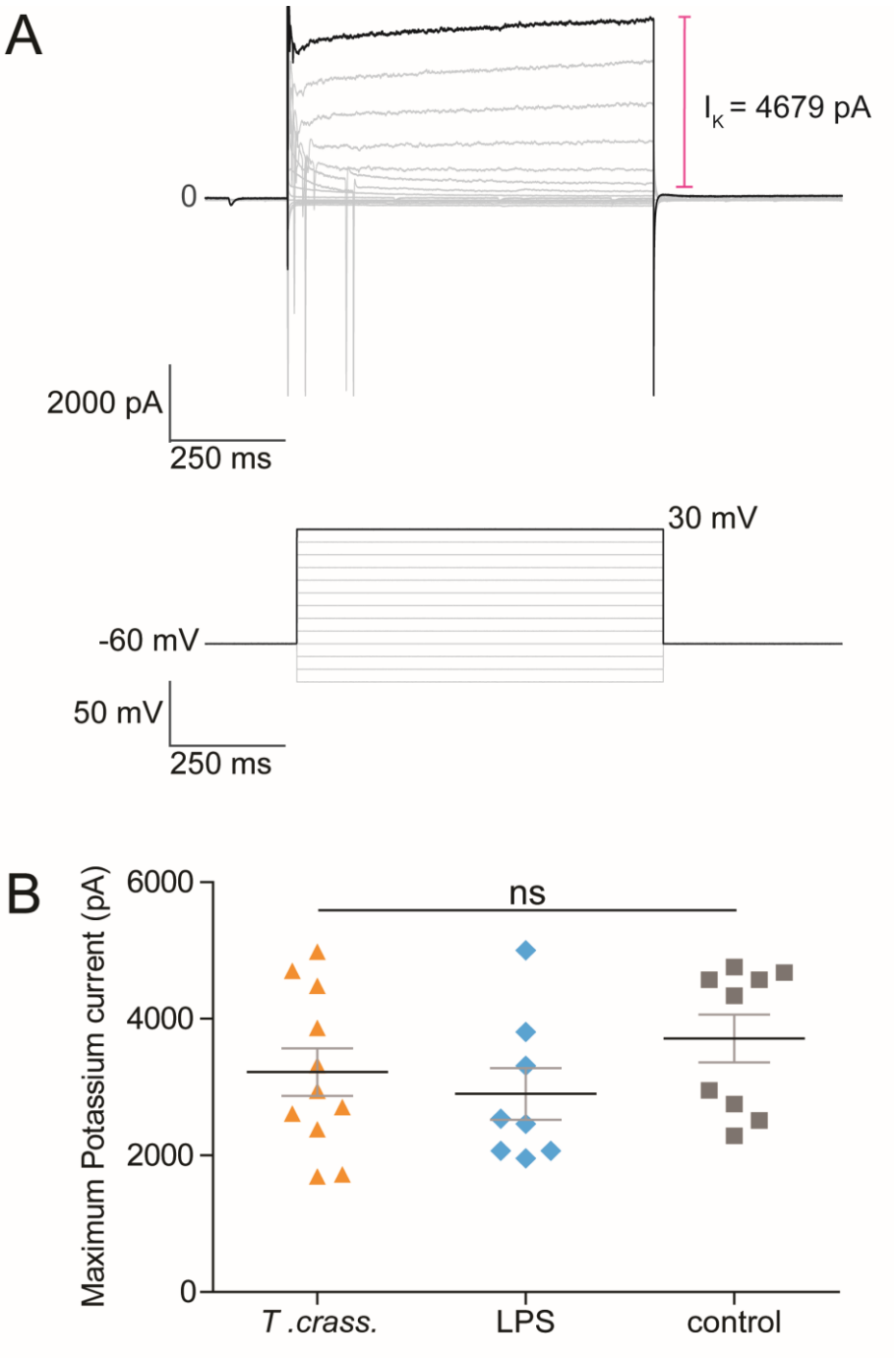

4.4 Sustained exposure to *Taenia crassiceps* homogenate does not affect the maximum size of potassium currents in neurons.
Whole–cell patch-clamp recordings in voltage clamp mode were made from CA3 pyramidal neurons in mouse hippocampal organotypic slice cultures. Slices were treated for 24 hours pre-electrophysiological recording with either; 50 µg/ml *Taenia crassiceps* homogenate, 10 µg/ml LPS or standard growth media. A) Example trace showing the measurement of the maximum K^+ current in voltage clamp following a positive voltage step to 30 mV. B) The mean maximum K^+ current was not significantly different between the groups. Values with means ± SEM; ns = not significant, each data point represents a cell.

4.6 SUSTAINED EXPOSURE TO *TAENIA CRASSICEPS* HOMOGENATE DOES NOT AFFECT THE EXCITABILITY OF THE NEURONAL NETWORK.

In order to understand if treatment with *T. crass.* makes the neuronal network more excitable I used the well-established 0 Mg^{2+} model to investigate how quickly the network would enter epileptiform states given this excitatory stimulus. I compared the time to first seizure-like event (SLE) as well as the power spectral density for each recording.

Seizure-like events could be identified by large depolarizations of the neuronal membrane potential with rapid firing of action-potentials lasting more than five seconds. SLEs were also observable as large increases in signal power (4.5 A).

The median power in the frequency range (1-100 Hz) from the start of recording for each of the *T. crass.*, LPS and media groups were 0.018 mV^2/Hz (IQR 0.005 – 0.115 mV^2/Hz, N = 12), 0.011 mV^2/Hz (IQR 0.005 – 0.025 mV^2/Hz, N = 6) and 0.027 mV^2/Hz (IQR 0.019 – 0.065 mV^2/Hz, N = 11), respectively and were not significantly different from one another ($p > 0.05$, Kruskal-Wallis test, 4.5 B).

The median power from the start of the first SLE for each of the *T. crass.*, LPS and media groups were 0.031 mV^2/Hz (IQR 0.011 – 0.210 mV^2/Hz, N = 12), 0.069 mV^2/Hz (IQR 0.028 – 0.252 mV^2/Hz, N = 6) and 0.069 mV^2/Hz (IQR 0.052 – 0.179 mV^2/Hz, N = 11), respectively and again were not significantly different from one another ($p = 0.50$, Kruskal-Wallis test, 4.5 C).

The median time from the start of 0 Mg^{2+} wash in to the first SLE for each of the *T. crass.*, LPS and media groups were 354.2 s (IQR 316.4 – 580.6 sec, N = 12), 396.3 s (IQR 359.7 – 553.8 sec, N = 7) and 354.6 s (IQR 335.5 – 378.7 sec, N = 11), respectively. No significant difference was observable between the groups ($p > 0.05$, Kruskal-Wallis test, 4.5 D).

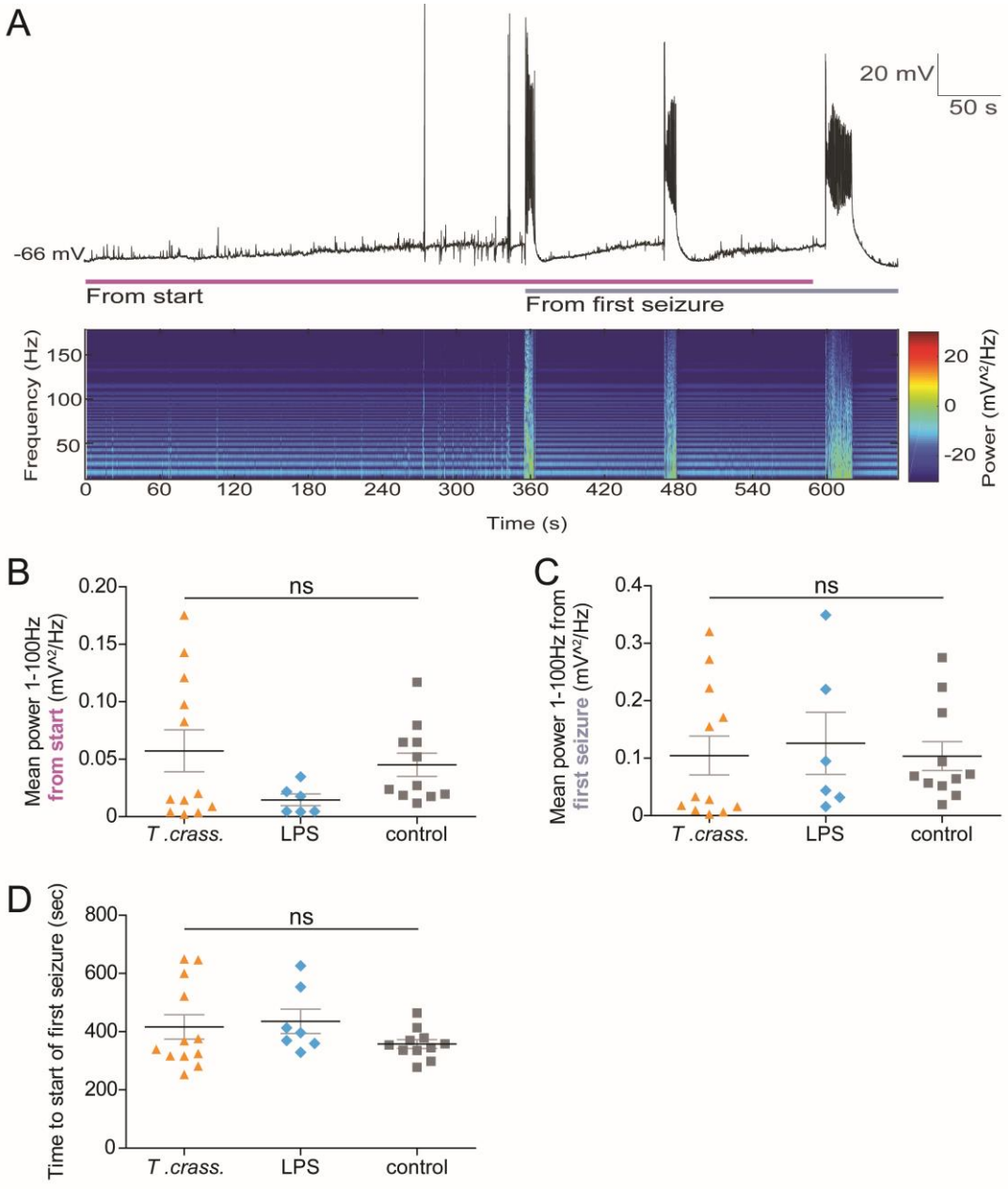

4.5 Sustained exposure to *Taenia crassiceps* homogenate does not affect the excitability of the neuronal network.

Whole–cell patch-clamp recordings were made from CA3 pyramidal neurons in mouse hippocampal organotypic slice cultures. Slices were treated for 24 hours pre-electrophysiological recording with either; 50 µg/ml *Taenia crassiceps* homogenate, 10 µg/ml LPS or standard growth media. A) The 0 Mg2+ model was then used to elicit seizure-like activity. Top, neuronal membrane potential following wash in of the 0 Mg2+ solution. Bottom, spectrogram indicating the signal power at each frequency. B & C) Neither the mean power (1-100 Hz) from the start nor the mean power from the first SLE were significantly different between the groups. D) The time to first SLE was also not significantly different between the groups. Values with means ± SEM; ns = not significant each data point represents a cell.

4.7 DISCUSSION

In Chapter 3 I described the discovery that *T. crass.* (and *T. solium*) larvae contain and actively produce glutamate, which is the mechanism by which the larval homogenate is able to have a depolarising effect on neurons, with the potential to evoke epileptiform activity under the correct conditions. However, that set of experiments only explored the very acute effects (ms to s) of larval homogenate, without being able to probe effects on longer-term processes, such as innate immunity, gene expression or second messenger cascades. Therefore in the current chapter I investigated possible longer term effects on neuronal intrinsic properties and network excitability elicited by 24 hour application of *T. crass.* homogenate and also compared this to LPS application, a known inflammatory stimulant.

My overriding, and perhaps surprising finding, was that for all of the many metrics tested, I found no detectable difference between *T. crass.* homogenate treated and control brain slices. That is, 24 hours of exposure to *T. crass.* homogenate drove no differences in neuronal membrane properties, active firing properties nor overall network excitability. Potential changes could either have been driven by the glutamate in the homogenate (as identified in Chapter 3) or by some hitherto unidentified factor. Given that I observed no changes, it is worth considering why the glutamate in the homogenate appeared to drive no changes in the slices. Using our glutamate measurements of the *T. crass.* homogenate taken in Chapter 3 I calculated that treating the slices with *T. crass.* homogenate at a concentration of 50 µg protein / ml equated to a final concentration in the media of 3 µM of glutamate. This is ultimately not a particularly high extracellular glutamate concentration as the concentration of glutamate in normal cerebrospinal fluid is 10 µM (Moussawi *et al.* 2011) and estimates of brain physiological extracellular glutamate concentration range from 0.02 to 30 µM (Herman and Jahr 2007; Chefer *et al*. 2015). In addition, it is quite possible that glutamate uptake mechanisms by neurons and glia would have further reduced the extracellular concentration of *T. crass.* derived glutamate (*i.e.* below the initial 3 µM) (Moussawi *et al.* 2011). At this low concentration of glutamate (< 3 µM), it is perhaps unsurprising that we did not see any evidence of changes in intrinsic properties or network excitability as these typically require extended exposure to much higher concentrations of glutamate (Ziobro, Deshpande, and DeLorenzo 2011).

Given that glutamate in the *T. crass.* homogenate at the concentrations used was unlikely to drive changes in excitability it is therefore interesting to note that other potential factors in the homogenate also did not drive any changes in intrinsic properties or network excitability. There are several potentials reasons for this. Firstly, it is possible that the concentration of *T. crass.* homogenate was too low (50 µg protein / ml). I was unable to increase this further without significantly modifying the composition of the media. At the concentration used, the *T. crass.* homogenate consisted of approximately 5 % of the total volume of media.

Nonetheless larval derived secreted factors or homogenate at concentrations well below 50 µg protein / ml have been shown to modulate inflammatory signalling (Palma *et al.* 2019; Y. Sun *et al.* 2014; Emilia Vendelova *et al.* 2016; Amit *et al.* 2011; Prasad *et al.* 2009). Therefore if factors within the *T. crass.* homogenate were to stimulate neurons either directly or via modulating inflammatory signalling, we would expect this to occur at the concentration utilised. As a result we can conclude that *T. crass.* homogenate exposure does not drive changes in neuronal excitability over a 24 hour timescale. Future work could expose brain slices to *T. crass.* larval product for longer than 24 hours. To my knowledge no studies have looked at the functional properties of cells following exposure to *T. crass.*, so there are no comparisons to draw as of yet in terms of the optimal length of exposure to begin to alter neuronal properties.

It has long been suggested that neuroinflammation plays a key role in the epileptogenic process (Vezzani *et al.* 2011). LPS is a potent and prototypical inflammatory stimulant which is known to cause classical activation of microglia and the release of inflammatory cytokines (Lively and Schlichter 2018; Papageorgiou *et al.* 2016). It was thus surprising that our intended positive control consisting of 24 hrs of LPS application did not drive particularly strong changes in neuronal intrinsic properties or network excitability. However, I did observe that LPS increased the action potential threshold in the neurons, making them less excitable. In many of the other metrics, despite not reaching the $p < 0.05$ threshold, the general trend of LPS exposure was to reduce the excitability of neurons and the network. It was therefore surprising to observe that this potent inflammatory stimulant, was having a mild inhibitory effect. However, this finding is consistent with the literature. For example, Hellstrom *et al.* (2005), found that one week exposure of organotypic hippocampal brain slices with 100 ng/ml of LPS also increased the action potential threshold of neurons and reduced excitability.

It is also worth noting the *T. crass.* homogenate did not result in the same moderate changes as LPS, which suggests that perhaps the homogenate used did not drive an inflammatory response in the same way as LPS, although this would be better assessed by measuring cytokine release or changes in microglial morphology.

It is also possible that we saw no changes due to the “type” or “state” of the *T. crass.* larvae prior to homogenization. It is known that whilst *Taenia* larvae are viable / alive within the brain, patients are typically asymptomatic (Stringer *et al.* 2003; Y. Sun *et al.* 2014), and that it is only once the larvae die naturally, or are killed using anti-helminthic agents that the likelihood of seizures occurring increases (Verma *et al.* 2010; Nash, Pretell, and Garcia 2002). In my experiments, *T. crass.* homogenate was prepared from live, viable larvae which were first freeze-thawed to lyse the cells before homogenization. Perhaps, a factor that could possibly

increase neuronal excitability is only present in dead or dying larvae. Future work could use *T. crass.* homogenate where the larvae are either starved or treated with anti-helminthic agents to see if this might contain additional factors, which could modulate neuronal excitability in this paradigm.

Lastly, the organotypic brain slice model, whilst containing all resident brain cells including microglia, lacks cells of the adaptive immune response such as T helper type 1 cells and/or natural killer cells. It is possible that for *T. crass.* homogenate to evoke seizures, a fully integrated immune response and/or blood brain barrier disruption is required. It is also possible that longer exposure to the *T. crass.* homogenate (longer than 24 hours) is required in order to generate an effect either mediated by immune signalling or otherwise. To address these issues, in the following chapter I set out to establish an *in vivo* model of NCC, whereby *T. crass.* homogenate was repeatedly injected into the cortex and hippocampus of freely moving rats over several weeks.

Chapter 5

THE CHRONIC EFFECTS OF *TAENIA CRASSICEPS* ON NEURONS *IN VIVO*

5.1 INTRODUCTION

In Chapter 3 I observed that *T. crass.* had an acute excitatory effect on neurons mediated by glutamatergic signalling. However, in Chapter 4, a 24 hour exposure to *T. crass.* homogenate *in vitro*, did not alter the excitability of individual neurons nor the network. Whilst the organotypic brain slice culture model retains innate immune cells such as microglia, a key difference between it and the human disease condition is the presence of an adaptive immune response. Neuroinflammation is thought to play an important role in epileptogenesis (Vezzani *et al.* 2011), therefore in this chapter I sought to investigate whether challenging an intact animal with *T. crass.* larval product could lead to the development of seizures similar to those seen in human NCC. In effect I sought to create an *in vivo* animal model of NCC resulting in seizures.

Only a handful of studies have attempted to generate *in vivo* animal models of NCC, and most either did not track or measure seizure occurrence, the main phenotypic feature of NCC, or only recorded seizures for up to several hours (Stringer *et al.* 2003; Robinson *et al.* 2012), when in humans the disease has a time course more akin to years. One study by Verastegui *et al.* (2015) injected activated oncospheres of *T. solium* into rats and monitored them sporadically for between 4 and 6 months. In order to recapitulate the time-course of the disease from the moment when the tapeworm larvae die, I injected larval homogenate, rather than activated oncospheres. Symptoms can often take months to years to develop in people with NCC therefore it was important to monitor animals for possible seizure activity for a long enough time period. The rats used in this study were approximately 3 months of age (young adults) at the time of the surgery and as such between 10.5 and 11.8 rat days would equate to 1 human year (Andreollo *et al.* 2012; Sengupta 2013). Therefore, the chosen 12 week (84 day) experimental timeline would equate to between 7.12 and 8 human years (e.g. 84 / 11.8 rat days = equivalent # human years) and would afford enough time to effectively model NCC disease progression.

In this chapter, homogenate of *T. crass.* larvae were injected intradermally as well as intracranially and the animals were monitored continuously using wireless ECoG. This is the first time, to my knowledge, that such technology has been utilised in a model of NCC. In addition, this technique enabled the recording of a full range of ECoG representing different brain activity corresponding to rest, wakefulness, anaesthesia as well as seizures following injection of a known pro-convulsant. All the while rats were able to perform all of their normal behaviours in their cage unhindered. After the 12 weeks of recording, an intradermal and 3 intracranial injections of *T. crass.* larval homogenate, and a seizure threshold test, the brains were harvested for fluorescent immunohistochemical labelling of astrocytes and microglia.

In this chapter I found that intradermal and intracranial injections of *T.crass.* homogenate did not result in the development of seizure activity *in vivo* and did not affect the seizure threshold in these animals. Astrocytes appear to be unaffected in this model of NCC but microglial morphology showed some changes in response to *T. crass.* injection.

5.2 SETUP AND PROCEDURE FOR RECORDING ECOG IN FREELY MOVING RATS.

To establish the method for chronic, continuous recording of ECoG in rats I utilised wireless telemetry which included a transmitter and receiver from Open Source Instruments (OSI). Electrodes placed into the brain parenchyma enabled the activity of the nearby neurons to be recorded, this information was sent wirelessly via a subcutaneous transmitter to a receiver coil near the animal's cage. From there signals were recorded and analysed by Neuroarchiver software running on a laptop. The wireless nature of the system allowed for the rat to go about all their regular activities; eating, sleeping and grooming, and allowed for 24 hour per day recordings to be made. This is vital for the development of any seizure type model as the chance of missing a seizure would be high were the recording time limited. Seizures are sometimes more common during certain behavioural tasks depending on where the epileptic focus is in the brain, so having the technology to record wirelessly while a rat exhibits all of his regular behaviours was ideal.

The OSI transmitter and battery are situated inside of a well-insulated, round container during fabrication that is small enough to sit comfortably within an adult rat but is also large enough to contain a battery that can power the transmitter for over 12 weeks (Figure 5.1 A). During surgery a large, subcutaneous pocket was made over the dorsum of the animals into which the transmitter was placed such that the transmitter coil (wire with transparent insulation) and body sit adjacent to the incision site, which was then well stitched (Figure 5.1 C). A subcutaneous tunnel was made from this pocket so that the two electrode wires (orange and

black) burrowed up the right side of the body to the cranium where they reached an oval-shaped skin excision exposing the skull (Figure 5.1 C). Burr holes were drilled through the skull at 2 locations on contralateral sides for placement of the electrodes into the cortex of each recording site. The wire ends of each electrode were prepared; stripped, straightened and bent at a 90° angle; and then inserted through the hole in the skull into the brain. Each electrode was held in place by either a screw or cannula (Figure 5.1 C). A further partial burr hole was drilled and into it was placed the 'fixing screw' which helped to add stability to the final headpiece construction when the dental cement was added (Figure 5.1 B).

The locations and depth of the electrodes for both hemispheres was kept consistent for all rats and was calculated using 'The Rat Atlas in Stereotaxic Coordinates, 6th edition (Paxinos and Watson 2007). The reference electrode location was in the visual cortex (V2) above the hippocampus (CA1) of the left hemisphere (injections into both the hippocampus and the cortex for half of the rats, X: -2.60 mm, Y: -4.44 mm) and the recording electrode location was in the visual cortex (V1) of the right hemisphere (injection into the cortex for all rats, X: +3 mm, Y: -7 mm) (Figure 5.1 D, F).

Once surgery was complete and the electrodes were fixed in place, rats were housed in a standard rat cage placed inside of a faraday cage, with a receiver coil to transmit the ECoG signals to a nearby laptop (Figure 5.1 E). ECoG was recorded 24 hours per day for the full 12 weeks giving a reliable indication of the state of activity of the rats' brains.

5.3 CHARACTERISATION OF RECORDED ECOG PATTERNS IN FREELY MOVING RATS.

In order to validate that the recording system was working correctly I analysed some initial ECoG and found that I could easily characterise different waveforms based upon the activity of the rat. Baseline activity consisted of low amplitude but varied signals with no discernible pattern (Figure 5.2 A).

I noted alpha waveforms when the rats were deeply relaxed or about to fall sleep, with notable enhanced spectral power at 8 Hz (Figure 5.2 B). Characteristic slow wave oscillations in the 2 – 4 Hz range (Delta waves) were seen when rats were sleeping (Figure 5.2 C).

The most extreme change observed was the marked reduction in ECoG activity when rats were anaesthetised (Figure 5.2 D) and the burst suppression observed when rats were exiting or entering a deeply anaesthetised state (Figure 5.2 E).

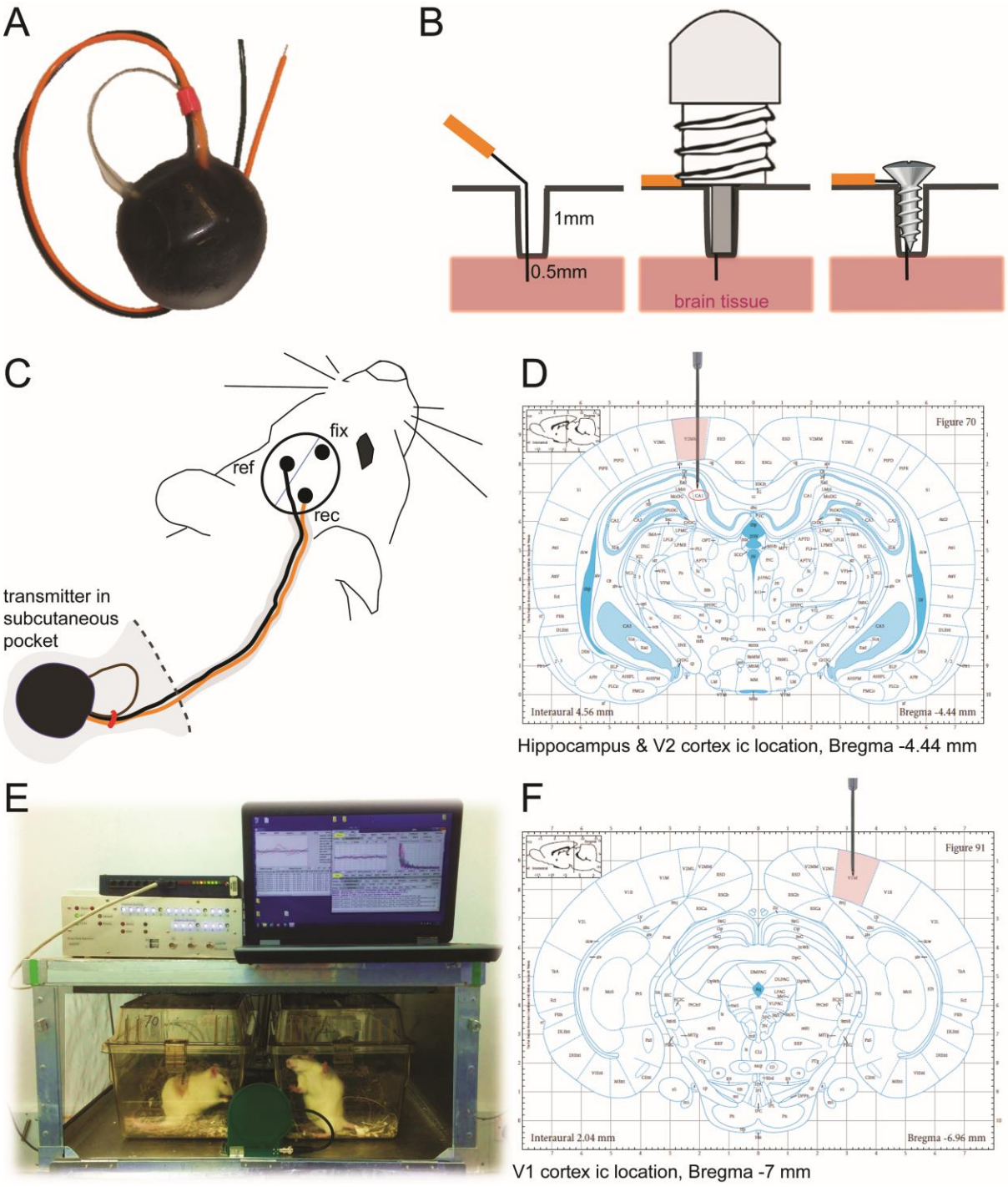

Figure 5.1 Setup and procedure for recording ECoG in freely moving rats.
A) OSI wireless transmitter; black battery pack, transmitter coil, recording electrode (orange) and reference electrode (black). B) The end of each electrode was placed through a burr hole in the skull into the brain parenchyma, where it was secured in place either by a cannula or by a screw. C) The wireless transmitter body was placed into a subcutaneous pocket over the dorsum from which the electrode wires were subcutaneously tunnelled to the cranium where each was fixed in place over their designated burr hole. D) The reference electrode was placed in the left hemisphere at bregma -4.44 mm. F) The recording electrode was placed in the right hemisphere at bregma -6.96 mm. E) The setup of two rat cages side by side inside a faraday cage (to reduce electrical noise) with the green receiver coil and signal transduction and recording equipment above.

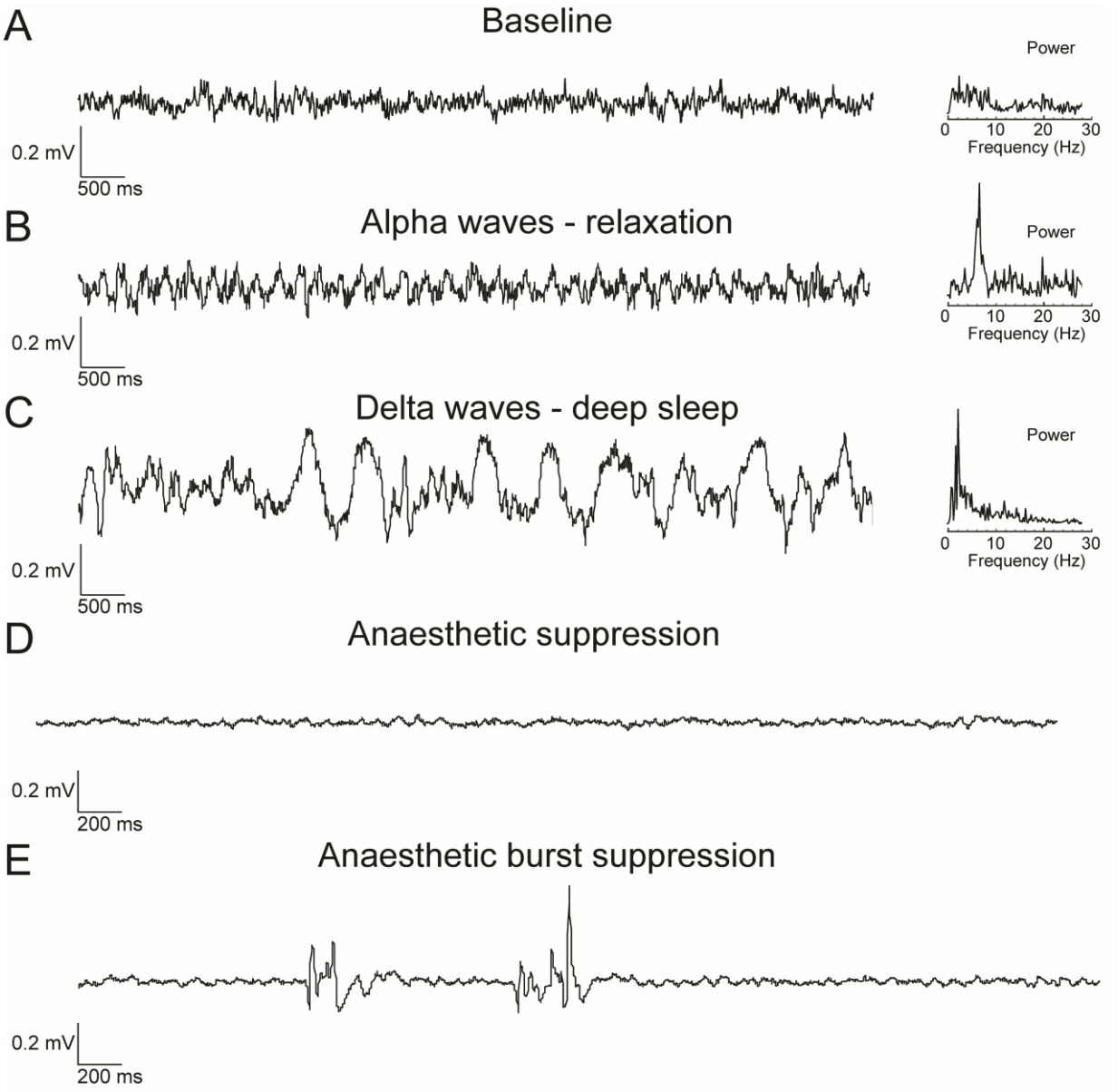

Figure 5.2 Characterisation of recorded ECoG in freely moving rats.
A) Characteristic baseline ECoG. B) Alpha waves with a predominant frequency of 8 Hz were observed when rats were relaxed. C) Delta waves with a predominant frequency of 3 Hz were observed when rats were sleeping. D) Suppression of ECoG was observed when rats were fully anaesthetised. E) Characteristic “burst suppression” was observed when rats were lightly anaesthetised or waking from anaesthesia.

5.4 CHARACTERISATION OF RECORDED ECoG FOR AUTOMATED SEIZURE DETECTION IN FREELY MOVING RATS.

A batch classifier was used to automatically identify and classify different waveforms, but most specifically ictal-like events. An 'Event library' of examples was built for the batch classifier to use to identify each type of ECoG event. The Event Classifier application (OSI) was used to do the batch classification by classifying 1 s segments of ECoG according to several metrics (coastline, intermittency, coherence and spikiness) enabling similar events to cluster together when plotted according to the metrics. Each type of event (*e.g.* chewing artefact, ictal-like events) formed separate clusters (coloured accordingly, Figure 5.3 A). Also depicted are example traces of baseline and ictal-like activity from the library as well as the type of ECoG I saw when the rats were grooming (and therefore touching their headpieces).

To further ensure the recording set up and batch classifier could reliably detect seizures should the injection of *T. crass.* result in them, one rat was injected intracranially with picrotoxin (400 nl, 10 µM), an excitotoxin, to serve as a positive control. Seizures (such as the one depicted in Figure 5.3 B & C) were recorded for 2 hours before they ceased spontaneously. These ECoG recordings demonstrated the distinct repetitive spikes characteristic of seizure-states (Figure 5.3 C) reflecting ictal activity. Seizures differed in length; some could be approximately 30 seconds long (Figure 5.3 B) whilst others were shorter (Figure 5.3 D). This demonstrated that my recording system could sensitively detect seizure activity should it occur.

5.5 INJECTION OF *TAENIA CRASSICEPS* HOMOGENATE DOES NOT RESULT IN THE DEVELOPMENT OF SEIZURE ACTIVITY *IN VIVO*.

Confident in my ability to detect seizures, I next proceeded with the full experimental timeline. This included 12 weeks of ECoG recordings in the following manner. 2 weeks of baseline recordings were performed post electrode implantation, following this all the animals (both control and experimental groups) were injected intradermally with *T. crass.* homogenate in Freund's incomplete adjuvant (100 µl) at the same time experimental animals received intracranial injections of *T. crass.* homogenate (600 nl per injection site, maximum of 1.8 µl) whilst control animals received identical injections of PBS containing an equivalent quantity of endotoxin as the *T. crass.* homogenate. 2 weeks later, and 2 weeks after that, the animals received further repeat intracranial injections. For the final intracranial injection, injected volumes were doubled. Following a further 6 weeks of ECoG recordings (*i.e.* a total of 12

weeks) animals underwent a seizure threshold test using intracranial injection of picrotoxin (Figure 5.4 A).

The wireless transmitter technology made it possible to record 24 hours/day, yielding a significant amount of data to process but safeguarding the emergence of even subtle differences between groups. First I quantified the number and frequency of 1 s segments classified as ictal-like events in *T. crass.* injected vs control animals. These ictal-like events were 1 s segments of ECoG recordings which met the classification criteria as demonstrated in Figure 5.4 A, but which did not necessarily reflect actual seizures. Although there was significant variability between animals, the mean number of ictal-like events detected per day for the *T. crass.* and control groups did not differ substantially over the course of the 12 week study and did not differ significantly from one another (Figure 5.4 B). In addition, the number of ictal-like events did not increase following each intracranial injection of *T. crass.* The number of ictal-like events detected was a median of 1952 events per day (IQR 1588 – 2225, N = 8) for the *T. crass.* group and a median 1332 events per day (IQR 1196 – 1386, N = 3) for the control group. The large majority of these likely reflect false positives as I designed the library in order to stringently limit false negatives, as I wanted to be sure to capture all possible seizures, which were defined as 5 consecutive ictal-like events (see below).

The *T. crass.* and control groups also do not differ in terms of the number of ictal-like events per hour over the 12 weeks (Figure 5.4 C). When the seizure-threshold test was conducted on Day 89 by injecting picrotoxin, it was clear that the number of ictal-like events detected increased dramatically. This confirmed the ability of the algorithm to detect possible seizures.

In order to possibly detect actual seizures, I used the batch-classifier to find instances where five 1 s ictal-like events occurred in succession, this would represent a 5 s long event with a strong likelihood of being a seizure. When these were detected, I visually verified each to rule out false positives (Figure 5.4 D). In this manner I observed that despite continuous recordings, 24 hours a day over 12 weeks (3 months), none of the animals had seizures. Both groups had a median of 0 detected seizures until the seizure-threshold test with picrotoxin, during which the *T. crass.* and control groups had a median of 7.50 (IQR 0 – 66.50, N = 6) and 9.00 (IQR 1 – 20.00, N = 3) seizures per hour, respectively, Figure 5.4 D). This revealed that serial intracranial injection of *T. crass.* homogenate did not result in the development of seizures.

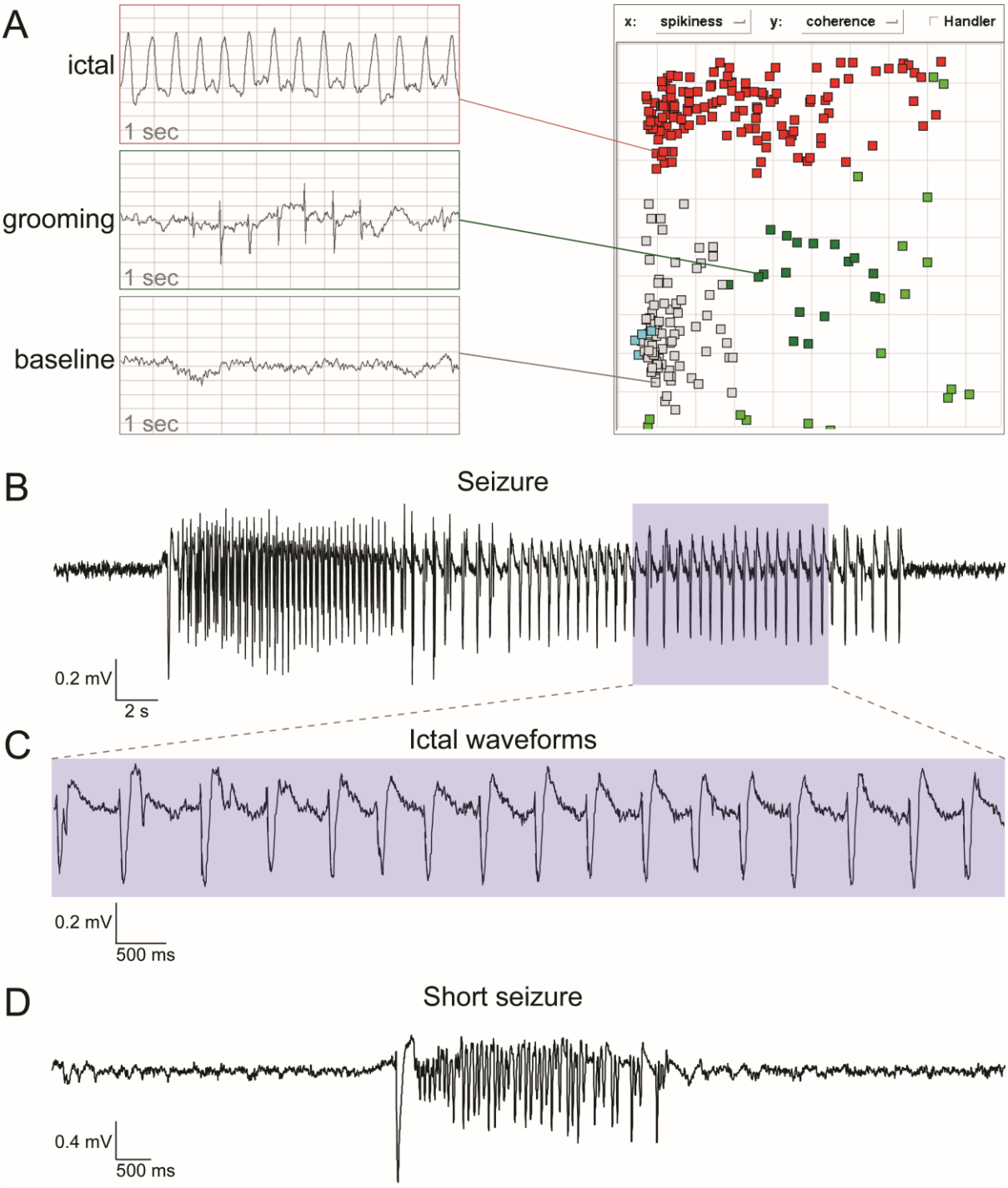

Figure 5.3 Characterisation of recorded ECoG for automated detection of seizures in freely moving rats. A) Batch classification utilised an 'event library' consisting of specific examples of 1 s traces recorded and identified as having occurred during different activities (ictal, grooming, baseline *etc.*) plotted here according to two of the four classification metrics used, spikiness and coherence. Note how the different activities cluster separately. B) Example of a definitive seizure recorded following picrotoxin injection to verify that the equipment could detect seizures reliably. C) A portion of (B) expanded to show the repetitive synchronous waveforms characteristic of seizures. D) Another example of a seizure of shorter duration.

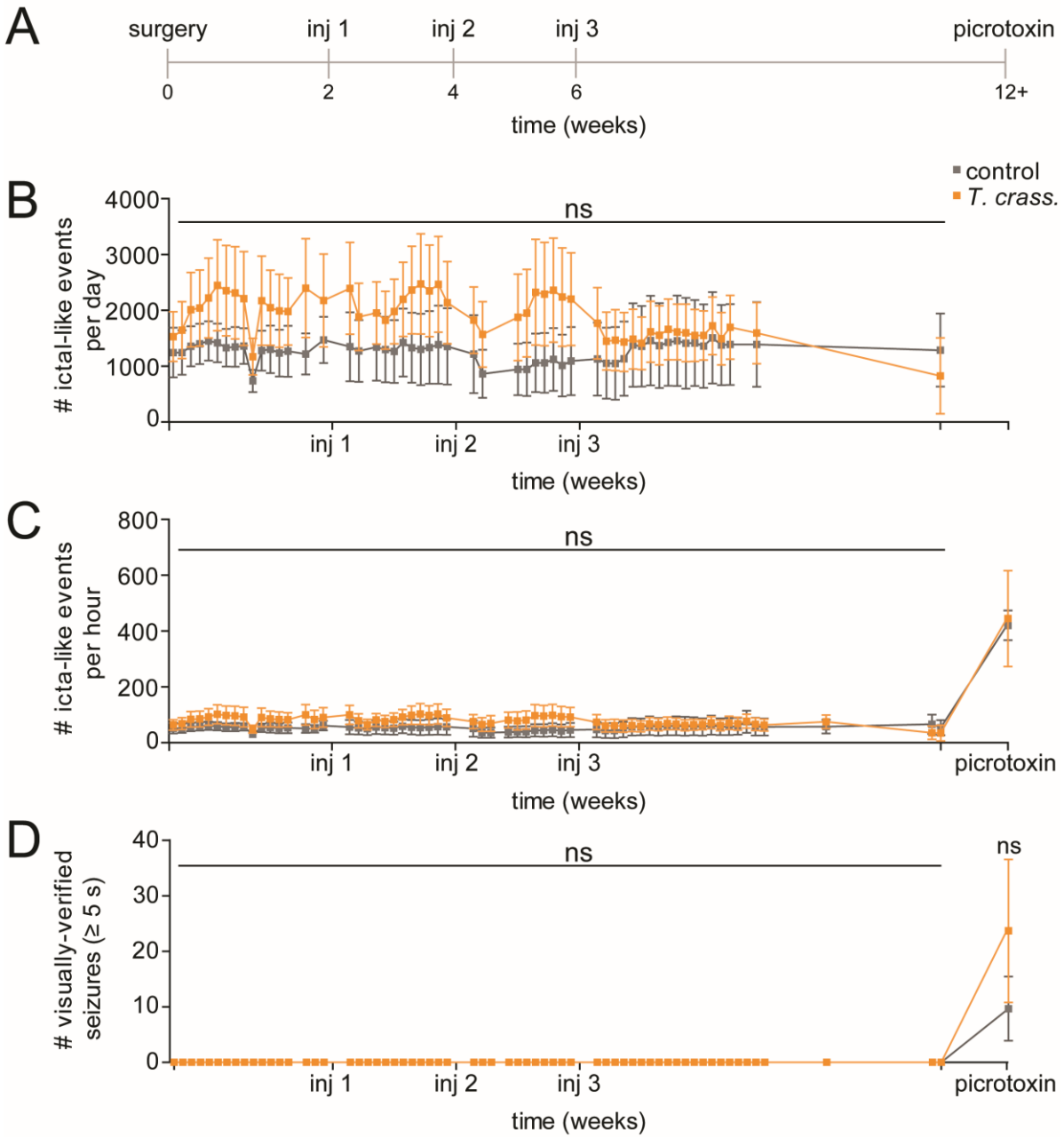

Figure 5.4 Injection of *Taenia crassiceps* homogenate did not result in the development of seizures *in vivo*.
A) ECoG was recorded from 10 rats for up to 12 weeks and analysed for ictal-like events to assess whether intracranial injection of *Taenia crassiceps* has any effect on neuronal circuitry, compared to the control condition. Following the surgery, two weeks of baseline recording were performed before the first injection both intradermally and intracranially. Thereafter, two more injections were performed at two week intervals followed after six weeks by the seizure threshold test. B) The number of detected ictal-like events per day did not differ between the *Taenia crassiceps (T. crass.)* group (n=6) and the control group (n=4) at any time interval during the 12 week experiment. C) The number of ictal-like events per hour did not differ significantly between the groups but did increase dramatically as a result of the picrotoxin injection at the end of the 12 weeks. D) The number of visually verified five second long ictal-like events was zero for both groups until the seizure threshold test, during which the two groups did not have a statistically different number of seizures. Values with means ± SEM; ns = not significant, n=10.

5.6 *TAENIA CRASSICEPS* HOMOGENATE DOES NOT AFFECT THE SEIZURE THRESHOLD OF NEURONAL NETWORKS *IN VIVO*.

Having determined that intracranial injection of *T. crass.* homogenate did not result in the generation of seizures I next wanted to assess whether it could alter neuronal networks in such a way as to make the brain more susceptible to seizures initiated via other means. That is, could the *T. crass.* homogenate lower the seizure threshold? To do so I used intracranial injection of picrotoxin at a relatively low dose, to potentially trigger seizures in the animals. Therefore, after the 12 weeks of ECoG recordings, 1 intradermal injection of *T. crass.*, 3 intracranial injections of *T. crass./*control saline, rats were briefly anaesthetised and injected with 400 nl of picrotoxin (10 µM, ic) to induce mild seizures lasting a couple of hours. Recordings were analysed for seizure activity using the batch classifier as before. The bulk of the animals developed pronounced electrographic seizure activity in response to the picrotoxin injection (Figure 5.5 A).

The number of ictal-like events that lasted for 1 or more seconds was determined for each rat, following picrotoxin injection. The median number of picrotoxin-induced ictal-like events per hour for the *T. crass.* and control groups were 361.8 (IQR 65.0 – 844.1, N = 6) and 390.0 (IQR 348.0 – 523.5, N = 3), respectively, and were not significantly different from one another ($p > 0.05$, Mann-Whitney U test, Figure 5.5 B).

The median number of picrotoxin-induced seizures (a seizure was detected when at least five consecutive ictal-like events occurred) per hour for the *T. crass.* and control groups were 7.50 (IQR 0 – 66.50, N = 6) and 9.00 (IQR 1.00 – 20.00, N = 3), respectively, and were not significantly different from one another ($p > 0.05$, Mann-Whitney U test Figure 5.5 C).

The median picrotoxin-induced seizure duration for the *T. crass.* and control groups were 13.38 (IQR 0 – 20.99, N = 6) and 15.20 (IQR 14.00 – 32.00, N = 3), respectively, and were not significantly different from one another ($p > 0.05$, Mann-Whitney U test, Figure 5.5 D).

As *T. crass.* homogenate did not result in a difference in the number or duration of picrotoxin induced seizures I could conclude that *T. crass.* homogenate did not appear to make the neuronal networks more susceptible or sensitive to induced seizure activity.

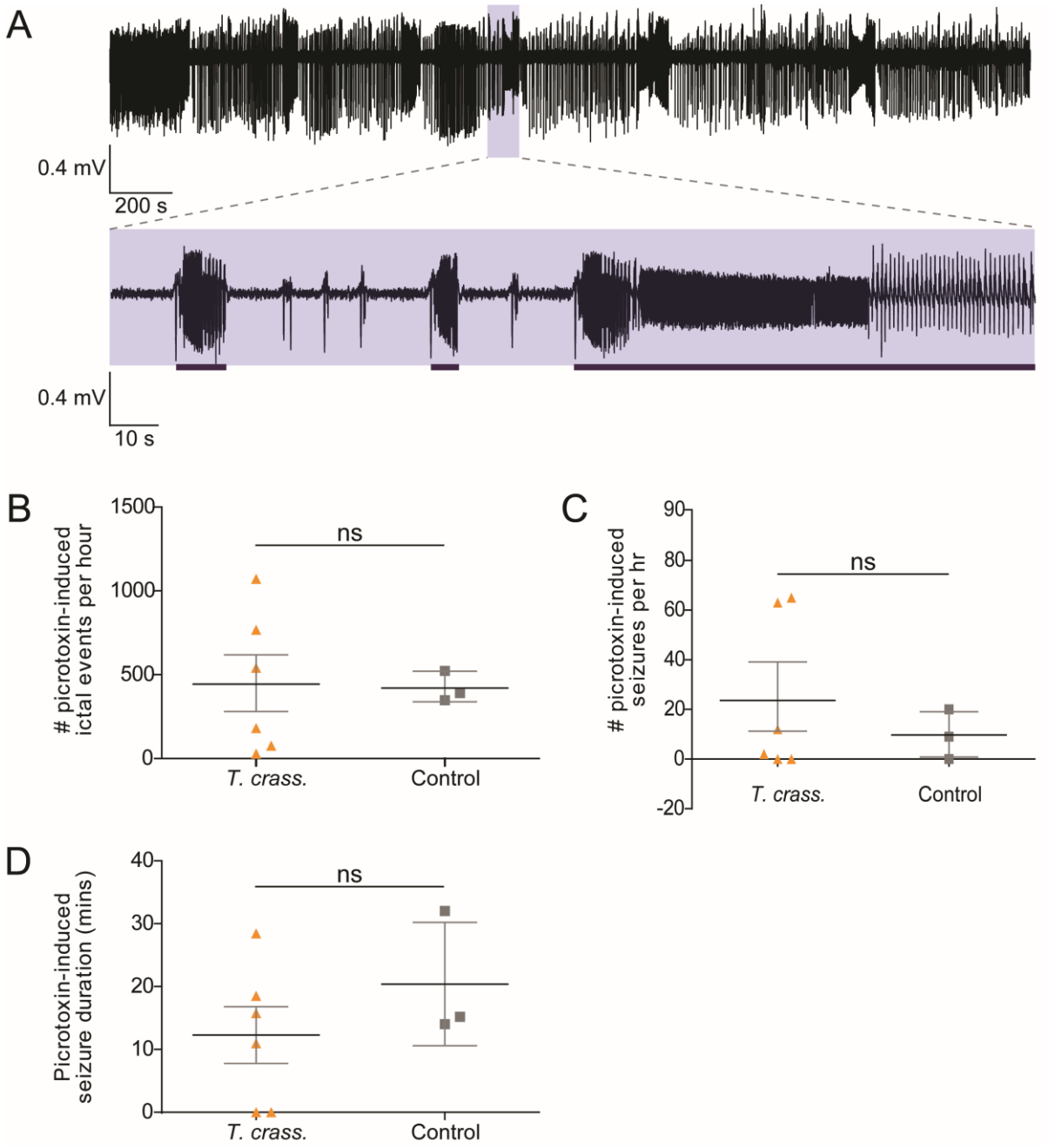

Figure 5.5 *Taenia crassiceps* homogenate did not affect the seizure threshold of neuronal networks *in vivo*.
A) An example ECoG trace following picrotoxin injection with a portion expanded below (blue box) to show three distinct seizures of differing lengths. B) The number of picrotoxin-induced ictal-like events (ictal-like events are 1 s of ECoG trace with the features of ictal activity) (per hour was not significantly different between the *Taenia crassiceps (T. crass.)* group (n=6) and control group (n=3). C) Picrotoxin-induced seizures were detected as at least 5 consecutive ictal-like events, which could last five seconds or longer. The number of these did not differ significantly between the groups. D) The picrotoxin-induced seizure duration was not different between *T. crass.* and control groups. Values with means ± SEM; ns = not significant, n=9.

5.7 ASTROCYTE STAINING WAS NOT AFFECTED BY *TAENIA CRASSICEPS* HOMOGENATE INJECTION.

Since *T. crass.* does not result in the generation of seizures or indeed in a predisposition to seizures within our 12 week model, I next wanted to assess whether it could result in any changes to the surrounding glial cells, which could constitute a neuroinflammatory response. Astrocytes respond to tissue injury and foreign antigens. Their dysregulation may contribute heavily to the generation of seizure activity (Sofroniew 2005) and *T. solium* larval product has been shown to modulate the release of chemokines from astrocytes (Uddin *et al.* 2005).

I therefore fluorescently labelled astrocytes using the anti-GFAP antibody. Glial fibrillary acidic protein (GFAP) is an intermediate filament protein predominantly expressed in astrocytes and clearly delineates the major astrocyte processes. It is a good indicator of glial scar formation as GFAP expression is typically increased surrounding areas of damage or neuroinflammation (Sofroniew 2005).

Tile scan images were taken of coronal sections of the brains of animals, which included the tract in the cortex made by the cannula and recording electrode in the right hemisphere (Figure 5.6 A). Higher magnification images (200x magnification) were taken of the area just below the electrode tract where the *T. crass.* homogenate / saline was injected to measure the amount of fluorescence associated with GFAP antibody staining. In addition, similar high resolution images were taken from a corresponding area in the left hemisphere (LH). The images taken of the LH, where no cannula or electrode had been placed, were used to normalise fluorescence measurements and account for any differences in staining between animals or slices (Figure 5.6 A). These normalised average fluorescence values for each image might reflect the number or activation status of astrocytes in the slice. The median normalised average GFAP fluorescence for the *T. crass.* and control groups were 111.3 % of LH (IQR 96.10 – 118.5 % of LH, N = 12) and 114.4 % of LH (IQR 108.6 – 145.5 % of LH, N = 6) respectively, and were not significantly different from one another ($p > 0.05$, Mann-Whitney U test, Figure 5.6 B).

I then analysed the number of pixels above a particular fluorescence threshold for each image in order to determine whether one condition potentially resulted in more astrocytes, more astrocytic processes, or more astrocytic scar material being present. Again values were normalised for each slice against a corresponding region from the opposite hemisphere. The median normalised GFAP-labelled pixels above threshold for the *T. crass.* and control groups were 179.5 % of LH (IQR 102.5 – 352.5 % of LH, N = 12) and 158.1 % of LH (IQR 82.73 – 512.5 % of LH, N = 6), respectively and were not significantly different from one another ($p > 0.05$, Mann-Whitney U test, Figure 5.6 C). The number of astrocytes or the amount of

GFAP expressed appears to not have been altered by intracranial injection of *T. crass.* homogenate.

5.8 MICROGLIAL STAINING WAS AFFECTED BY *TAENIA CRASSICEPS* HOMOGENATE INJECTION.

Microglia, as the resident macrophages of the nervous system, play an important role in epileptogenesis. Multiple studies suggest that neuroinflammation and excitability have a bi-directional effect on one another (Vezzani *et al.* 2011; Sheng *et al.* 1994; Ravizza *et al.* 2005; M. G. De Simoni *et al.* 2000; Balosso *et al.* 2008; Cerri *et al.* 2016; Maroso *et al.* 2011).

To assess potential microglial changes in my model, I fluorescently labelled microglia using the anti-Iba1 antibody. Ionized calcium binding adaptor molecule 1 (Iba1) is a protein that is involved in the phagocytic process (Ohsawa *et al.* 2004). It is found in all microglia, including at rest, but its expression is increased when microglia are classically activated. As such, increased Iba1 staining is indicative of an inflammatory response.

As before, tile scan images were acquired of coronal sections of the brains of animals, which included the injection tract in the cortex made by the cannula and recording electrode in the right hemisphere (Figure 5.7 A). Higher magnification images (200x magnification) were taken of the area just below the electrode tract where the *T. crass.* homogenate / saline was injected to measure the amount of fluorescence associated with Iba1 antibody staining. Again, similar high magnification images were taken from a corresponding area in the left hemisphere in order to normalise fluorescence measurements and account for any potential differences in staining between slices (Figure 5.7 A). The normalised average Iba1 fluorescence just below the injection site might represent the number or activation status of microglia. The median normalised average Iba1 fluorescence for the *T. crass.* versus the control groups was 114.0 % of LH (IQR 107.3 – 119.6 % of LH, N = 12) and 103.7 % of LH (IQR 99.13 – 111.0 % of LH, N = 6) respectively, and were not significantly different from one another ($p > 0.05$, Mann-Whitney U test, Figure 5.7 B).

I then also analysed the number of pixels above threshold for each image in order to ascertain whether one group might have had more numerous or enlarged cells. Once again values were normalised for each slice against a corresponding region from the opposite hemisphere. The median normalised number of Iba1-labelled pixels above threshold was increased for the *T. crass.* as compared to control groups (144.6 % of LH [IQR 104.5 – 225.1 % of LH, N = 12] versus 66.0 % of LH [IQR 52.04 – 105.3 % of LH, N = 6]). This was a statistically significant

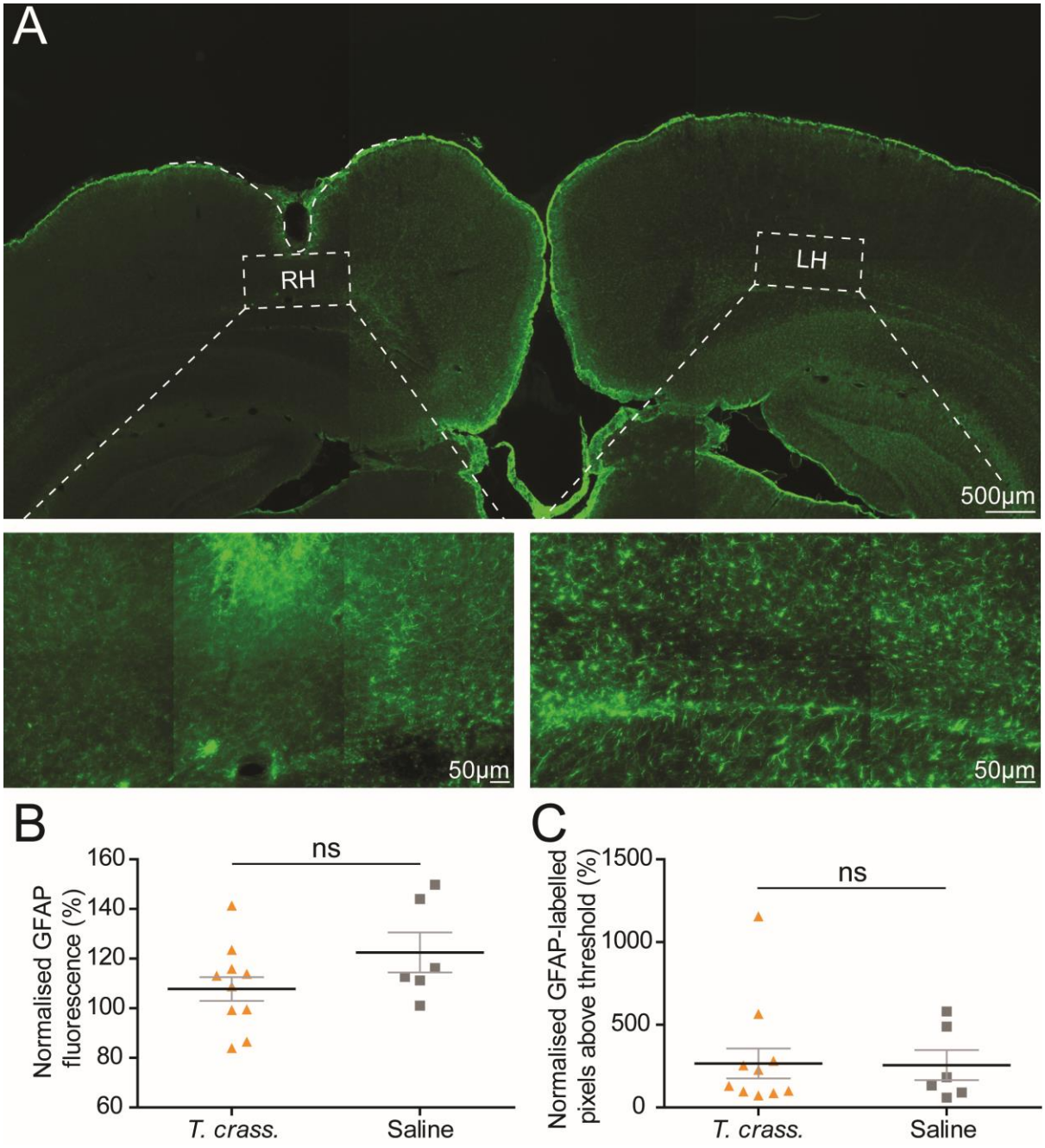

Figure 5.6 Astrocytes were not affected by *Taenia crassiceps* homogenate injection.
Rats were transcardially perfused and the brains processed and frozen for sectioning at 40 µm thickness. Fluorescent immunohistochemistry was then performed on the slices labelling astrocytes with an antibody against glial fibrillary acidic protein (GFAP), green. A) Top, overview tile scan using a confocal microscope of a coronal section containing both hemispheres. Bottom, higher magnification images (200x) were taken from specific regions of interest in the left and right hemispheres for average fluorescence and pixel comparisons. B) The average GFAP fluorescence from the region of interest below the *Taenia crassiceps (T. crass.)* injection site (normalised by an equivalent region of interest from the non-injected hemisphere) was not statistically different from that of the control group. C) The number of pixels with fluorescence values above a certain threshold from the same region of interest (again normalised by an equivalent region from the non-injected hemisphere) also did not differ significantly between the groups indicating that the astrocytes appear unaffected by the presence of *Taenia crassiceps* homogenate. Values with means ± SEM; ns = not significant, n=8.

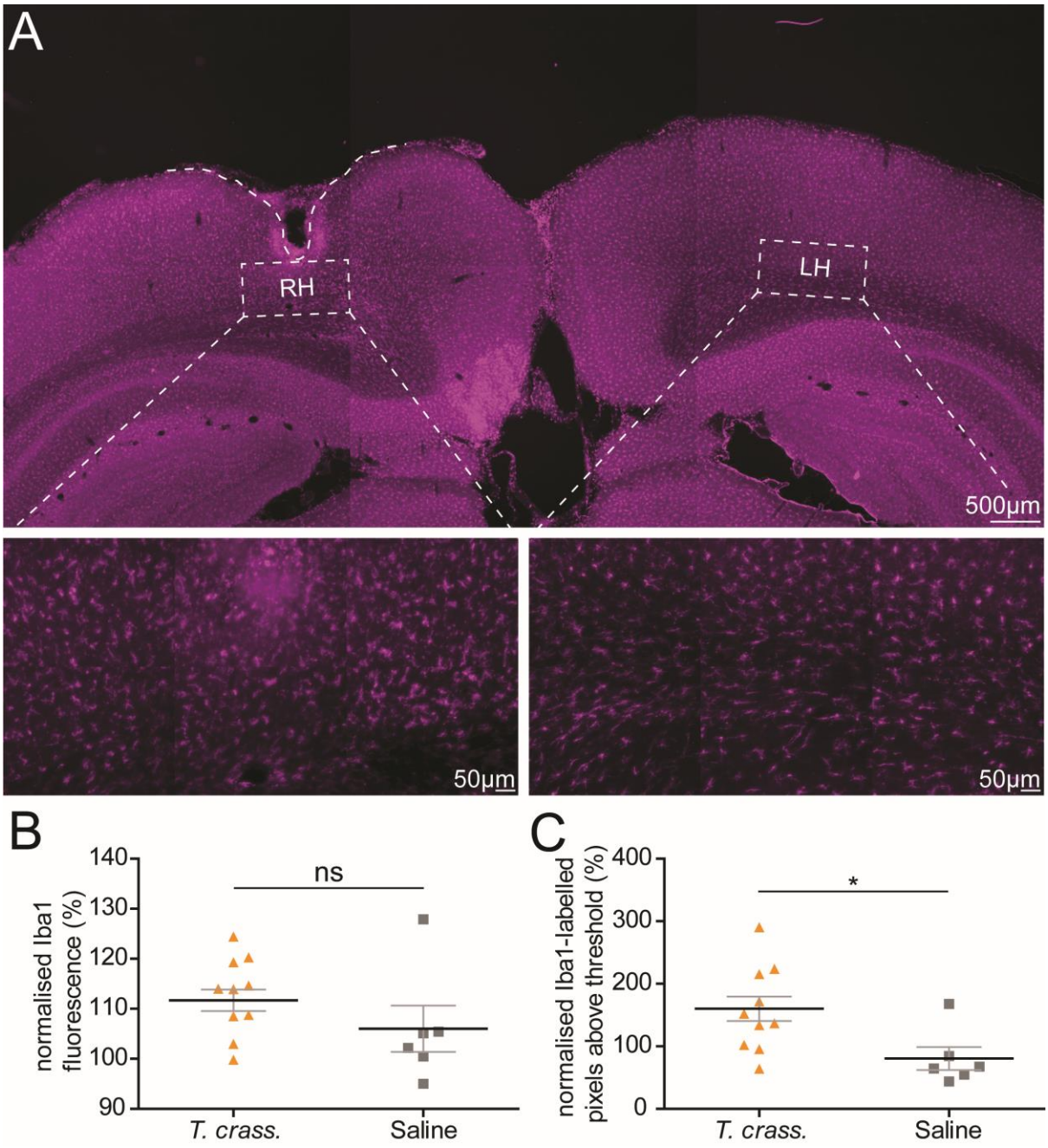

Figure 5.7 Microglial staining was affected by *Taenia crassiceps* homogenate injection.
Rats were transcardially perfused and the brains processed and frozen for sectioning at 40 µm thickness. Fluorescent immunohistochemistry was performed on the brain slices labelling astrocytes with an antibody against ionized calcium binding adaptor molecule 1 (Iba1), magenta. A) Top, overview tile scan using a confocal microscope of a coronal section containing both hemispheres. Bottom, higher magnification images (200x) were taken from specific regions of interest in the left and right hemispheres for average fluorescence and pixel comparisons. B) The average Iba1 fluorescence from the region of interest in the hemisphere injected with *Taenia crassiceps (T. crass.)* (normalised by the non-injected hemisphere) was not statistically different from that of the control group. C) However, the number of pixels with fluorescence values above threshold (and also normalised for the non-injected side) was significantly higher in the *Taenia crassiceps* group indicating either an increase in the number of microglia or that the size of microglial cells had increased. Values with means ± SEM; ns = not significant, n=8.

difference (p = 0.023, Mann-Whitney U test, Figure 5.7 A). This could indicate either an increase in the number of microglial cell bodies or an increase in the size of the cell bodies, or the size and number of their processes.

5.9 MICROGLIAL POPULATION SIZE AND SPATIAL CLUSTERING WERE UNAFFECTED BY INJECTION OF *TAENIA CRASSICEPS* HOMOGENATE.

Given the difference observed above in terms of Iba1-labelled pixels above threshold, I next sought to investigate whether this might be due to a change in the number or distribution of microglia following cortical *T. crass.* injection. To do so I performed further imaging at 630x magnification (using an oil immersion lens) of the area between the injection tract (above) and a white matter tract (below, both blacked out) (Figure 5.8 A). Microglia were then manually counted by placing a turquoise dot onto each and using Image J's count, area and nearest neighbour functions (Figure 5.8 B).

The median microglial density for the *T. crass.* and control groups were 674.4 cells/mm^2 (IQR 539.7 – 768.6 cells/mm^2, N = 5) and 546.4 cells/mm^2 (IQR 422.4 – 646.5 cells/mm^2, N = 3), respectively and were not significantly different from one another (p > 0.05, Mann-Whitney U test, Figure 5.8 C).

Since the number of cells did not differ between conditions I then sought to investigate whether the way the cells were distributed spatially might have differed. To determine this I performed several analyses. The first was a nearest neighbour measurement, which computes the distance to the closest neighbouring cell for each cell. The median nearest neighbour distance for the *T. crass.* and control groups were 25.70 mm^2 (IQR 24.91 – 29.17mm^2, N = 5) and 28.35 mm^2 (IQR 25.93 – 33.10 mm^2, N = 3), respectively and were not significantly different from one another (p > 0.05, Mann-Whitney U test, Figure 5.8 D). Next I computed the microglial spacing index which indicates how clustered (higher value) or spaced out (lower value) the cells are. The median microglial spacing index for the *T. crass.* and control groups were 4.53 AU (IQR 4.44 – 4.78 AU, N = 5) and 4.39 AU (IQR 4.35 – 4.63 AU, N = 3), respectively and again were not significantly different from one another (p > 0.05, Mann-Whitney U test, Figure 5.8 E). Thus the intracranial injections of *T. crass.* did not appear to alter the number or spread of microglia in the vicinity of the injection site.

5.10 *TAENIA CRASSICEPS* HOMOGENATE INJECTION INDUCED CHANGES IN MICROGLIAL MORPHOLOGY.

In order to investigate if there were any *T. crass.* induced changes to the morphology of the microglia I imaged approximately 20 individual microglia per slice again at 630x magnification (using an oil immersion lens). The imaged microglia were from the same area, *i.e.* surrounding the injection tract. I observed that the microglial processes appeared to be more elaborate and spread out further in the control group as compared to the *T. crass.* group (Figure 5.9 A & B).

One way to quantitatively analyse morphological changes is to measure the soma size and the spread of the microglial processes. I therefore traced out the soma for each cell in order to calculate its size (Figure 5.9 C). A polygon was then also drawn connecting the distal processes in order to calculate the process arbour area and shape (Figure 5.9 C).

The median arbour area for the *T. crass.* group was significantly smaller than the control group, at 680.4 μm^2 (IQR 369.1 – 1081 μm^2, N = 99) and 1156 μm^2 (IQR 866.1 – 1501.0 μm^2, N = 62), respectively ($p < 0.0001$, Mann-Whitney U test, Figure 5.9 D). This is of interest as a smaller arbour area could result from the retracting of microglial processes, which is a typical neuroinflammatory phenotype (Hui *et al.* 2019).

The shape of the microglial arbours could also potentially change as a result of microglial activation. I therefore also calculated the arbour circularity for each cell. The median arbour circularity for the *T. crass.* and control groups were 0.75 AU (IQR 0.68 – 0.81 AU, N = 99) and 0.76 AU (IQR 0.66 – 0.80 AU, N = 62), respectively and were not significantly different from one another ($p > 0.05$, Mann-Whitney U test, Figure 5.9 E).

It is also possible that the microglial soma sizes could be altered. I found that the median soma area for the *T. crass.* and control groups were 150.1 μm^2 (IQR 119.5 – 222.3 μm^2, N = 99) and 168.7 μm^2 (IQR 130.3 – 215.5 μm^2, N = 62), respectively and were not significantly different from one another ($p > 0.05$, Mann-Whitney U test, Figure 5.9 F). This means that even though the *T. crass.* group have shorter, retracted, processes their cell bodies were not enlarged compared to controls.

A further metric to quantify possible morphological differences between microglia is the morphological index. This is calculated by dividing the soma area by the arbour area. The median morphological index for the *T. crass.* and control groups were 0.24 AU (IQR 0.14 – 0.46 AU, N = 99) and 0.16 AU (IQR 0.11 – 0.22 AU, N = 62), respectively and were significantly different from one another ($p < 0.0001$, Mann-Whitney U test, Figure 5.9 G). This measure demonstrates that the *T. crass.* group had shortened/retracted microglial processes relative to their soma size as compared to the control condition. This measure provides evidence that

T. crass. injection caused microglia to have retracted processes, one morphological characteristic of enhanced activation of this cell type.

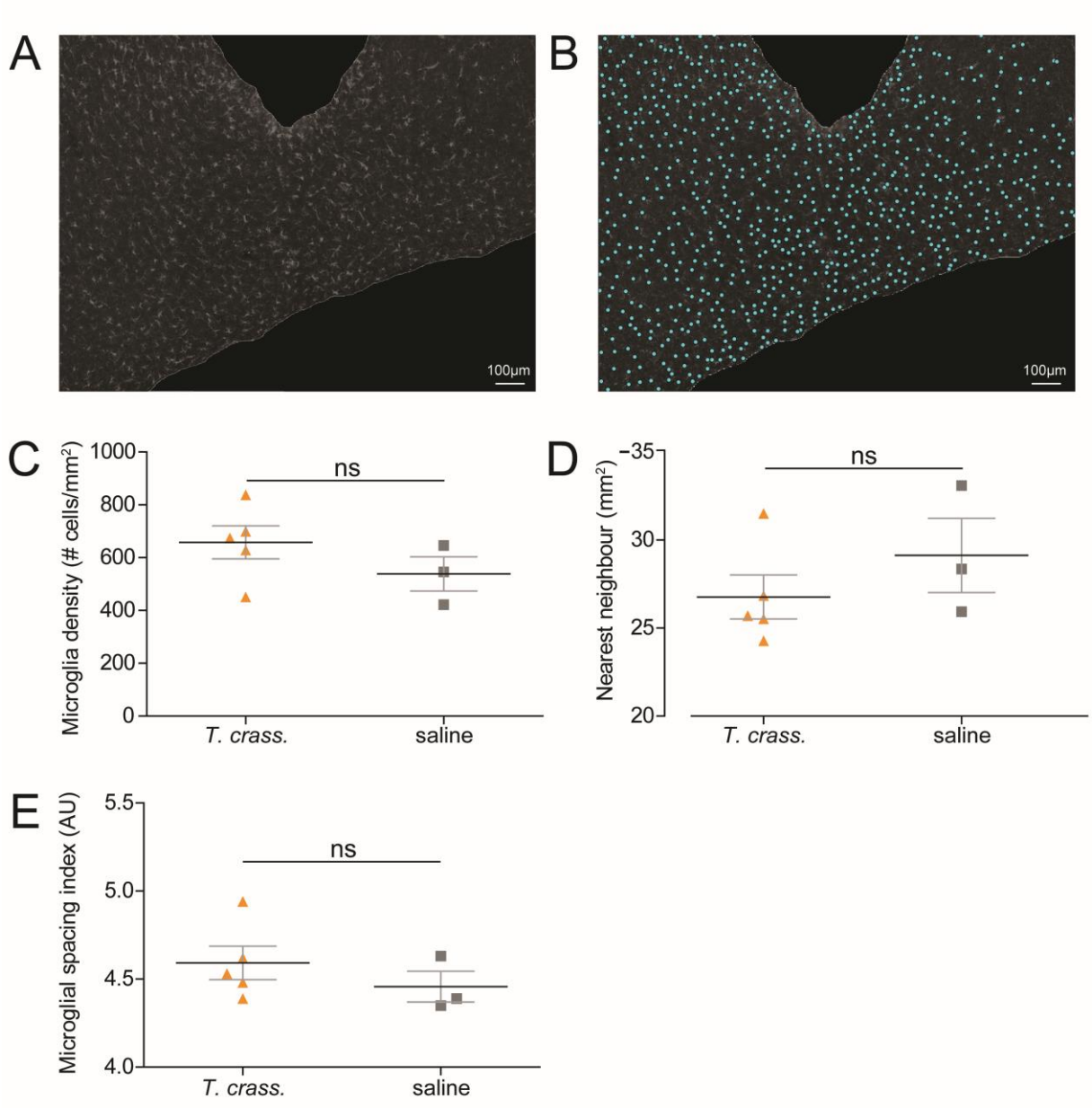

Figure 5.8 Microglial population size and spatial distribution are unaffected by injection of *Taenia crassiceps* homogenate.
A) Confocal microscopy image of microglia stained with Iba1 at 630x magnification from a region just below the injection tract. Accurate area measurements were taken, excluding the injection site and any white matter tracts, using Image J software. B) The number of microglia with the images were manually counted by placing a dot (cyan) on top of each microglial cell. C) The microglial density (the number of cells divided by the area) was calculated and found not to differ between *Taenia crassiceps (T. crass.)* and control groups. D) The nearest neighbour calculation in Image J was used to analyse how the cells were dispersed and also did not differ between the groups. E). The microglial spacing index (a metric to test for clustering of cells) did not differ statistically between the *Taenia crassiceps* and control groups. Values with means ± SEM; ns = not significant, n=8.

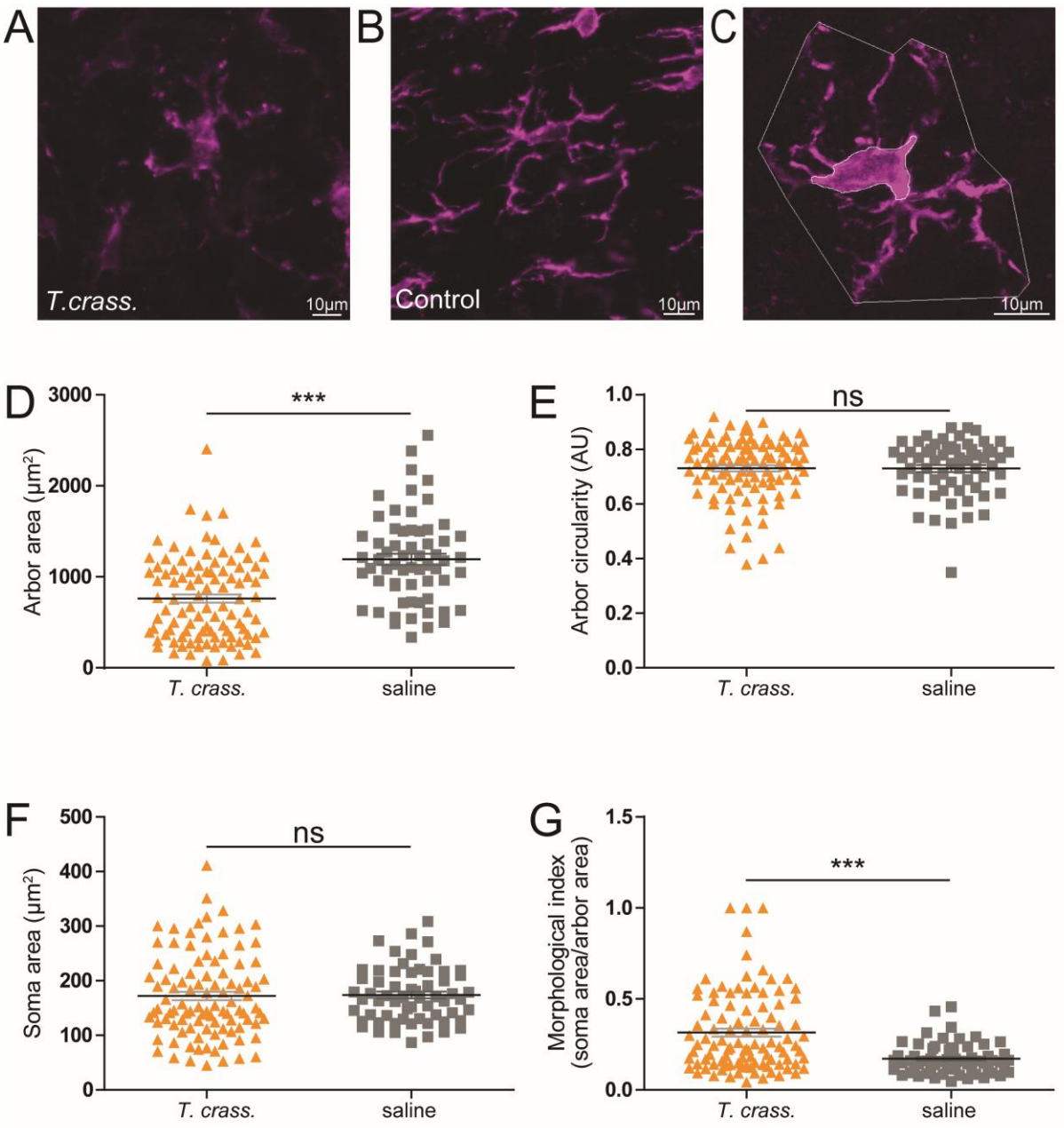

Figure 5.9 *Taenia crassiceps* homogenate injection induces changes in microglial morphology.
A) Confocal microscopy image at 630x magnification of an Iba1-labelled microglial cell from the *Taenia crassiceps (T. crass.)* group showing retracted processes. B) An Iba1-labelled microglial cell from a control showing a large arbour area with extended processes. C) An image showing the tracing of the soma and process arbour (inner and outer lines respectively) used to calculate the soma and arbour areas respectively. D) The arbour area was significantly smaller in the *Taenia crassiceps* group, possibly suggestive of activation of the microglia. E) The arbour circularity did not differ significantly between the groups. F) The soma area was not significantly different between the groups. G) The morphological index (calculated as the area of the soma divided by the area of the arbour) was significantly greater in the *Taenia crassiceps* group, likely because they on average had smaller arbour areas, demonstrating that *Taenia crassiceps* results in a retraction of microglial processes possibly indicative of inflammation. Values with means ± SEM; ***p<0.0001, ns = not significant, n=99 cells from 5 rats and 62 cells from 3 rats for the *Taenia crassiceps* and control groups, respectively.

5.11 DISCUSSION

In Chapter 4 I determined that *T. crass.* homogenate prepared from viable larvae had no effect on the excitability of neurons or neural networks following a 24 hour treatment in an organotypic brain slice preparation, which necessarily lacked the ability to generate an adaptive immune response. In this chapter I used continuous ECoG recordings, seizure threshold tests and post-mortem immunohistological analysis to determine whether the serial intracranial injection of *T. crass.* homogenate *in vivo* could evoke seizures, modify neuronal networks or drive neuroinflammatory changes.

My most important finding was that despite 12 weeks of continuous ECoG recordings, none of the animals displayed electrographic seizure activity. This was despite several manipulations to both maximise the likelihood of evoking seizures and the likelihood of detecting them. Firstly, in order to "prime" the adaptive immune system, and to maximise the chance of evoking an inflammatory response to the intracranial injection of *T. crass.* homogenate, all animals received an intradermal injection of *T. crass.* homogenate in incomplete Freund's adjuvant, which would allow for sustained release of *T. crass.* antigen in the animals. Secondly, animals received at least three injections of *T. crass.* homogenate (2 weeks apart) into the right visual cortex. Thirdly, during each injection session three of the animals received *T. crass.* homogenate injections into three separate brain areas (left and right visual cortex and right hippocampus). These animals therefore received a total of 9 intracranial injections of *T. crass.* homogenate over 6 weeks, with double the volume in the final injection session. Finally, by making use of wireless telemetry technology to measure ECoG continuously, *i.e.* 24 hours a day, and by making use of a sophisticated automated detection algorithms I could be sure that if any seizures did occur during the 12 week period they would be detected. In addition, the frequency of short ictal-like events could also be detected and compared within animal (*i.e.* prior to and following *T. crass.* homogenate injection) as well as between control and *T. crass.* injected groups. Despite all of these measures I found that none of the animals experienced seizures and there was no detectable difference in ictal-like events following *T. crass.* injection, or between *T. crass.* injected and control animals.

I could therefore conclude that at least in my system, *T. crass.* homogenate did not evoke detectable changes in neuronal network function *in vivo*. Why was this the case? Firstly, it is likely that glutamate homeostasis mechanisms were able to deal with the volumes and concentrations of glutamate in the *T. crass.* homogenate to prevent any long-term epileptogenic processes from occurring. Secondly, beyond glutamate, it is still possible that I did not allow sufficient time for seizures to develop following *T. crass.* homogenate injection,

as in human patients this can often take several years. This is unlikely as according to my calculations (see Chapter 5.1) 12 weeks in a rat should be roughly equivalent to several years in a human patient. Furthermore, I also saw no trends or increases in the number of short ictal-like events detected over time following *T. crass.* homogenate injection. Following the picrotoxin injection at 12 weeks (the seizure threshold test) there was no difference in the number or duration of seizures evoked between *T. crass.* and control groups. Together this suggests that injection of *T. crass.* homogenate did not appear to enhance excitability within brain circuits and was therefore unlikely to evoke seizures at a later time point. Never-the-less, in the future the recording period could be lengthened for an *in vivo* study by intermittently turning the batteries of the wireless transmitters off, whilst being wary that this may reduce the reliability of capturing seizure events. Thirdly, it is possible that as could have been the case for Chapter 4, I injected *T. crass.* larvae of the wrong "state" into the brain. As described before, whilst *Taenia* larvae are viable within the brain, human patients can often be asymptomatic (Stringer *et al.* 2003), and that it is only once the larvae die naturally, or are killed using anti-helminthic agents that the likelihood of seizures occurring increases (Verma *et al.* 2010; Nash, Pretell, and Garcia 2002). In these experiments, the *T. crass.* homogenate used was prepared from live, viable larvae, which were freeze-thawed to lyse the cells before homogenization. Utilising homogenate from dead or dying larvae may have had a different outcome. In support of this idea, Stringer *et al.* (2003) demonstrated that early stage *T. crass.* granulomas, presumably containing material from dead or dying *T. crass.* larvae and surrounding inflammatory cells, evoked acute seizures when injected intracranially in rats. There are several caveats to this work however, including the fact that seizures were elicited acutely (no chronic recordings were performed), and the granulomas were developed in the peritoneum of mice and not in the brain parenchyma itself. Fourthly, it is possible that larvae of the ORF strain of *T. crass.* are simply not as virulent as *T. solium,* the pathogenic agent in humans. Indeed, Verastegui *et al.* (2015) showed that injection of *T. solium* ova intracranially into rats resulted in the development of seizures in 9% of animals (2 of 23 animals infected). This could suggest that a) as very few animals developed seizures in the Verastegui *et al.* study we did not use sufficient numbers of animals in our study to detect this low incidence (only 6 animals were injected with *T. crass.* homogenate due to cost constraints associated with the transmitters) or b) that the species of cestode is important for seizure development (*i.e. T. solium* vs *T. crassiceps*) or c) that it is important to inject ova rather than larval homogenate. Future work could seek to address these potential limitations by injecting different types of cestode material in animals where continuous ECoG recordings can be performed.

A reasonable, but intriguing interpretation of my data is that the *T. crass.* homogenate I injected failed to evoke a sufficiently large inflammatory response or in fact had anti-inflammatory properties. Indeed, my immunohistochemical analysis revealed no changes in astrocyte staining between *T. crass.* and control animals. In contrast however, I did observe some changes in microglial staining and morphology between the groups, namely that the processes of microglia in *T. crass.* injected animals were more retracted than in controls. This is in line with the literature, which reports that microglia take on a more amoeboid shape and retract their processes when in an activated state (Hui *et al.* 2019). This suggests that the *T. crass.* homogenate did drive some phenotypic changes constituting part of a neuroinflammatory response, which is broadly consistent with neuroinflammation ultimately observed in NCC (Shabab *et al.* 2017; Feng *et al.* 2019).

A reasonable question, however, which I was unable to answer, is whether the injection of foreign material from a different organism, or even endogenous proteins not normally found in the brain might have elicited more of a neuroinflammatory response as compared to that observed following *T. crass.* homogenate injections. This is because our control injections, the point of comparison, were saline containing an equivalent level of endotoxin as the *T. crass.* homogenate. For example, serum albumin, robustly activates microglia and astrocytes if it enters the extravascular space within the brain parenchyma following injury (Ralay Ranaivo and Wainwright 2010; Weissberg *et al.* 2016; Ivens *et al.* 2007; Seiffert *et al.* 2004). It is likely that other foreign proteins may have generated more of an inflammatory response than *T. crass.* Indeed, *Taenia* larvae have likely evolved multiple mechanisms to modulate and prevent host immune responses to maintain their viability *in situ* (Peón, Ledesma-Soto, and Terrazas 2016). For example, homogenate from viable cestode larvae has been shown to prevent activation of microglia (Y. Sun *et al.* 2014). It is therefore possible that one explanation for our inability to elicit seizure activity and a robust neuroinflammatory response is because the *T. crass.* homogenate prepared from larvae also contain factors with anti-inflammatory properties.

Taken together, in this chapter I demonstrated that serial intracranial injection of *T. crass.* larval homogenate did not result in epileptogenesis *in vivo* and was associated with moderate neuroinflammatory changes.

Chapter 6

OVERALL DISCUSSION AND CONCLUSIONS

In this thesis I have used patch-clamp electrophysiology, and calcium imaging in hippocampal organotypic brain slice cultures to demonstrate that *Taenia* larval products cause neuronal depolarization and can initiate seizure-like events via glutamate receptor activation. Glutamate assays revealed that both *T. crass.* and *T. solium* larvae contain and release considerable quantities of glutamate (Chapter 3). A 24 hour treatment with 50 µg/ml of *T. crass.* larval homogenate, however, was not enough to evoke any changes in neuronal membrane properties, firing rates or network excitability (Chapter 4). Furthermore, repeated intracranial injections of *T. crass.* larval homogenate also affected no observable change on nearby neurons as measured by ECoG and wireless telemetry over 12 weeks. Immunohistochemically stained microglia in the surrounding area of *T. crass.* injection showed signs of activation indicative of a mild inflammatory response (Chapter 5), but this was not observed in astrocytes. I discuss below how these seemingly divergent findings may fit together and confer what future work could be performed to further elucidate and characterise seizure development in NCC.

Clinical evidence and animal models conclusively demonstrate that the presence of cestode larvae in the brain can result in the generation of seizures (Verastegui *et al.* 2015; Nash *et al.* 2015). Importantly, the majority of previous work has centred around the host inflammatory response and how this plays a role in seizure generation (Stringer *et al.* 2003; Robinson *et al.* 2012). Whilst this is likely important, it does not preclude the involvement of additional or exacerbating pathogenic mechanisms for seizure generation and epileptogenesis in NCC. In this thesis I identified that *Taenia* larvae have a direct excitatory effect on neurons via glutamatergic signalling. This is important as the central role of glutamatergic signalling in epileptogenesis has conclusively been shown using multiple cell culture (D. A. Sun, Sombati, and DeLorenzo 2001; Sombati and DeLorenzo 1995; DeLorenzo, Pal, and Sombati 1998), slice (Anderson *et al.* 1986; Ziobro, Deshpande, and DeLorenzo 2011; Stasheff *et al.* 1989), and *in vivo* models of epilepsy (M. J. Croucher and Bradford 1990; Martin J. Croucher *et al.* 1988; Rice and Delorenzo 1998).

Clinically, in addition to NCC, the other major causes of adult acquired epilepsy are stroke, traumatic brain injury and CNS tumours (Hauser, Annegers, and Kurland 1991; Forsgren *et al.* 2005). In these other causes of acquired epilepsy, glutamatergic signalling and glutamate

excitotoxicity are thought to be central to the pathogenic process. Glutamate excitotoxicity occurs when depolarized, damaged or dying neurons release glutamate, which activate surrounding neurons via NMDA and AMPA receptors, resulting in sustained neuronal depolarization, Ca^{2+} influx and the subsequent activation of signalling cascades and enzymes. These in turn lead to cell death via necrosis and apoptosis (Ankarcrona *et al.* 1995), the further release of intracellular glutamate and the propagation of the excitotoxic process to neighbouring cells. In the neurons that survive, the prolonged exposure to glutamate has been shown to cause hyperexcitability and seizures (DeLorenzo, Pal, and Sombati 1998; D. A. Sun, Sombati, and DeLorenzo 2001) via multiple mechanisms including enhanced intrinsic excitability and NMDA receptor dependent disruption of GABAergic inhibition (Lee *et al.* 2011; Terunuma *et al.* 2010; Buckingham *et al.* 2011). Given our finding that *Taenia* larvae contain and release significant quantities of glutamate, it is possible that should homeostatic mechanisms for taking up and metabolizing glutamate fail to compensate for larval derived glutamate in the extracellular space, similar glutamate-dependent excitotoxic and epileptogenic processes that occur in stroke, traumatic brain injury and CNS tumours are likely to also occur in NCC.

Glioma, a common adult primary brain tumour, which typically presents with seizures in over 80% of patients (Santosh and Sravya 2017), is an intriguing condition for comparison to NCC. Glioma tumour cells themselves have been shown to release glutamate into the extracellular space via the system x_c^-cystine-glutamate antiporter (Buckingham *et al.* 2011). Interestingly, there is compelling evidence that tumoural release of glutamate via this mechanism causes seizures and in addition, favours glioma preservation, progression and invasion in cases of malignant glioma (Sontheimer 2008; Takano *et al.* 2001; Huang *et al.* 2013). Analogously, it is possible that *Taenia* larvae in the brain utilize the release of glutamate and the induction of glutamate excitotoxicity to facilitate their growth and expansion, with the accompanying effect of seizure generation. In the case of glioma, where the mechanism of glutamate release by tumour cells is known, pharmacological agents (*e.g.* sulfasalazine), which block glutamate release have considerable potential as therapeutic agents for reducing seizure burden in this condition. Therefore, it is important that future work attempts to identify the molecular mechanisms underlying the *Taenia*-specific production of glutamate in order to inform the development of new therapeutic strategies to potentially reduce larval expansion and treat seizures in NCC. In terms of further elucidating the possible glutamate mechanism of *Taenia in vivo*; glutamate receptor expression could be analysed post treatment *in vivo* to determine whether any glutamate receptors are upregulated and on which cells preferentially. Assessing the effect of different levels of environmental glutamate on cestode larval growth would also be of interest, in terms of a mechanistic comparison to tumour cells.

An important consideration is how we might reconcile my findings of continuous glutamate release by *Taenia* larvae with the clinical picture of delayed symptom onset in NCC. In people with NCC, acute seizures may be experienced by some immediately following infection whilst it takes months to years following initial infection for others (Foyaca-sibat *et al.* 2009; Stringer *et al.* 2003). This suggests that multiple different, or possibly interacting mechanisms might be involved in the epileptogenic process in NCC. Neuroinflammation is one possible mechanism that has long been thought to be central to the development of seizures in NCC. In support of this, larval suppression of host inflammatory responses explains why many patients may remain asymptomatic for years following infection (Garcia, Gonzalez, and Gilman 2003). My findings are not at odds with this line of thinking when considering the effect of neuroinflammation on extracellular glutamate uptake. In the healthy brain parenchymal astrocytes are optimized to maintain extracellular glutamate at low concentrations (Perea and Araque 2010). However, the inflammatory transition of astrocytes to a reactive phenotype is known to impede their ability to buffer extracellular uptake (Seifert, Carmignoto, and Steinhäuser 2010). It is therefore conceivable that cyst-associated reactive astrocytosis may gradually erode the ability of homeostatic mechanisms to compensate for larval derived extracellular glutamate, resulting in delayed symptom onset in NCC. Astrocytes are usually activated by microglial TNF-α and IL-1β release, which places the attention on activated microglia (exhibiting retracted processes and enlarged somas) as the first indicator of neuroinflammation (Vezzani and Viviani 2015). In my study there was evidence of activated microglia in response to the intracranial injection of *T. crass.* (see Chapter 5), however, the astrocytes did not exhibit a characteristic increase in size or GFAP fluorescence (Figure 5.6), as has been seen in the literature (Wilhelmsson *et al.* 2006). The inflammatory response was therefore likely still in its early stages because the microglia didn't have enlarged somas (despite their processes being retracted) and the astrocytes had a non-reactive morphology.

A further way we might explain a delayed onset of epileptogenesis following *Taenia* infection is that the presence of multiple cysts at different stages of development may be required, perhaps even multiple rounds of infection. It is common place for a person to suffer with different stages of cysts at the same time (Wagner and Newton 2009, Figure 2), whether from the same or a different infection. A degenerating larval cyst starting to evoke an inflammatory response may on its own not result in seizures. This is because the amount of glutamate contained within a larvae is relatively small and may only exert a local effect, despite a declining astrocyte glutamate buffering capability. Patients who additionally have a viable cyst that is constantly producing glutamate into an environment where astrocytes are unable to adequately buffer it, akin to glioma tumoural cells, would possibly be more vulnerable to developing seizures. Given that NCC occurs in areas where there is poor sanitation and the

recognition and diagnosis of the disease can take years, the chance of a person being infected multiple times, and thus experiencing cysts at a variety of stages, is a statistical possibility. Thus, future work could expose neurons, either *in vitro* or *in vivo*, to dead larval product, which should activate an immune response, followed by viable larva, which would continually produce glutamate.

In addition to identifying an important role for glutamate in this thesis, I have also demonstrated that at the concentrations delivered, other factors within *T. crass.* homogenate from viable larvae do not drive changes in neuronal or network excitability over 24 hrs *in vitro* or over 12 weeks *in vivo*, which I believe is important information for the field. An important limitation of my study is that all investigations used only a single type of larval homogenate. It is important to note that utilising a different form of the larval product could result in different functional effects on neurons *in vitro* and *in vivo*. The larvae could be killed in a different way or the homogenate prepared in such a way as to preserve the cell wall fraction that in these experiments was separated out by centrifuging. Whole dead larvae could be used in the *in vitro* model, but, due to their size, would be difficult to inject intracranially *in vivo*. Activated oncospheres could be injected, as has been done in other models, but may take considerable time to develop into larvae and then cysticerci.

It is clear that there is still considerable uncertainty regarding the precise sequences of events leading to seizure onset in NCC. Nonetheless, my thesis has demonstrated the utility of using modern techniques in cellular neuroscience such as patch-clamp electrophysiology and wireless ECoG together with new models of NCC to study how neuronal networks might be affected in this disorder. My findings provide the first evidence that, as is the case with the other common causes of adult acquired epilepsy (*i.e.* stoke, traumatic brain injury and glioma), increased extracellular glutamate likely plays an important role in the development of seizures in NCC. I hope this thesis will encourage and inform future research studying seizure mechanisms in NCC.

REFERENCES

Akiyoshi, Ryohei, Hiroaki Wake, Daisuke Kato, Hiroshi Horiuchi, Riho Ono, Ako Ikegami, Koichiro Haruwaka, et al. 2018. 'Microglia Enhance Synapse Activity to Promote Local Network Synchronization'. *Eneuro* 5 (5): ENEURO.0088-18.2018. https://doi.org/10.1523/eneuro.0088-18.2018.

Aluja, A. S. De, A. N.M. Villalobos, A. Plancarte, L. F. Rodarte, M. Hernández, and E. Sciutto. 1996. 'Experimental Taenia Solium Cysticercosis in Pigs: Characteristics of the Infection and Antibody Response'. *Veterinary Parasitology* 61 (1–2): 49–59. https://doi.org/10.1016/0304-4017(95)00817-9.

Alyu, Feyza, and Miriş Dikmen. 2017. 'Inflammatory Aspects of Epileptogenesis: Contribution of Molecular Inflammatory Mechanisms'. *Acta Neuropsychiatrica* 29 (1): 1–16. https://doi.org/10.1017/neu.2016.47.

Amit, Prasad, Kashi Nath Prasad, Gupta Rakesh Kumar, Tripathi Shweta, Jha Sanjeev, Paliwal Vimal Kumar, and Tripathi Mukesh. 2011. 'Immune Response to Different Fractions of Taenia Solium Cyst Fluid Antigens in Patients with Neurocysticercosis'. *Experimental Parasitology* 127 (3): 687–92. https://doi.org/10.1016/j.exppara.2010.11.006.

Anderson, William W., Darrell V. Lewis, H. Scott Swartzwelder, and Wilkie A. Wilson. 1986. 'Magnesium-Free Medium Activates Seizure-like Events in the Rat Hippocampal Slice'. *Brain Research* 398 (1): 215–19. https://doi.org/10.1016/0006-8993(86)91274-6.

Andreollo, Nelson Adami, Elisvânia Freitas, Marina Rachel Araújo, and Luiz Roberto Lopes. 2012. 'Rat's Age versus Human's Age : What Is the Relationship?' *Arquivos Brasileiros de Cirurgia Digestiva* 25 (1): 49–51.

Ankarcrona, Maria, Jeannette M. Dypbukt, Emanuela Bonfoco, Boris Zhivotovsky, Sten Orrenius, Stuart A. Lipton, and Pierluigi Nicotera. 1995. 'Glutamate-Induced Neuronal Death: A Succession of Necrosis or Apoptosis Depending on Mitochondrial Function'. *Neuron* 15 (4): 961–73. https://doi.org/10.1016/0896-6273(95)90186-8.

As, A D van, and J Joubert. 1991. 'Neurocysticercosis in 578 Black Epileptic Patients.' *South African Medical Journal* 80 (7): 327–28.

Avanzini, Giuliano, and Silvana Franceschetti. 2003. 'Cellular Biology of Epileptogenesis'.

Lancet Neurology 2 (1): 33–42. https://doi.org/10.1016/S1474-4422(03)00265-5.

Balosso, Silvia, Ã Mattia Maroso, Ã Manuel Sanchez-alavez, Teresa Ravizza, Angelisa Frasca, Tamas Bartfai, and Annamaria Vezzani. 2008. 'A Novel Non-Transcriptional Pathway Mediates the Proconvulsive Effects of Interleukin-1'. *Brain* 131 (November): 3256–65. https://doi.org/10.1093/brain/awn271.

Baron, Anne, Rainer Waldmann, and Michel Lazdunski. 2002. 'ASIC-like, Proton-Activated Currents in Rat Hippocampal Neurons'. *Journal of Physiology* 539 (2): 485–94. https://doi.org/10.1113/jphysiol.2001.014837.

Bear, Mark F, Barry W Connors, and Michael A Paradiso. 2007. *Neuroscience: Exploring the Brain*. Edited by Emily Lupash, Elizabeth Connolly, Betsy Dilernia, and Paula Williams. Third. Philadelphia, Baltimore, New York, London, Buenos Aires, Hong Kong, Sydney, Tokyo: Lippincott Williams & Wilkins.

Bird, A V, H J Heinz, and S Klintwork. 1962. 'Convulsive Disorders in Bantu Mine Workers'. *Epilepsia* 3: 175–87.

Buckingham, Susan C., Susan L. Campbell, Brian R. Haas, Vedrana Montana, Stefanie Robel, Toyin Ogunrinu, and Harald Sontheimer. 2011. 'Glutamate Release by Primary Brain Tumors Induces Epileptic Activity'. *Nature Medicine* 17 (10): 1269–74. https://doi.org/10.1038/nm.2453.

Campbell, G.D., and V.J.R Farrell. 1987. 'Brain Scans, Epilepsy and Cerebral Cysticercosis.' *South African Medical Journal* 72: 885–86.

Carpio, Arturo, Alfonso Escobar, and W. Allen Hauser. 1998. 'Cysticercosis and Epilepsy: A Critical Review'. *Epilepsia* 39 (10): 1025–40. https://doi.org/10.1111/j.1528-1157.1998.tb01287.x.

Carpio, Arturo, and Matthew L. Romo. 2014. 'The Relationship between Neurocysticercosis and Epilepsy: An Endless Debate'. *Arquivos de Neuro-Psiquiatria* 72 (5): 383–90. https://doi.org/10.1590/0004-282X20140024.

Cerri, Chiara, Sacha Genovesi, Manuela Allegra, Francesco Pistillo, Ursula Pu, Angelo Guglielmotti, V Hugh Perry, Yuri Bozzi, and Matteo Caleo. 2016. 'The Chemokine CCL2 Mediates the Seizure-Enhancing Effects of Systemic Inflammation'. *Neurobiology of Disease* 36 (13): 3777–88. https://doi.org/10.1523/JNEUROSCI.0451-15.2016.

Chefer, Vladimir I, Alexis C Thompson, Agustin Zapata, and Toni S Shippenberg. 2015. *Antagónico Frente a Phytophthora Palmivora , Agente Causal de La Pudrición Del*

Cogollo. https://doi.org/10.1002/0471142301.ns0701s47.Overview.

Chile, Nancy, Taryn Clark, Yanina Arana, Ynes R. Ortega, Sandra Palma, Alan Mejia, Noelia Angulo, et al. 2016. 'In Vitro Study of Taenia Solium Postoncospheral Form'. *PLoS Neglected Tropical Diseases* 10 (2): 1–15. https://doi.org/10.1371/journal.pntd.0004396.

Christensen, Nina M., Chiara Trevisan, Páll S. Leifsson, and Maria V. Johansen. 2016. 'The Association between Seizures and Deposition of Collagen in the Brain in Porcine Taenia Solium Neurocysticercosis'. *Veterinary Parasitology* 228: 180–82. https://doi.org/10.1016/j.vetpar.2016.09.008.

Chun, Eugene, Argyle V. Bumanglag, Sara N. Burke, and Robert S. Sloviter. 2019. 'Targeted Hippocampal GABA Neuron Ablation by Stable Substance P–Saporin Causes Hippocampal Sclerosis and Chronic Epilepsy in Rats'. *Epilepsia* 60 (5): e52–57. https://doi.org/10.1111/epi.14723.

Croucher, M. J., and H. F. Bradford. 1990. 'NMDA Receptor Blockade Inhibits Glutamate-Induced Kindling of the Rat Amygdala'. *Brain Research* 506 (2): 349–52. https://doi.org/10.1016/0006-8993(90)91279-P.

Croucher, Martin J., Henry F. Bradford, David C. Sunter, and Jeffrey C. Watkins. 1988. 'Inhibition of the Development of Electrical Kindling of the Prepyriform Cortex by Daily Focal Injections of Excitatory Amino Acid Antagonists'. *European Journal of Pharmacology* 152 (1–2): 29–38. https://doi.org/10.1016/0014-2999(88)90832-1.

Czeh, Boldizsár, Mária Simon, Marieke G.C. Van Der Hart, Barthel Schmelting, Mayke B. Hesselink, and Eberhard Fuchs. 2005. 'Chronic Stress Decreases the Number of Parvalbumin-Immunoreactive Interneurons in the Hippocampus: Prevention by Treatment with a Substance P Receptor (NK1) Antagonist'. *Neuropsychopharmacology* 30 (1): 67–79. https://doi.org/10.1038/sj.npp.1300581.

DeLorenzo, Robert J, Shubhro Pal, and Sompong Sombati. 1998. 'Prolonged Activation of the N-Methyl-d-Aspartate Receptor–Ca2+ Transduction Pathway Causes Spontaneous Recurrent Epileptiform Discharges in Hippocampal Neurons in Culture.' *Proceedings of the National Academy of Sciences of the United States of America* 95 (24): 14482–87.

Diaz Verdugo, Carmen, Sverre Myren-Svelstad, Celine Deneubourg, Robbrecht Pelgrims, Akira Muto, Koichi Kawakami, Nathalie Jurisch-Yaksi, and Emre Yaksi. 2019. 'Glia-Neuron Interactions Underlie State Transitions to Generalized Seizures'. *BioRxiv*, 509521. https://doi.org/10.1101/509521.

Diop, Amadou Gallo, Hanneke M De Boer, Custodia Mandlhate, Leonid Prilipko, and Harry

Meinardi. 2003. 'The Global Campaign against Epilepsy in Africa'. *Acta Tropica* 87: 149–59. https://doi.org/10.1016/S0001-706X(03)00038-X.

Douglas, Steven. D, and Susan. E Leeman. 2011. 'Neurokinin-1 Receptor: Functional Significance in the Immune System in Reference to Selected Infections and Inflammation'. *Annals of the New York Academy of Sciences* 1217: 83–95. https://doi.org/10.1111/j.1749-6632.2010.05826.x.Neurokinin-1.

Dzik, Jolanta M. 2006. 'Molecules Released by Helminth Parasites Involved in Host Colonization'. *Acta Biochimica Polonica* 53 (1): 33–64.

Edelstein, Arthur, Nenad Amodaj, Karl Hoover, Ron Vale, and Nico Stuurman. 2010. 'Computer Control of Microscopes Using MManager'. In *Current Protocols in Molecular Biology*, 92:14.20.1-14.20.17. Hoboken, NJ, USA: John Wiley & Sons, Inc. https://doi.org/10.1002/0471142727.mb1420s92.

'Endemicity of Taenia Solium'. 2015. World Health Organisation. 2015. https://www.who.int/taeniasis/Endemicity_Taenia_Solium_2015.jpg.

Erta, María, Albert Quintana, and Juan Hidalgo. 2012. 'Interleukin-6, a Major Cytokine in the Central Nervous System'. *International Journal of Biological Sciences* 8 (9): 1254–66. https://doi.org/10.7150/ijbs.4679.

Feng, Lijie, Madhuvika Murugan, Dale B Bosco, Yong Liu, Jiyun Peng, Gregory A Worrell, Hai-long Wang Lauren, E Ta Jason, and Yuxian Shen Long-jun Wu. 2019. 'Microglial Proliferation and Monocyte Infiltration Contribute to Microgliosis Following Status Epilepticus'. *Glia*, 1–15. https://doi.org/10.1002/glia.23616.

Fleury, Agnes, Alain Dessein, PierreMarie Preux, Michel Dumas, Graciela Tapia, Carlos Larralde, and Edda Sciutto. 2004. 'Symptomatic Human Neurocysticercosis'. *Journal of Neurology* 251 (7): 830–37. https://doi.org/10.1007/s00415-004-0437-9.

Fleury, Agnès, Armando Trejo, Humberto Cisneros, Roberto García-Navarrete, Nelly Villalobos, Marisela Hernández, Juana Villeda Hernández, et al. 2015. 'Taenia Solium: Development of an Experimental Model of Porcine Neurocysticercosis'. *PLoS Neglected Tropical Diseases* 9 (8): 1–18. https://doi.org/10.1371/journal.pntd.0003980.

Flores-Bautista, Jeanette, José Navarrete-Perea, Gladis Fragoso, Ana Flisser, Xavier Soberón, and Juan P. Laclette. 2018. 'Fate of Uptaken Host Proteins in Taenia Solium and Taenia Crassiceps Cysticerci'. *Bioscience Reports* 38 (4): 1–10. https://doi.org/10.1042/BSR20180636.

Forman, Chris J, Hayley Tomes, Buchule Mbobo, Richard J Burman, Muazzam Jacobs, Tom Baden, and Joseph V Raimondo. 2017. 'Openspritzer: An Open Hardware Pressure Ejection System for Reliably Delivering Picolitre Volumes'. *Scientific Reports* 7 (2188): 1–11. https://doi.org/10.1038/s41598-017-02301-2.

Forsgren, Lars, E. Beghi, A. Oun, M. Sillanpaa, A. Õun, and M. Sillanpää. 2005. 'The Epidemiology of Epilepsy in Europe - A Systematic Review'. *European Journal of Neurology* 12 (4): 245–53. https://doi.org/10.1111/j.1468-1331.2004.00992.x.

Foyaca-sibat, Humberto, Linda D Cowan, Helene Carabin, Irene Targonska, Mushtaq A Anwary, Gilberto Serrano-ocana, Rosina C Krecek, and A Lee Willingham. 2009. 'Accuracy of Serological Testing for the Diagnosis of Prevalent Neurocysticercosis in Outpatients with Epilepsy , Eastern Cape Province , South Africa'. *PLOS Neglected Tropical Diseases* 3 (12): 1–8. https://doi.org/10.1371/journal.pntd.0000562.

Garcia, Hector H., and Oscar H. Del Brutto. 2005. 'Neurocysticercosis: Updated Concepts about an Old Disease'. *Lancet Neurology* 4 (10): 653–61. https://doi.org/10.1016/S1474-4422(05)70194-0.

Garcia, Hector H., Armando E. Gonzalez, and Robert H. Gilman. 2003. 'Diagnosis, Treatment and Control of Taenia Solium Cysticercosis'. *Current Opinion in Infectious Diseases* 16 (5): 411–19. https://doi.org/10.1097/00001432-200310000-00007.

Garcia, Hector H, and Oscar H Del. 2017. 'Antiparasitic Treatment of Neurocysticercosis - The Effect of Cyst Destruction in Seizure Evolution'. *Epilepsy & Behavior* 76: 158–62. https://doi.org/10.1016/j.yebeh.2017.03.013.

García, Héctor H, Armando E Gonzalez, Carlton A W Evans, Robert H Gilman, and Cysticercosis Working. 2003. 'Taenia Solium Cysticercosis'. *The Lancet* 361: 547–56.

Garza, Armandina, David J. Tweardy, Joel Weinstock, Balaji Viswanathan, and Prema Robinson. 2010. 'Substance P Signaling Contributes to Granuloma Formation in Taenia Crassiceps Infection, a Murine Model of Cysticercosis'. *Journal of Biomedicine and Biotechnology* 2010. https://doi.org/10.1155/2010/597086.

Hamlet, W. R., and Y. Lu. 2016. 'Intrinsic Plasticity Induced by Group II Metabotropic Glutamate Receptors via Enhancement of High-Threshold KV Currents in Sound Localizing Neurons'. *Neuroscience* 324: 177–90. https://doi.org/10.1016/j.neuroscience.2016.03.010.

Harrison, S, and P Geppetti. 2001. 'Substance P'. *The International Journal of Biochemistry & Cell Biology* 33 (6): 555–76. https://doi.org/10.1016/S1357-2725(01)00031-0.

Hauser, W. Allen, John F. Annegers, and Leonard T. Kurland. 1991. 'Prevalence of Epilepsy in Rochester, Minnesota: 1940–1980'. *Epilepsia* 32 (4): 429–45. https://doi.org/10.1111/j.1528-1157.1991.tb04675.x.

Heinz, H.J, and G.M MacNab. 1965. 'Cysticercosis in the Bantu of Southern Africa'. *South African Journal of Medical Sciences* 30 (1): 19–31.

Hellstrom, Ian C., Marc Danik, Giamal N. Luheshi, and Sylvain Williams. 2005. 'Chronic LPS Exposure Produces Changes in Intrinsic Membrane Properties and a Sustained IL-β-Dependent Increase in GABAergic Inhibition in Hippocampal CA1 Pyramidal Neurons'. *Hippocampus* 15 (5): 656–64. https://doi.org/10.1002/hipo.20086.

Herman, Melissa A., and Craig E. Jahr. 2007. 'Extracellular Glutamate Concentration in Hippocampal Slice'. *Journal of Neuroscience* 27 (36): 9736–41. https://doi.org/10.1523/JNEUROSCI.3009-07.2007.

Herrick, Jesica A., Biswajit Maharathi, Jin Suh Kim, Gerardo G. Abundis, Anjali Garg, Isidro Gonzales, Herbert Saavedra, Javier A. Bustos, Hector H. Garcia, and Jeffrey A. Loeb. 2018. 'Inflammation Is a Key Risk Factor for Persistent Seizures in Neurocysticercosis'. *Annals of Clinical and Translational Neurology* 5 (5): 630–39. https://doi.org/10.1002/acn3.562.

Hotez, Peter J., Paul J. Brindley, Jeffrey M. Bethony, Charles H. King, Edward J. Pearce, and Julie Jacobson. 2008. 'Helminth Infections: The Great Neglected Tropical Diseases'. *Journal of Clinical Investigation* 118 (4): 1311–21. https://doi.org/10.1172/JCI34261.

Huang, Weijiao, Wooyoung Choi, Yuling Chen, Qi Zhang, Haiteng Deng, Wei He, and Yigong Shi. 2013. 'A Proposed Role for Glutamine in Cancer Cell Growth through Acid Resistance'. *Cell Research* 23 (5): 724–27. https://doi.org/10.1038/cr.2013.15.

Hui, Chin Wai, Sanjeev K Bhardwaj, Kaushik Sharma, Antoneta T Joseph, Kanchan Bisht, Katherine Picard, Marie-ève Tremblay, and Lalit K Srivastava. 2019. 'Microglia in the Developing Prefrontal Cortex of Rats Show Dynamic Changes Following Neonatal Disconnection of the Ventral Hippocampus'. *Neuropharmacology* 146: 264–75. https://doi.org/10.1016/j.neuropharm.2018.12.007.

Id, Ruud H P Wilbers, Roger Schneiter, Martijn H M Holterman, Claire Drurey, Geert Smant, Oluwatoyin A Asojo, Rick M Maizels, and Jose L Lozano-Torres. 2018. 'Secreted Venom Allergen-like Proteins of Helminths : Conserved Modulators of Host Responses in Animals and Plants'. *PLoS Pathogens* 14 (10): 1–14.

'International Task Force for Disease Eradication'. n.d. The Carter Center. Accessed 20

September 2007. https://www.cartercenter.org/health/itfde/index.html.

———. 2008. ‘Recommendations of the International Task Force for Disease Eradication’. *Morbidity and Mortality Weekly Report* 42 (April).

Ivens, Sebastian, Daniela Kaufer, Luisa P Flores, Ingo Bechmann, Dominik Zumsteg, Oren Tomkins, Ernst Seiffert, Uwe Heinemann, and Alon Friedman. 2007. ‘TGF- b Receptor-Mediated Albumin Uptake into Astrocytes Is Involved in Neocortical Epileptogenesis’, 535–47. https://doi.org/10.1093/brain/awl317.

Jiang, C., and G. G. Haddad. 1991. ‘Effect of Anoxia on Intracellular and Extracellular Potassium Activity in Hypoglossal Neurons in Vitro’. *Journal of Neurophysiology* 66 (1): 103–11. https://doi.org/10.1152/jn.1991.66.1.103.

Johnson, Martha B., Kun Lin Jin, Manabu Minami, Dexi Chen, and Roger P. Simon. 2001. ‘Global Ischemia Induces Expression of Acid-Sensing Ion Channel 2a in Rat Brain’. *Journal of Cerebral Blood Flow and Metabolism* 21 (6): 734–40. https://doi.org/10.1097/00004647-200106000-00011.

Johnston, Jessica M., Cecilia D. Dyer, Susan Madison-Antenucci, Kimberly AM Mergen, Christin L. Veeder, and Angela K. Brice. 2016. ‘Neurocysticercosis in a Rhesus Macaque (Macaca Mulatta)’. *Comparative Medicine* 66 (6): 499–502.

Jones, Simon A. 2005. ‘Directing Transition from Innate to Acquired Immunity: Defining a Role for IL-6’. *The Journal of Immunology* 175 (6): 3463–68. https://doi.org/10.4049/jimmunol.175.6.3463.

Lange, Anja De, Siddhartha Mahanty, and Joseph V Raimondo. 2018. ‘Model Systems for Investigating Disease Processes in Neurocysticercosis’. *Parasitology* 146 (5): 553–62. https://doi.org/10.1017/S0031182018001932.

Lee, Henry H.C. C, Tarek Z. Deeb, Joshua A. Walker, Paul A. Davies, and Stephen J. Moss. 2011. ‘NMDA Receptor Activity Downregulates KCC2 Resulting in Depolarizing GABAA Receptor-Mediated Currents’. *Nature Neuroscience* 14 (6): 736–43. https://doi.org/10.1038/nn.2806.

Lesage, Florian. 2003. ‘Pharmacology of Neuronal Background Potassium Channels’. *Neuropharmacology* 44 (1): 1–7. https://doi.org/10.1016/S0028-3908(02)00339-8.

Lieberman, David N., and Istvan Mody. 1998. ‘Substance P Enhances NMDA Channel Function in Hippocampal Dentate Gyms Granule Cells’. *Journal of Neurophysiology* 80 (1): 113–19. https://doi.org/10.1152/jn.1998.80.1.113.

Liu, H., A. M. Mazarati, H. Katsumori, R. Sankar, and C. G. Wasterlain. 2002. 'Substance P Is Expressed in Hippocampal Principal Neurons during Status Epilepticus and Plays a Critical Role in the Maintenance of Status Epilepticus'. *Proceedings of the National Academy of Sciences* 96 (9): 5286–91. https://doi.org/10.1073/pnas.96.9.5286.

Lively, Starlee, and Lyanne C. Schlichter. 2018. 'Microglia Responses to Pro-Inflammatory Stimuli (LPS, IFNγ+TNFα) and Reprogramming by Resolving Cytokines (IL-4, IL-10)'. *Frontiers in Cellular Neuroscience* 12 (July): 1–19. https://doi.org/10.3389/fncel.2018.00215.

Mafojane, N A, C C Appleton, R C Krecek, and L M Michael. 2003. 'The Current Status of Neurocysticercosis in Eastern and Southern Africa'. *Acta Tropica* 87: 25–33. https://doi.org/10.1016/S0001-706X(03)00052-4.

Mahanty, Siddhartha, and Hector H. Garcia. 2010. 'Cysticercosis and Neurocysticercosis as Pathogens Affecting the Nervous System'. *Progress in Neurobiology* 91 (2): 172–84. https://doi.org/10.1016/j.pneurobio.2009.12.008.

Mahanty, Siddhartha, Elise M. Madrid, and Theodore E. Nash. 2013. 'Quantitative Screening for Anticestode Drugs Based on Changes in Baseline Enzyme Secretion by Taenia Crassiceps'. *Antimicrobial Agents and Chemotherapy* 57 (2): 990–95. https://doi.org/10.1128/AAC.01022-12.

Maroso, Mattia, Silvia Balosso, Teresa Ravizza, Valentina Iori, Christopher Ian Wright, Jacqueline French, and Annamaria Vezzani. 2011. 'Interleukin-1β Biosynthesis Inhibition Reduces Acute Seizures and Drug Resistant Chronic Epileptic Activity in Mice'. *Journal of the American Society for Experimental NeuroTherapeutics* 8 (April 2011): 304–15. https://doi.org/10.1007/s13311-011-0039-z.

Martin, Jennifer L., and Robert S. Sloviter. 2001. 'Focal Inhibitory Interneuron Loss and Principal Cell Hyperexcitability in the Rat Hippocampus after Microinjection of a Neurotoxic Conjugate of Saporin and a Peptidase-Resistant Analog of Substance P'. *Journal of Comparative Neurology* 436 (2): 127–52. https://doi.org/10.1002/cne.1065.

Matos-Silva, Hidelberto, Bruno Pereira Reciputti, Élbio Cândido de Paula, André Luiz Oliveira, Vânia Beatriz Lopes Moura, Marina Clare Vinaud, Milton Adriano Pelli Oliveira, and Ruy de Souza Lino-Júnior. 2012. 'Experimental Encephalitis Caused by Taenia Crassiceps Cysticerci in Mice'. *Arquivos de Neuro-Psiquiatria* 70 (4): 287–92. https://doi.org/10.1590/s0004-282x2012005000010.

McQuiston, A. Rory. 2014. 'Acetylcholine Release and Inhibitory Interneuron Activity in

Hippocampal CA1'. *Frontiers in Synaptic Neuroscience* 6 (SEP): 1–7. https://doi.org/10.3389/fnsyn.2014.00020.

Mejia Maza, Alan, Rogger P. Carmen-Orozco, Emma S. Carter, Danitza G. Dávila-Villacorta, Gino Castillo, Jemina D. Morales, Javier Mamani, et al. 2019. 'Axonal Swellings and Spheroids: A New Insight into the Pathology of Neurocysticercosis'. *Brain Pathology* 29 (3): 425–36. https://doi.org/10.1111/bpa.12669.

Moussawi, Khaled, Arthur Riegel, Satish Nair, and Peter W. Kalivas. 2011. 'Extracellular Glutamate: Functional Compartments Operate in Different Concentration Ranges'. *Frontiers in Systems Neuroscience* 5 (NOVEMBER 2011): 1–9. https://doi.org/10.3389/fnsys.2011.00094.

Naidoo, DV, MV Pammenter, A Moosa, JR van Dellen, and JE Cosnett. 1987. 'Seventy Black Epileptics. Cysticercosis, Computed Tomography and Electro-Encephalography.' *South African Medical Journal* 72: 837–38.

Nash, Theodore E., Javier Pretell, and Hector H. Garcia. 2002. 'Calcified Cysticerci Provoke Perilesional Edema and Seizures'. *Clinical Infectious Diseases* 33 (10): 1649–53. https://doi.org/10.1086/323670.

Nash, Theodore E, Siddhartha Mahanty, Jeffrey a Loeb, William H Theodore, Alon Friedman, Josemir W Sander, Gagandeep Singh, et al. 2015. 'Neurocysticercosis: A Natural Human Model of Epileptogenesis.' *Epilepsia* 56 (2): 177–83. https://doi.org/10.1111/epi.12849.

Ndimubanzi, Patrick C., Héleѣe Carabin, Christine M. Budke, Hai Nguyen, Ying Jun Qian, Elizabeth Rainwater, Mary Dickey, Stephanie Reynolds, and Julie A. Stoner. 2010. 'A Systematic Review of the Frequency of Neurocyticercosis with a Focus on People with Epilepsy'. *PLoS Neglected Tropical Diseases* 4 (11). https://doi.org/10.1371/journal.pntd.0000870.

Newsholme, Philip, Joaquim Procopio, Manuela Maria Ramos Lima, Tania Cristina Pithon-Curi, and Rui Curi. 2002. 'Glutamine and Glutamate—Their Central Role in Cell Metabolism and Function'. *Cell Biochemistry and Function* 21: 1–9.

Nguekam, A., A. P. Zoli, L. Vondou, S. M R Pouedet, E. Assana, P. Dorny, J. Brandt, B. Losson, and S. Geerts. 2003. 'Kinetics of Circulating Antigens in Pigs Experimentally Infected with Taenia Solium Eggs'. *Veterinary Parasitology* 111 (4): 323–32. https://doi.org/10.1016/S0304-4017(02)00391-6.

Ohsawa, Keiko, Yoshinori Imai, Yo Sasaki, and Shinichi Kohsaka. 2004. 'Microglia/Macrophage-Specific Protein Iba1 Binds to Fimbrin and Enhances Its Actin-

Bundling Activity.' *Journal of Neurochemistry* 88 (4): 844–56. https://doi.org/10.1046/j.1471-4159.2003.02213.x.

Osmakov, Dmitry I., Sergey G. Koshelev, Yaroslav A. Andreev, and Sergey A. Kozlov. 2017. 'Endogenous Isoquinoline Alkaloids Agonists of Acid-Sensing Ion Channel Type 3'. *Frontiers in Molecular Neuroscience* 10 (September): 1–7. https://doi.org/10.3389/fnmol.2017.00282.

Palma, Sandra, Nancy Chile, Rogger P. Carmen-Orozco, Grace Trompeter, Kayla Fishbeck, Virginia Cooper, Laura Rapoport, et al. 2019. 'In Vitro Model of Postoncosphere Development, and in Vivo Infection Abilities of Taenia Solium and Taenia Saginata'. *PLOS Neglected Tropical Diseases* 13 (3): e0007261. https://doi.org/10.1371/journal.pntd.0007261.

Papageorgiou, Ismini E., Andrea Lewen, Lukas V. Galow, Tiziana Cesetti, Jörg Scheffel, Tommy Regen, Uwe-Karsten Karsten Hanisch, and Oliver Kann. 2016. 'TLR4-Activated Microglia Require IFN- γ to Induce Severe Neuronal Dysfunction and Death in Situ'. *Proceedings of the National Academy of Sciences* 113 (1): 212–17. https://doi.org/10.1073/pnas.1513853113.

Paxinos, George, and Charles Watson. 2007. *The Rat Brain in Stereotaxic Coordinates*. 6th ed. Amsterdam: Elsevier Inc.

Peón, A. N., Y. Ledesma-Soto, and L. I. Terrazas. 2016. 'Regulation of Immunity by Taeniids: Lessons from Animal Models and in Vitro Studies'. *Parasite Immunology* 38 (3): 124–35. https://doi.org/10.1111/pim.12289.

Perea, Gertrudis, and Alfonso Araque. 2010. 'GLIA Modulates Synaptic Transmission'. *Brain Research Reviews* 63 (1–2): 93–102. https://doi.org/10.1016/j.brainresrev.2009.10.005.

Prasad, Amit, Rakesh K. Gupta, Sunil Pradhan, Mukesh Tripathi, Chandra M. Pandey, and Kashi N. Prasad. 2008. 'What Triggers Seizures in Neurocysticercosis? A MRI-Based Study in Pig Farming Community from a District of North India'. *Parasitology International* 57 (2): 166–71. https://doi.org/10.1016/j.parint.2007.12.001.

Prasad, Amit, Kashi Nath Prasad, Rakesh Kumar Gupta, and Sunil Pradhan. 2009. 'Increased Expression of ICAM-1 among Symptomatic Neurocysticercosis'. *Journal of Neuroimmunology* 206 (1–2): 118–20. https://doi.org/10.1016/j.jneuroim.2008.09.015.

Preux, Pierre-marie, and Michel Druet-cabanac. 2005. 'Epidemiology and Aetiology of Epilepsy in Sub-Saharan Africa'. *Lancet Neurology* 4 (January): 21–31.

Raimondo, Joseph V., Richard J. Burman, Arieh A. Katz, and Colin J. Akerman. 2015. 'Ion Dynamics during Seizures'. *Frontiers in Cellular Neuroscience* 9 (October): 1–14. https://doi.org/10.3389/fncel.2015.00419.

Raimondo, Joseph V., Louise Kay, Tommas J. Ellender, and Colin J. Akerman. 2012. 'Optogenetic Silencing Strategies Differ in Their Effects on Inhibitory Synaptic Transmission'. *Nature Neuroscience* 15 (8): 1102–4. https://doi.org/10.1038/nn.3143.

Ralay Ranaivo, Hantamalala, and Mark S. Wainwright. 2010. 'Albumin Activates Astrocytes and Microglia through Mitogen-Activated Protein Kinase Pathways'. *Brain Research* 1313 (51): 222–31. https://doi.org/10.1016/j.brainres.2009.11.063.

Rana, Amna, and Alberto Musto. 2018. 'The Role of Inflammation in the Development of Epilepsy'. *Journal of Neuroinflammation* 15 (144): 1–12. https://doi.org/10.1186/s12974-018-1192-7.

Rasamoelina-Andriamanivo, Harentsoaniaina, Vincent Porphyre, and Ronan Jambou. 2013. 'Control of Cysticercosis in Madagascar: Beware of the Pitfalls.' *Trends in Parasitology* 29 (11): 538–47. https://doi.org/10.1016/j.pt.2013.09.002.

Ravizza, Teresa, Massimo Rizzi, Carlo Perego, Cristina Richichi, Jana Velískŏvá, Solomon L. Moshé, M. Grazia De Simoni, and Annamaria Vezzani. 2005. 'Inflammatory Response and Glia Activation in Developing Rat Hippocampus after Status Epilepticus'. *Epilepsia* 46 (SUPPL. 5): 113–17. https://doi.org/10.1111/j.1528-1167.2005.01006.x.

Restrepo, B. I., J. I. Alvarez, J. A. Castaño, L. F. Arias, M. Restrepo, J. Trujillo, C. H. Colegial, and J. M. Teale. 2001. 'Brain Granulomas in Neurocysticercosis Patients Are Associated with a Th1 and Th2 Profile'. *Infection and Immunity* 69 (7): 4554–60. https://doi.org/10.1128/IAI.69.7.4554-4560.2001.

Rice, Ann C., and Robert J. Delorenzo. 1998. 'NMDA Receptor Activation during Status Epilepticus Is Required for the Development of Epilepsy'. *Brain Research* 782 (1–2): 240–47. https://doi.org/10.1016/S0006-8993(97)01285-7.

Robinson, Prema, Armandina Garza, Joel Weinstock, Jose a Serpa, Jerry Clay Goodman, Kristian T Eckols, Bahrom Firozgary, and David J Tweardy. 2012. 'Substance P Causes Seizures in Neurocysticercosis.' *PLoS Pathogens* 8 (2): e1002489. https://doi.org/10.1371/journal.ppat.1002489.

Román, G., J. Sotelo, O. Del Brutto, a. Flisser, M. Dumas, N. Wadia, D. Botero, et al. 2000. 'A Proposal to Declare Neurocysticercosis an International Reportable Disease'. *Bulletin of the World Health Organization* 78 (99): 399–406. https://doi.org/10.1590/S0042-

96862000000300016.

Roseti, Cristina, Erwin A. van Vliet, Pierangelo Cifelli, Gabriele Ruffolo, Johannes C. Baayen, Maria Amalia Di Castro, Cristina Bertollini, et al. 2015. 'GABA-A Currents Are Decreased by IL-1β in Epileptogenic Tissue of Patients with Temporal Lobe Epilepsy: Implications for Ictogenesis'. *Neurobiology of Disease* 82: 311–20. https://doi.org/10.1016/j.nbd.2015.07.003.

Sabbagh, Amr Mohamed El, Samah Sabry El Kazzaz, Ghada El Saeed Mashaly, Dina Salama Abd Elmagid, and Noha Tharwat. 2017. 'Tumor Necrosis Factor-Alpha and Interleukin-1 Beta in Febrile Seizures'. *International Journal of Current Microbiology and Applied Sciences* 6 (10): 849–54. https://doi.org/10.20546/ijcmas.2017.610.101.

Saleque, A., N. Chowdhury, P. K.R. Iyer, and G. Baruah. 1988. 'Induced Taenia Solium Cysticercosis in Rhesus Monkeys (Macaca Mulatta): A Clinicopathological Study'. *Annals of Tropical Medicine and Parasitology* 82 (1): 103–5. https://doi.org/10.1080/00034983.1988.11812215.

Santosh, Vani, and Palavalasa Sravya. 2017. 'Glioma, Glutamate (SLC7A11) and Seizures - a Commentary.' *Annals of Translational Medicine* 5 (10): 214. https://doi.org/10.21037/atm.2017.02.18.

Sciutto, E., G. Fragoso, L. Trueba, D. Lemus, R. M. Montoya, M. L. Diaz, T. Govezensky, C. Lomeli, G. Tapia, and C. Larralde. 1990. 'Cysticercosis Vaccine: Cross Protecting Immunity with T. Solium Antigens against Experimental Murine T. Crassiceps Cysticercosis'. *Parasite Immunology* 12 (6): 687–96. https://doi.org/10.1111/j.1365-3024.1990.tb00997.x.

Seifert, Gerald, Giorgio Carmignoto, and Christian Steinhäuser. 2010. 'Astrocyte Dysfunction in Epilepsy'. *Brain Research Reviews* 63 (1–2): 212–21. https://doi.org/10.1016/j.brainresrev.2009.10.004.

Seiffert, Ernst, Jens P Dreier, Sebastian Ivens, Ingo Bechmann, Oren Tomkins, Uwe Heinemann, and Alon Friedman. 2004. 'Lasting Blood – Brain Barrier Disruption Induces Epileptic Focus in the Rat Somatosensory Cortex'. *Neurobiology of Disease* 24 (36): 7829–36. https://doi.org/10.1523/JNEUROSCI.1751-04.2004.

Sengupta, Pallav. 2013. 'The Laboratory Rat: Relating Its Age With Human's.' *International Journal of Preventive Medicine* 4 (6): 624–30.

Shabab, Tara, Ramin Khanabdali, Soheil Zorofchian Moghadamtousi, Habsah Abdul Kadir, and Gokula Mohan. 2017. 'Neuroinflammation Pathways: A General Review'.

International Journal of Neuroscience 127 (7): 624–33. https://doi.org/10.1080/00207454.2016.1212854.

Sheng, Jin, Frederick Boop, Robert Mrak, and W Sue Griffin. 1994. 'Increased Neuronal β-Amyloid Precursor Protein Expression in Human Temporal Lobe Epilepsy: Association with Interleukin-1α Immunoreactivity'. *Journal of Neurochemistry* 63 (5): 1872–79. https://doi.org/10.1038/jid.2014.371.

Simoni, Anna De, and Lily M.Y. Yu. 2006. 'Preparation of Organotypic Hippocampal Slice Cultures: Interface Method'. *Nature Protocols* 1 (3): 1439–45. https://doi.org/10.1038/nprot.2006.228.

Simoni, Maria Grazia De, Carlo Perego, Teresa Ravizza, Daniela Moneta, Mirko Conti, Francesco Marchesi, Ada De Luigi, Silvio Garattini, and Annamaria Vezzani. 2000. 'Inflammatory Cytokines and Related Genes Are Induced in the Rat Hippocampus by Limbic Status Epilepticus'. *European Journal of Neuroscience* 12 (7): 2623–33. https://doi.org/10.1046/j.1460-9568.2000.00140.x.

Singhi, Pratibha. 2011. 'Infectious Causes of Seizures and Epilepsy in the Developing World'. *Developmental Medicine and Child Neurology* 53 (7): 600–609. https://doi.org/10.1111/j.1469-8749.2011.03928.x.

Sloviter, Robert S., Leila Ali-Akbarian, Kathryn D. Horvath, and Kent a. Menkens. 2001. 'Substance P Receptor Expression by Inhibitory Interneurons of the Rat Hippocampus: Enhanced Detection Using Improved Immunocytochemical Methods for the Preservation and Colocalization of GABA and Other Neuronal Markers'. *Journal of Comparative Neurology* 430 (3): 283–305. https://doi.org/10.1002/1096-9861(20010212)430:3<283::AID-CNE1031>3.0.CO;2-V.

Snowball, Albert, Elodie Chabrol, Robert C Wykes, Tawfeeq Shekh-ahmad, Jonathan H Cornford, Andreas Lieb, Michael P Hughes, et al. 2019. 'Epilepsy Gene Therapy Using an Engineered Potassium Channel'. *Neurobiology of Disease* 39 (16): 3159–69.

Sofroniew, Michael V. 2015. 'Astrocyte Barriers to Neurotoxic Inflammation'. *Nature Reviews Neuroscience* 16 (5): 249–63. https://doi.org/10.1038/nrn3898.

Sofroniew, Michael V. 2005. 'Reactive Astrocytes in Neural Repair and Protection'. *The Neuroscientist* 11 (5): 400–407. https://doi.org/10.1177/1073858405278321.

Sombati, S., and R. J. DeLorenzo. 1995. 'Recurrent Spontaneous Seizure Activity in Hippocampal Neuronal Networks in Culture'. *Journal of Neurophysiology* 73 (4): 1706–11. https://doi.org/10.1152/jn.1995.73.4.1706.

Sontheimer, Harald. 2008. ‘A Role for Glutamate in Growth and Invasion of Primary Brain Tumors’. *Journal of Neurochemistry* 105 (2): 287–95. https://doi.org/10.1111/j.1471-4159.2008.05301.x.

South African National Standard: The Care and Use of Animals for Scientific Purposes. 2008. Pretoria, South Africa: SABS Standards Division.

Stasheff, SF, WW Anderson, S Clark, and WA Wilson. 1989. ‘NMDA Antagonists Differentiate Epileptogenesis from Seizure Expression in an in Vitro Model’. *Science* 245 (4918): 648–51. https://doi.org/10.1126/science.2569762.

Stellwagen, D., E. Beattie, J. Seo, and R. Malenka. 2005. ‘Differential Regulation of AMPA Receptor and GABA Receptor Trafficking by Tumor Necrosis Factor-α’. *Journal of Neuroscience* 25 (12): 3219–28. https://doi.org/10.1523/jneurosci.4486-04.2005.

Stellwagen, David, and Robert C. Malenka. 2006. ‘Synaptic Scaling Mediated by Glial TNF-α’. *Nature* 440 (7087): 1054–59. https://doi.org/10.1038/nature04671.

Stoppini, L., P.-A. Buchs, and D. Muller. 1991. ‘A Simple Method for Organotypic Cultures of Nervous Tissue’. *J. Neurosci. Meth.* 37 (2): 173–182. https://doi.org/10.1016/0165-0270(91)90128-M.

Stringer, Janet L., LaToia M. Marks, A. Clinton White, and Prema Robinson. 2003. ‘Epileptogenic Activity of Granulomas Associated with Murine Cysticercosis’. *Experimental Neurology* 183 (2): 532–36. https://doi.org/10.1016/S0014-4886(03)00179-1.

Sun, David A., Sompong Sombati, and Robert J. DeLorenzo. 2001. ‘Glutamate Injury–Induced Epileptogenesis in Hippocampal Neurons’. *Stroke* 32 (10): 2344–50. https://doi.org/10.1161/hs1001.097242.

Sun, Yuyang, Arun Chauhan, Pramod Sukumaran, Jyotika Sharma, Brij B Singh, and Bibhuti B Mishra. 2014. ‘Inhibition of Store-Operated Calcium Entry in Microglia by Helminth Factors: Implications for Immune Suppression in Neurocysticercosis’. *Journal of Neuroinflammation* 11 (210): 1–12. https://doi.org/10.1186/s12974-014-0210-7.

Takano, Takahiro, Jane H.C. H.-C. Lin, Gregory Arcuino, Qun Gao, Jay Yang, and Maiken Nedergaard. 2001. ‘Glutamate Release Promotes Growth of Malignant Gliomas’. *Nature Medicine* 7 (9): 1010–15. https://doi.org/10.1038/nm0901-1010.

Terunuma, Miho, Karina J. Vargas, Megan E. Wilkins, Omar A. Ramírez, Matías Jaureguiberry-Bravo, Menelas N. Pangalos, Trevor G. Smart, Stephen J. Moss, and

Andrés Couve. 2010. ‘Prolonged Activation of NMDA Receptors Promotes Dephosphorylation and Alters Postendocytic Sorting of GABA B Receptors’. *Proceedings of the National Academy of Sciences of the United States of America* 107 (31): 13918–23. https://doi.org/10.1073/pnas.1000853107.

The World Health Organisation. n.d. ‘Neglected Tropical Diseases’. The World Health Organisation. Accessed 20 September 2007. https://www.who.int/neglected_diseases/diseases/en/.

The World Health Organization. 2006. ‘Neurological Disorders: Public Health Challenges’. Switzerland.

Thomson, A. J. G. 1993. ‘Neurocysticercosis - Experience at the Teaching Hospitals of the University of Cape Town’. *South African Medical Journal* 83 (5): 332–34.

Thomson, A.J, J.C de Villiers, A Moosa, and J van Dellen. 1984. ‘Cerebral Cysticercosis in Children in South Africa.’ *Annals of Tropical Paediatrics* 4 (2): 67–77.

Trevisan, Chiara, Ernatus M. Mkupasi, Helena A. Ngowi, Björn Forkman, and Maria V. Johansen. 2016. ‘Severe Seizures in Pigs Naturally Infected with Taenia Solium in Tanzania’. *Veterinary Parasitology* 220: 67–71. https://doi.org/10.1016/j.vetpar.2016.02.025.

Tsai, Isheng J., Magdalena Zarowiecki, Nancy Holroyd, Alejandro Garciarrubio, Alejandro Sanchez-Flores, Karen L. Brooks, Alan Tracey, et al. 2013. ‘The Genomes of Four Tapeworm Species Reveal Adaptations to Parasitism’. *Nature* 496 (7443): 57–63. https://doi.org/10.1038/nature12031.

Uddin, J., H. H. Garcia, R. H. Gilman, A. E. Gonzalez, and J. S. Friedland. 2005. ‘Monocyte-Astrocyte Networks and the Regulation of Chemokine Secretion in Neurocysticercosis’. *The Journal of Immunology* 175: 3273–81. https://doi.org/10.4049/jimmunol.175.5.3273.

Uddin, J., A. E. Gonzalez, R. H. Gilman, L. H. Thomas, S. Rodriguez, C. A. W. Evans, D. G. Remick, H. H. Garcia, and J. S. Friedland. 2010. ‘Mechanisms Regulating Monocyte CXCL8 Secretion in Neurocysticercosis and the Effect of Antiparasitic Therapy’. *The Journal of Immunology* 185: 4478–84. https://doi.org/10.4049/jimmunol.0904158.

Varadkar, Sophia, Christian G. Bien, Carol A. Kruse, Frances E. Jensen, Jan Bauer, Carlos A. Pardo, Angela Vincent, Gary W. Mathern, and J. Helen Cross. 2014. ‘Rasmussen’s Encephalitis: Clinical Features, Pathobiology, and Treatment Advances’. *The Lancet Neurology* 13 (2): 195–205. https://doi.org/10.1016/S1474-4422(13)70260-6.

Vendelova, E., G. Hrčková, M. B. Lutz, K. Brehm, and J. Nono Komguep. 2016. 'In Vitro Culture of Mesocestoides Corti Metacestodes and Isolation of Immunomodulatory Excretory–Secretory Products'. *Parasite Immunology* 38 (7): 403–13. https://doi.org/10.1111/pim.12327.

Vendelova, Emilia, Jeferson Camargo de Lima, Karina Rodrigues Lorenzatto, Karina Mariante Monteiro, Thomas Mueller, Jyotishman Veepaschit, Clemens Grimm, et al. 2016. 'Proteomic Analysis of Excretory-Secretory Products of Mesocestoides Corti Metacestodes Reveals Potential Suppressors of Dendritic Cell Functions'. *PLoS Neglected Tropical Diseases* 10 (10): 1–27. https://doi.org/10.1371/journal.pntd.0005061.

Verastegui, Manuela R, Alan Mejia, Taryn Clark, Cesar M Gavidia, Javier Mamani, Fredy Ccopa, and Noelia Angulo. 2015. 'Novel Rat Model for Neurocysticercosis Using Taenia Solium'. *The American Journal of Pathology* 185 (8): 2259–68. https://doi.org/10.1016/j.ajpath.2015.04.015.

Verma, Avantika, Kashi Nath Prasad, Rakesh Kumar Gupta, Aloukick Kumar Singh, Kishan Kumar Nyati, Arshi Rizwan, Chandra Mohan Pandey, and Vimal Kumar Paliwal. 2010. 'Toll-Like Receptor 4 Polymorphism and Its Association with Symptomatic Neurocysticercosis'. *The Journal of Infectious Diseases* 202 (8): 1219–25. https://doi.org/10.1086/656395.

Vezzani, Annamaria, Jacqueline French, Tamas Bartfai, and Tallie Z. Baram. 2011. 'The Role of Inflammation in Epilepsy'. *Nature Reviews Neurology* 7 (1): 31–40. https://doi.org/10.1038/nrneurol.2010.178.

Vezzani, Annamaria, Robert S Fujinami, H Steve White, Pierre-marie Preux, Ingmar Blümcke, Josemir W Sander, and Wolfgang Löscher. 2016. 'Infections, Inflammation and Epilepsy'. *Acta Neuropathologica* 131: 211–34. https://doi.org/10.1007/s00401-015-1481-5.

Vezzani, Annamaria, and Barbara Viviani. 2015. 'Neuromodulatory Properties of Inflammatory Cytokines and Their Impact on Neuronal Excitability'. *Neuropharmacology* 96: 70–82. https://doi.org/10.1016/j.neuropharm.2014.10.027.

Villa, Chiara, and Romina Combi. 2016. 'Potassium Channels and Human Epileptic Phenotypes: An Updated Overview'. *Frontiers in Cellular Neuroscience* 10 (MAR2016): 1–14. https://doi.org/10.3389/fncel.2016.00081.

Viviani, B, S Bartesaghi, F Gardoni, A Vezzani, M M Behrens, T Bartfai, M Binaglia, et al. 2003. 'Interleukin-1β Enhances NMDA Receptor-Mediated Intracellular Calcium Increase

through Activation of the Src Family of Kinases.' *The Journal of Neuroscience* 23 (25): 8692–8700.

Vliet, E. A. Van, S. Da Costa Araújo, S. Redeker, R. Van Schaik, E. Aronica, and J. A. Gorter. 2007. 'Blood-Brain Barrier Leakage May Lead to Progression of Temporal Lobe Epilepsy'. *Brain* 130 (2): 521–34. https://doi.org/10.1093/brain/awl318.

Wagner, R. G., and C. R. Newton. 2009. 'Do Helminths Cause Epilepsy?' *Parasite Immunology* 31 (11): 697–705. https://doi.org/10.1111/j.1365-3024.2009.01128.x.

Wang, Lihua, Suzie Dufour, Taufik A. Valiante, and Peter L. Carlen. 2016. 'Extracellular Potassium and Seizures: Excitation, Inhibition and the Role of Ih'. *International Journal of Neural Systems* 26 (8): 1–14. https://doi.org/10.1142/S0129065716500441.

Weissberg, Itai, Lydia Wood, Lyn Kamintsky, Oscar Vazquez, Dan Z Milikovsky, Allyson Alexander, Hannah Oppenheim, et al. 2016. 'Albumin Induces Excitatory Synaptogenesis through Astrocytic TGF-β/ALK5 Signaling in a Model of Acquired Epilepsy Following Blood-Brain Barrier Dysfunction'. *Neurobiology of Disease* 78: 115–25. https://doi.org/10.1016/j.nbd.2015.02.029.Albumin.

Weng, Xie-chuan, Jian-quan Zheng, Xiao-dan Gai, Jin Li, and Wen-bin Xiao. 2004. 'Two Types of Acid-Sensing Ion Channel Currents in Rat Hippocampal Neurons'. *Neuroscience Research* 50: 493–99. https://doi.org/10.1016/j.neures.2004.09.001.

Wilhelmsson, Ulrika, Eric A. Bushong, Diana L. Price, Benjamin L. Smarr, Van Phung, Masako Terada, Mark H. Ellisman, and Milos Pekny. 2006. 'Redefining the Concept of Reactive Astrocytes as Cells That Remain within Their Unique Domains upon Reaction to Injury'. *Proceedings of the National Academy of Sciences of the United States of America* 103 (46): 17513–18. https://doi.org/10.1073/pnas.0602841103.

Willms, Kaethe, and Rimma Zurabian. 2010. 'Taenia Crassiceps: In Vivo and in Vitro Models.' *Parasitology* 137 (3): 335–46. https://doi.org/10.1017/S0031182009991442.

Winkler, Andrea Sylvia, Arve Lee Willingham, Chummy Sikalizyo Sikasunge, and Erich Schmutzhard. 2009. 'Epilepsy and Neurocysticercosis in Sub-Saharan Africa'. *The Middle European Journal of Medicine* 121: 3–12. https://doi.org/10.1007/s00508-009-1242-3.

Zepeda, N, S Solano, N Copitin, and J L Chávez. 2017. 'Apoptosis of Mouse Hippocampal Cells Induced by Taenia Crassiceps Metacestode Factor'. *Journal of Helminthology*, 1–7. https://doi.org/10.1017/S0022149X16000146.

Ziobro, Julie M., Laxmikant S. Deshpande, and Robert J. DeLorenzo. 2011. ‘An Organotypic Hippocampal Slice Culture Model of Excitotoxic Injury Induced Spontaneous Recurrent Epileptiform Discharges’. *Brain Research* 1371 (January): 110–20. https://doi.org/10.1038/jid.2014.371.